The Hong Kong Polytechnic University

Department of Civil and Structural Engineering

Project Title:

Sensor Placement Method for Effective Monitoring of Structural Elements

The Hong Kong Polytechnic University
香港理工大學
Department of Civil and Structural Engineering

Memorandum

The accompanying dissertation entitled "Sensor placement method for effective monitoring of consistent elements" is submitted for the degree of Master of Philosophy in the Department of Civil and Structural Engineering in the Hong Kong Polytechnic University.

The dissertation is based on independent work carried out by the author from September 1997 to September 1999, except the experimental work of the five-storey plane steel frame, under the supervision of Dr. S.S. Law,. The work and ideas are original and all contributions from others are duly acknowledged in the text by reference.

Chi Kin, Iu

Abstract

A large civil engineering structure consists of a huge sum of components or elements with great variation of stiffness, and a damage identification algorithm for such a structure seems to be difficult with limited number of sensors. A question on how to place the sensors to monitor this large civil structure effectively has to be answered. This sensor placement problem can be based on the sensitivity, as presented by the Cobb and Liebst (1997), and the sensor locations according to this Co-linearity Matrix Method are fundamentally basded on the high eigenvector sensitivities at the degrees-of-freedom. Also these sensor locations may localize on some highly sensitive elements, when the sensor selection is based on the high eigenvector sensitivity. As a result, these selected sensor locations are impossible to monitor all elements effectively.

On the other hand, in the proposed method, the selection of the sensor locations is based on the eigenvector sensitivities according to the particular group of elements. These sensor locations therefore depend on the different elements which are chosen to be monitored. According to the different elements chosen for monitoring, the sensors are allocated around these elements. And the sensors are therefore not placed around some highly sensitive elements. Moreover, the reliable damage information emitting from the elements chosen for monitoring is also a

criterion for sensor selection in the proposed method. Hence the selected sensor locations enable the collection of adequate damage information from the elements for effective health monitoring.

The sensors according to the proposed method can collect relatively large damage information emitted from the elements by comparing with different sensor placement methods, such as Co-linearity Matrix Method and Effective Index Method. This damage information is an indicator of the effectiveness of health monitoring. It means that the selected elements are more effectively monitored by the given sensors configuration according to the proposed method.

For the analysis of the damage assessment, the damage localization and quantification for the damages is evaluated basing on the corresponding sensor locations from the different sensor placement methods as previously mentioned. This damage assessment is mainly based on the *MDLAC* method. The results for the proposed method indicate that the effectiveness of damage assessment is relatively better than those in accordance with other methods, but the accuracy of the damage assessment by using MDLAC method is a little bit poor. According to the same basis for comparison, this analysis of damage assessment for the different sensor placement methods is fairly comparable to be accepted at this stage.

As an example application, the sensor placement methods, including the proposed method and the Co-linearity Matrix Method, are applied to the Tsing Ma Bridge. According to the results of this analysis, the sensor locations basing on the Co-

linearity Matrix Method concentrate on some highly sensitive elements. On the other hand, the sensor locations from the proposed method are scattered around the different structural components of the bridge according to which elements need to be monitored. Intuitively, the structural health monitoring for this kind of large civil structure is relatively effective by means of the proposed method.

List of publication derived from this project

1. Iu, C.K. and Law, S.S. (1999) "Sensor placement method for consistent element grouping" Proceedings of international conference of the integrating dynamics, condition monitoring and control for the 21st century, pp575-580.
2. Iu, C.K. and Law, S.S. (1999) "Minimal sensor placement for monitoring structural element group" Journal of Sound and vibration (submitted)
3. Iu, C.K, Law, S.S. and Mak, P.S. (1999) "Sensor Placement for damage detection of a steel plane frame" Journal of Structural Engineering, ASCE (submitted)

Acknowledgements

At the very beginning, the author would like to thank a number of people who have provided much assistance in various ways to complete this research project. For my chief supervisor, Dr. S.S. Law, he gave me valuable advice on the research project. Also I would like to thank for the professional judgement from my co-supervisor, Prof. J.M. Ko, on my project.

Besides I wish to thank another research student Miss P.S. Mak, who has preformed most of the experimental work so that I could analyze and compare the effectiveness of health monitoring on a test structure basing on different sets of sensor locations. I also wish to thank all technical staff of the Civil and Structural En..neering Department of the Hong Kong Polytechnic for their assistance in the laboratory work.

Moreover, I would like to thank my parent and younger sister for all their loves and spiritual supports for the completion of my thesis. I wish to send my sincere appreciation to all my friends for all their supports and assistance during my weakest time.

Strong appreciation of the financial support given by the Hong Kong Polytechnic University is truly expressed.

List of symbols

C_k	scaling coefficient
$E[]$	expectation value;
h_{ii}	amount of leverage or ith diagonal element in the prediction matrix;
$\boldsymbol{H}$	prediction matrix;
H'	updated prediction matrix;
$\boldsymbol{K}_j$	stiffness matrix of jth element;
l	number of the accessible degrees-of-freedom;
m	number of target modes;
MAC	Modal Assurance Criterion
$MDLAC$	Multiple Damage Location Assurance Criterion;
n	number of total elements;
p_j	structural parameter of jth element;
$\boldsymbol{P}$	inverse of Fisher Information matrix;
$\boldsymbol{Q}$	covariance matrix of error in the estimator;
q	number of target elements;
r	number of analyzed elements;
s	number of non-analyzed elements;
x	Element Detectability;
$\overline{x}$	Receptability of a degree-of-freedom;
$\boldsymbol{X}$	sensitivity or eigenvector derivative matrix;
$\boldsymbol{Y}$	total Detectability of an element;
$\overline{Y}$	total Receptability of a degree-of-freedom;
$\hat{Y}$	best fit Total Detectability or Total Receptability;
δD_j	small change of structural parameter in jth element;
$\Delta\boldsymbol{\Phi}$	measured mode shape change vector;
$\delta\boldsymbol{\Phi}$	analytical mode shape change vector;
α	weighting factor on the Receptability of a degrees-of-freedom;
β	modal contribution factor;
$\hat{\beta}$	linear unbiased estimator;

λ_r the rth eigenvalue;

γ weighting factor on the contribution of damage information of an element to the Receptability at a degree-of-freedom;

ε random error vector;

μ reduction ratio

ϕ_i eigenvector at ith degree-of-freedom;

σ^2 variance of random error vector.

Contents

Memorandum

Abstract

List of publication derived from this project

Acknowledgements

List of symbols

Table of Content

List of tables

List of figures *Page No.*

Chapter 1: Introduction

Section 1.1	**Background of structural health monitoring**	1
Section 1.2	**Objective of the project**	2
Section 1.3	**Scope of the project**	3

Chapter 2: Literature review

Section 2.1	**Development of eigenvalue and eigenvector derivatives**	7
Section 2.2	**Development of sensor placement methods**	9
Section 2.3	**Development of damage assessment**	15

Chapter 3: Basic theory for the sensor placement method

Section 3.1	**Assumptions**	22
Section 3.2	**Sensitivity**	23
Section 3.2.1	Derivation of sensitivity by means of Nelson's method	24
Section 3.2.2	Implication of an eigenvector derivative	30
Section 3.3	**Detectability**	31
Section 3.3.1	Element Detectability	31
Section 3.3.2	Total Detectability	32
Section 3.4	**Receptability**	34
Section 3.4.1	Receptability of a degree-of-freedom	34
Section 3.4.2	Total Receptability of a degree-of-freedom	35
Section 3.4.3	Consistent element	36
Section 3.4.3.1	*Inconsistent Total Detectability*	36
Section 3.4.3.2	*Consistent element grouping*	38
Section 3.5	**Linear model analysis**	39
Section 3.5.1	Linear model on Total Detectability or Total Receptability	39
Section 3.5.2	Estimation of the best fit Total Detectability or Total Receptability	40
Section 3.5.3	Covariance matrix of unbiased estimator	42
Section 3.5.4	Use of prediction matrix	44
Section 3.6	**Consistency check for elements**	46
Section 3.6.1	Principle of determination of consistent elements	46
Section 3.6.2	Criterion for the determination of consistent elements	48

Chapter 4: Methodology for the sensor placement method

Section 4.1	**Introduction of the proposed sensor placement method**	51
Section 4.2	**Damage element classification**	52
Section 4.2.1	Target modal identification process	52
Section 4.2.2	Damage element classification	54
Section 4.3	**Sensor placement method**	56
Section 4.3.1	Criterion of sensor placement ratio	56
Section 4.3.2	Threshold value of sensor placement ratio	58
Section 4.4	**Minimization of the sensor number**	58
Section 4.4.1	Limitation of sensor number	58
Section 4.4.2	Criterion on minimizing the sensor number	59
Section 4.4.3	Formulation of sensor elimination process	59
Section 4.4.4	Criterion of the least loss of damage information	61
Section 4.4.5	Procedures of the sensor deletion process	62
Section 4.5	**Consistency check**	63
Section 4.5.1	Introduction of consistent elements grouping	63
Section 4.5.2	Criterion of the consistent elements grouping	64
Section 4.5.3	Model updating process for elimination of inconsistent elements	64

Chapter 5: Comparison of the sensor placement methods

Section 5.1	**Introduction**	67
Section 5.2	**Effective index method**	68
Section 5.2.1	Introduction	68
Section 5.2.2	Fisher Information matrix	68
Section 5.2.3	Fractional contribution of sensor locations	70
Section 5.2.3	Modification of the effective index method	72
Section 5.3	**Co-linearity matrix method**	73
Section 5.3.1	Introduction	73
Section 5.3.2	Sensor location prioritization	73
Section 5.3.3	Damage localization	75
Section 5.4	**Simulated structure for illustration**	77
Section 5.4.1	Structural properties and form of simulated structure	77
Section 5.4.2	Vibrational data of simulated structure	80
Section 5.5	**Results from proposed sensor placement method**	83
Section 5.5.1	Threshold values	83
Section 5.5.2	Undetectable elements	84
Section 5.5.3	Sensor location from proposed method	85
Section 5.6	**Results from other sensor placement methods**	90
Section 5.6.1	Sensor locations from Effective Index Method	90
Section 5.6.2	Sensor locations from Co-linearity Matrix Method	91
Section 5.6.3	Implication of symmetrical sensor placement	94

Section 5.7 **Comparison and discussion** 95

Section 5.7.1 Comparison of sensor locations 95

Section 5.7.2 Comparison of eigenvectors change due to unity damage 95

Section 5.7.3 Discussion on damage in different types of elements 98

Section 5.7.4 Discussion on consistent element grouping 99

Chapter 6: Damage localization and quantification

Section 6.1	**Introduction**	101
Section 6.2	**Damage assessment using incomplete mode shapes**	102
Section 6.2.1	Damage localization using *MDLAC*	102
Section 6.2.2	Damage quantification using *MDLAC*	104
Section 6.3	**Damage localization with simulated three-storey frame**	107
Section 6.4	**Experimental verification on five-storey steel frame**	110
Section 6.4.1	Test structure	110
Section 6.4.2	Setup of the experiment	113
Section 6.4.3	Identification of eigenvalues and eigenvectors of the damage states	117
Section 6.4.4	Damage in the test structure	122
Section 6.5	**Verification of the tested structure**	124
Section 6.5.1	Verification in the multi-damage states with the proposed method	124
Section 6.5.2	Verification in the multi-damage states with other methods	129
Section 6.5.3	Comparison using different Target Groups with proposed method	129
Section 6.5.3.1	*Effects of different Target Groups on damage localization*	129
Section 6.5.3.2	*Effects of different target Groups on damage quantification*	135
Section 6.5.3.3	*Effects of damage sequence on damage assessment*	137
Section 6.5.4	Comparison between different sensor placement methods	140

Section 6.5.5 Summary on the effectiveness of method in damage assessment 142

Chapter 7: Application on Tsing Ma Bridge

Section 7.1	**Background of Tsing Ma Bridge**	144
Section 7.1.1	Introduction	144
Section 7.1.2	Main features of the Tsing Ma Bridge	145
Section 7.1.3	Finite element modelling of Tsing Ma Bridge	147
Section 7.2	**Sensor locations on Tsing Ma Bridge from different methods**	149
Section 7.2.1	Sensor locations from Co-linearity Matrix Method	149
Section 7.2.2	Sensor locations from the proposed method for different groups of interested elements	151
Section 7.2.2.1	*Introduction*	151
Section 7.2.2.2	*Target Group of deck spines on Ma Wan side*	152
Section 7.2.2.3	*Target Group of deck spines on main span*	153
Section 7.3	Discussion on sensor locations from different methods	154

Chapter 8: Conclusions and recommendations

Section 8.1	Conclusion on damage information collected	156
Section 8.2	Conclusion on damage localization and quantification	157
Section 8.3	Conclusion on sensor locations on Tsing Ma Bridge	159
Section 8.4	Recommendation	160

Reference

List of tables

- Table 5.1 – Section properties of three-storey plane steel frame
- Table 5.2 – Natural frequencies of three-storey plane steel frame
- Table 5.3 – Sensor placement ratio for each sensor location
- Table 5.4 – Sensor locations remained according to the least loss of information
- Table 5.5 – Consistent elements with respect to each sensor locations
- Table 5.6 – Finalized sensor locations from proposed sensor placement method
- Table 5.7 – Linearly independent distribution by Effective Index Method
- Table 5.8 – Linearly independent information by Co-linearity Matrix Method (i)
- Table 5.9 – Linearly independent information by Co-linearity Matrix Method using method (ii)
- Table 5.10 – Summary of sensor locations from different sensor placement methods
- Table 6.1 – Summary of sensor locations from different sensor placement methods
- Table 6.2 – Ranking of the MDLAC values for damage element 38 and 42
- Table 6.3 – Natural frequencies for different damage states
- Table 6.4 – Correlation of mode shapes between different damage states
- Table 6.5 – True damage extent of damage elements in five-storey steel frame
- Table 6.6 – Sensor locations for corresponding Target Groups
- Table 6.6 – Summary of sensor locations from different sensor placement methods
- Table 6.7 – *MDLAC* ranking for damage elements of each Target Group
- Table 6.8 – *MDLAC* ranking based on all 75 elements
- Table 6.9 – Damage quantification in different damage states
- Table 7.1 – Different Tsing Ma Bridge components in finite element model
- Table 7.1 – The sensor locations from Co-linearity Matrix Method
- Table 7.3 – The sensor locations from proposed method for deck at Ma Wan side
- Table 7.4 – The sensor locations from proposed method for main deck spines

List of figures

- Figure 3.1 – Distribution of sensitivities in the linear model
- Figure 4.1 – Procedures of proposed sensor placement method
- Figure 5.1 – Evaluation view of three-storey plane steel frame
- Figure 5.2 – Mode shape of three-storey plane steel frame
- Figure 5.3 – Distribution of sensitivities at finalized sensor locations
- Figure 5.4 – Eigenvector change at sensor locations due to damage element 38
- Figure 5.5 – Eigenvector change at sensor locations due to damage element 42
- Figure 5.6 – Eigenvector change due to different elements in proposed method
- Figure 6.1 – Damage localization of *MDLAC* due to damage element 38
- Figure 6.2 – Damage localization of *MDLAC* due to damage element 42
- Figure 6.3 – Evaluation view of five-storey plane steel frame
- Figure 6.4 – Experimental setup to measure complete mode shapes
- Figure 6.5 – Photograph of experimental setup
- Figure 6.6 – Eigenvector change at 188.939Hz mode for multi damage states
- Figure 6.7 – Mode shapes of undamaged five-storey plane steel frame
- Figure 6.8 – Different target elements in five-storey plane steel frame
- Figure 6.9 – *MDLAC* values with different Target Groups in first damage state
- Figure 6.10 – *MDLAC* values with different Target Groups in second damage state
- Figure 6.11 – *MDLAC* values with different Target Groups in third damage state
- Figure 6.12 – *MDLAC* values with different Target Groups in third damage state (based on target mode)
- Figure 6.13 – *MDLAC* values with Target Group 4 for all three damage states
- Figure 6.14 – Damage extent with Target Group 4 for all three damage states

- Figure 6.15 – MDLAC values with Target Group 2 for all three damage states
- Figure 6.16 – Damage extent with Target Group 2 for all three damage states
- Figure 6.17 – MDLAC values with different methods in first damage state
- Figure 6.18 – MDLAC values with different methods in second damage state
- Figure 6.19 – MDLAC values with different methods in third damage state
- Figure 7.1 – The evaluation view of Tsing Ma Bridge
- Figure 7.2 – Sensor locations on Tsing Ma Bridge from Co-linearity Matrix Method
- Figure 7.3 – Sensor locations on Tsing Ma Bridge for deck at Ma Wan side
- Figure 7.4 – Sensor locations on Tsing Ma Bridge for main deck spines

Chapter 1
Introduction

Section 1.1) Background of structural health monitoring

The structural health monitoring of a structure is an essential process to guarantee that it is in a sound service condition. For simply speaking, the structural health monitoring is to find out the damages on a structure for maintenance. Otherwise, in the most serious cases, a structure loses its function and even collapses without warning, when the small damage develops. The risk to human life would be a serious problem, and the cost of health monitoring of the structure would be much less than the cost of subsequent remedial work. Therefore, health monitoring process for a large scale structure is advisable.

First of all, there are several types of damage that may exist in the structure, which are necessary to find out by all means. These different types of damage include the crack, fatigue and loosening of assembled components, etc. These damages can influence the structural stiffness of the elements, the structural mass and damping, etc. But only the structural stiffness is required for modeled as the damage in the project. For example, while extreme stress residual in an element causes the strain hardening, the structural stiffness of the element increases. However, in this project, the damage is modeled as a reduction of the element stiffness which comes

from crack or loosening of assembled components, because it is beneficial to detect the damages as increasing stiffness basing on eigenvector sensitivity. It is not on the emphasis of this project, and the case with the damage modeled as an increasing element stiffness is excluded from the project. But the change of the stiffness is confined to a small percentage due to the assumption as mentioned later. This percentage change of the stiffness is represented by a reduction of element property of the elastic modulus in this project. It is directly related to the element stiffness.

Section 1.2) Objective of the project

However, a large civil engineering structure consists of a huge sum of components or elements, and a damage identification algorithm for such a structure seems to be difficult with limited number of sensors. A question on how to place the sensors to monitor the structure effectively has to be answered. The effective sensor placement on a large civil structure can be based on sensitivity which is the eigenvector change with respect to damages, as presented by Cobb and Liebst (1997). According to their basic principle, the sensor should be placed on a degree-of-freedom with a large eigenvector change due to damages. However, this degree-of-freedom may not be sensitive to all damage elements, in which the damages would be most likely to occur, and most of the sensors will be localized around some highly sensitive elements. Furthermore, no method on the selection of element for monitoring in the pre-analysis is included in the Co-linearity Matrix Method. The results from this method indicate that the sensor locations are the

same for the same structure, no matter which elements are chosen for monitoring does not coincidence with engineering judgement.

Hence, for the relatively effective sensor placement method, the selection of sensor locations should depend on which elements to be monitored. According to the proposed method, these elements chosen to be included in the analysis are called the interested elements, and the potential damages may highly probably occur in these elements by engineering judgement. Moreover, this selection should also be based on those chosen elements, which are chosen for monitoring, emitting similar damage information. This sensor location therefore enable the collection of reliable damage information from these elements which are then assembled into a consistent element group with respect to this selected sensor location and are called the consistent elements. It means that a selected sensor location can provide the effective monitoring for these elements. The choice of which interested elements are monitored depends on the engineering considerations. In short, the sensor locations from the proposed method will therefore depend on the different components to be monitored.

Section 1.3) Scope of the project

As previously mentioned, the proposed method includes the engineering consideration on the sensor selection, which is different from the general sensor placement methods. The basic algorithms used in the proposed method is then briefly introduced in the following paragraphs. It is based on the sensitivity and

statistical approach to determine the sensor locations. The eigenvector sensitivity is mainly used for the sensor selection and it is defined as the eigenvector change at a degree-of-freedom with respect to a small parameter change in an element. This change can be regarded as a measure of the damage information generated from the element which can be formulated as the summation of the eigenvector sensitivities for the elements at a degree-of-freedom. Basing on the locations collecting the high damage information, these locations are selected as sensor locations. Subsequently, when the degrees-of-freedom are relatively sensitive to the elements and they receive the reliable damage information from the consistent elements basing on the statistical approach, these degrees-of-freedom are finalized as the sensor locations.

The proposed sensor placement problem is also subdivided into two smaller problems. They are element classification and sensor placement method. Firstly, the element classification process eliminates the elements exhibiting small sensitivity or little damage information. They are classified as the undetectable elements. Secondly, the process of sensor placement method determines the optimal sensor locations which are relatively sensitive to the elements. In addition, a particular degree-of-freedom can collect the reliable and similar damage information from the consistent elements, which are selected as a sensor location for effective monitoring of these elements.

After the development of the proposed sensor placement method, its effectiveness is judged basing on the amount of damage information collected from a simulated

structure from using different sensor placement methods. They include Co-linearity Matrix Method (i) and (ii) and Effective Index Method. This damage information can be regarded as the indicator of the effective health monitoring, as the damage information at a sensor location can be represented by the total sum of the eigenvector sensitivity from the elements. When this damage information at a degree-of-freedom is large, it means that this location is sensitive to these corresponding elements and a sensor placing at this location can effectively monitor these elements.

Subsequently, the verification is also based on the accuracy of localizing and quantifying the damages on a simulated structure and a test structure by means of Multiple Damage Location Assurance Criterion (*MDLAC*) with incomplete measured mode shapes at the corresponding sensor locations. And the effectiveness on damage assessment is then compared between the different sensor placement methods. The simulated and tested structures are a three-storey plane steel frame in the computer modeling and a five-storey plane steel frame in the laboratory, respectively. Using the *MDLAC* method on the damage assessment for the test structure, the eigenvector changes at the degrees-of-freedom are required and they can be obtained from the measurement under different damage states. On the other hand, eigenvectors changes under different damage states of the stimulated structure are computed in the program by including the specified damages in the interested elements.

Finally, the application of the proposed method for the real structure, such as the

Tsing Ma Bridge, is performed, the Tsing Ma Bridge is modeled in the computer program by means of the finite element method. The corresponding sensor locations from the proposed method and Co-linearity Matrix Method are evaluated in accordance with this finite element model of the Tsing Ma Bridge. This model of the Tsing Ma Bridge comprises a thousand of one-dimensional beam elements with or without shear effects and cable elements. And they are then compared for verification.

Chapter 2

Literature review

Section 2.1) Development of eigenvalue and eigenvector derivatives

In the early stages, sensitivity analysis found its predominant use in assessing the effect of varying parameters in mathematical models of the system. The applications of the sensitivity analysis are in several fields. They are approximate analysis, the analytical model improvement and the assessment of structural properties. The structural sensitivity analysis has become more than a utility for optimization and is a versatile assessment tool. A survey of different types of derivatives is presented by Adelman and Haftka (1986). The different types of derivatives are the derivatives of static response, such as displacement and stresses, eigenvalues and eigenvectors, transient response and derivatives of optimum designs with respect to problem parameters. In this project, the eigenvalue and eigenvector derivatives are used as a general criteria for the selection of sensor locations.

The eigenvalue and eigenvector derivatives are termed as the sensitivities which mean that the eigenvector at a degree-of-freedom or eigenvalue of a mode change due to the variation of design parameter in an element. This modal parameter change is useful in estimating the analysis of modified designs and in the

automated optimum design of structures under dynamic response restrictions.

The first group of investigators on the eigenvalue and eigenvector derivatives were Fox and Kapoor (1968), that they provided an exact expression for the eigenvalue derivatives and expressed the eigenvector derivatives as a linear combination of eigenvectors for real symmetric eigensystem. However, this expression of eigenvector derivatives was very cumbersome such that the numerical analysis indicate the predominant consumption of the cost and time in the calculation of these derivatives. As a consequence, emerging interest in sensitivity analysis for the eigenvalue and eigenvector derivatives has emphasized efficient computational procedures.

The determination of eigenvalue derivatives was shown by Fox and Kapoor to be a straightforward and simple calculation, but the calculation of eigenvector derivatives was found to be much more complicated. Nelson (1976) then improved the previous work of the sensitivity by Fox and Kapoor to develop a simpl.ed approach of calculation of eigenvector derivatives. This method is based on arbitrary *n-th* order symmetric or non-symmetric eigenvalue system, and it gives an alternate and simplified procedure for calculating eigenvector derivatives. The simplified method of eigenvector derivatives requires only the left-hand-side and right-hand-side eigenvectors and the associated eigenvalue under consideration. Since the characteristic equation of the eigensystem is rank deficient, the (n-1) rank matrix is converted to a full rank matrix by taking out only certain row and column entries of the matrix of the eigenvalues system. This gives a matrix with exactly

the same banded characteristics as the original system. The modified equations, therefore, may be solved by the use of the same banded equation in the eigenvalues system analysis. Therefore, the eigenvector derivative or sensitivity can be derived from his formulation in a simplified and powerful way.

Section 2.2) Development of sensor placement methods

The sensor placement can help to deal with different types of problems, such as the system identification technique, health monitoring and damage assessment. To achieve the different objectives, many criteria on how to place the sensors are developed by many researchers in their own right. For example, the sensor locations can be based on the minimal noise in the data collection. Or the sensor locations receiving linear independence information of the target mode is a common criterion in the sensor placement methods. In addition, the sensitivities of the modal parameters, such as damping ratio, eigenvector and eigenvalue derivatives, are the new criteria to placing the sensors for damage assessment or health monitoring.

The aim of system identification technique is to modify the structural properties in the analytical modeling such that the structural behaviour of the model can compromise the actual structural behaviour. It can make use of the model updating techniques by matching the analytical model with the measurement data. However, the topic of the model updating techniques is beyond the scope of this project. This technique updates the modeling structural properties generally by means of the

measurement data at the sensor locations. These structural properties include the natural frequencies, damping and joint stiffness, etc.. It is therefore important that placing the sensors at the best locations though the automatic process obtains the accurate structural properties for modeling the structure. In a general sense, the best degree-of-freedom means that the measurements at the small number of sensor locations can give the accurate values of the structural properties that can be used to correlate the finite element model to the actual structure.

According to the development by Stabb and Blelloch, the best degrees-of-freedom of the model to be instrumented are evaluated basing on the flexibility shapes to collect adequate information for model identification. The flexibility shapes is originated by Flanigan and Botos (1992).

In addition, Lim (1992) addresses a systematic procedure of placing the sensors to identify modal parameters of the flexible structure. It is employed to select the best locations among the candidate sensor locations, which is called the effective independence approach. In this analysis, the combined information on natural frequencies, mode shapes, and modal damping ratios are considered for the sensor placement.

In the experiment of the parameter identification, the measurement locations chosen have a major influence on the quality of the results. For the simple structures, an experienced engineer is able to make a reasonable selection of locations. However, for more complex structures, the choice of the sensor locations

is often difficult. In this case, the selection of the measurement locations prefer to base on the automatic process, as presented by Penny, Friswell and Garvey (1994). In this paper, two methods of selecting measurement locations are used. One based on Guyan reduction as originally conceived by Guyan (1965) and the other is on the Fisher Information Matrix.

However, the accuracy of measurement is subjected to the sensor noise distributed non-uniformly throughout the structure. The noise can induce inaccuracy in determining the model property from the measurement for any system identification technique. A study of the effect of noise on sensor placement is proposed by Kammer (1992a). In the development of the Effective Index Method by Kammer (1991), a rather restrictive assumption is made concerning the form of the sensor noise statistics. This sensor placement analysis extends this previous works to include a much more general representation of the sensor noise statistics. A criterion is also derived by which the minimum number of sensors required to maintain desired minimum signal-to-noise ratio in the target modal response can be determined.

Furthermore, the error in the system identification is also due to inaccuracy of determining the best locations from the analysis. However, there are few sensor placement methods which consider the effect of model error in the optimal sensor placement problem. This error can be due to incorrect input parameters, incorrect modeling techniques, unmodeled dynamic and small non-linearity. For improving the accuracy of the analytical model, Kammer (1992b) presents the error analysis

basing on his previous works of the Effective Index Method. This analysis provides a lower bound on the number of sensors required to guarantee independent identification of the real target modes. It can be used to correct preliminary analytical models using the correlation between the test and analysis with the model updating techniques.

For another sensor placement problem, health monitoring is an essential process of maintenance to ensure the structure in a sound service condition. An effective monitoring system is necessary for a large civil structure because its continuous operation is essential. However, it has a large number of structural components, and it is impossible to allocate sensors at all degrees-of-freedom of the structure. The question of where to place the sensors for an effective monitoring of the structure has to be answered. This question will be emphasized on and solved in this study.

In the past, the optimal sensor placement problem was solved by positioning the given number of sensors in a structure such that the measured data obtained at those locations is used to fit a specific estimator. Chen and Graba (1985) identified the location of sensors by minimizing the covariance of a location estimator, and this procedure is repeated for different sets of sensor locations. The set of sensor locations yielding the best parameter estimate is the required solution. An ordinary least squares techniques is used to obtain this estimator, and this requires the solution of an optimization and the identification problems simultaneously in general. Thus the optimal locations are estimator dependent, and an exhaustive

search is performed for each specific estimator. Such a procedure suffers from the major drawback of not yielding any physical insight into why certain locations are preferable to others.

To overcome the exhaustive search of optimal sensor locations, Kammer (1991) developed an Effective Index Method as previously stated that is based on a backward elimination approach to minimize covariance of the Fisher Information matrix. It implies that the determinant of Fisher Information matrix is maximal, which represents the independent modal information of mode shapes obtained by the sensors. The corresponding sensor locations must be placed to obtain independent mode shapes information. Details of the mathematical formulation of the Effective Index Method will be mentioned in Chapter 5.

Basing on the development by Kammer, Tasker and Liu (1995) presented a iterative method of using backward elimination and sequential replacement approaches. It applied the covariance trace criterion and a condition number of the Fisher Information matrix as a measure of the effective independence on the optimal sensor locations.

Apart from the criterion of modal information, a sensitivity parameter as a quantitative measure of the eigenvalue and eigenvector derivative is utilized in the sensor placement method as Co-linearity Matrix Method, which is developed by Cobb and Liebst (1997). They defined the sensitivity as the total amount of eigenvalue or eigenvector changes with respect to an element parameter change.

When these total amount of eigenvalue or eigenvector changes are small, those elements that cause little or no change in the measured data are difficult to detect. The eigenstructure will be difficult or impossible to distinguished when damaged. In addition, the correlation of information collected by two sets of sensors is gauged from the sensitivities at two sets of selected locations. When the correlation between two sets of the locations is well matched, these two sets of locations produce similar or identical information. Therefore, the sensor locations are selected basing on independent information on the damaged element, as well as the most sensitivity locations. The basic concept of the Co-linearity Matrix Method is only briefly mentioned, and the details of mathematical formulation will be stated in Chapter 5.

However, some of these sensor placement methods do not provide the procedures for target modes selection to benefit the analysis. Therefore, Kashangaki (1992) proposed a sensitivity parameter as a quantitative measure of the eigenvalue and eigenvector derivatives for the sensor placement problem on damage detection scheme. Also he determines which mode should be used to benefit the damage detection.

When dealing with a complex large civil structure, the sensors are placed only at a limited number of locations due to constraints such as cost and physical accessibility. Therefore, the sensor placement method should maintain its effectiveness as well as the optimal sensor number. And a class of optimal sensor placement methods should include the sensor elimination algorithms. Three

algorithms for the sensor elimination have been developed using different elimination criterion which are the determinant of the Fisher Information matrix, modal assurance criterion and condition number, are compared in the study performed by Yap and Zimmerman (2000). This study pointed out that all three sensor elimination algorithms achieves its own optimal objective better than the others.

Section 2.3) Development of damage assessment

After optimally allocating the sensors on the structure, a problem arises on how to identify the damage configuration using the sensor locations from the sensor placement methods. It is another issue to be continued the most common damage assessment for the structures is visual inspection. This method is costly, time consuming and in many cases difficult to perform due to the inaccessibility to certain parts of the structure. In addition, visual inspection does not give a quantitative value for the remaining strength of the structure. Recently, alternate testing procedures have been employed to assess the integrity of structures by the system identification techniques.

In principle, these techniques are often based on the correlation of modal parameters between measurement and analysis to assess the damages on the structure. Therefore, the system identification techniques for damage assessment can be categorized into several sub-streams basing on different modal parameters, such as natural frequencies or mode shapes. It is expected that the modal

parameters of the structure can provide useful information in determining the location and extent of damage by means of the system identification techniques. If the structure is in a sound condition and there is no measurement error, the measured and analytical modal parameters are in agreement. On the other hand, any change of the structural properties, such as mass, damping and stiffness, due to damage will cause changes in the modal parameters. Therefore, measuring the changes in the modal parameters to assess the damages is a popular approach for the damage assessment.

According to the system identification techniques, the main difficulties in measuring the change of modal parameters for the damage assessment lie in the measurement errors, such as measurement noise. Subjected to this limitation, it has been realized that the measurement locations included in the analysis have a great influence on the accuracy of damage assessment. Therefore, proper measurement locations need to be determined before field measurement so that damage can be detected reliably.

A technique, which is presented by Xia and Hao (2000), selects an optimal set of measurement locations so that the sensors at the corresponding locations measure the change of modal parameters for structural damage assessment with minimal measurement error. A new parameter of damage measurability is therefore introduced basing on the damage sensitivity and the noise sensitivity for minimizing the measurement error. Based on this definition, the measurement locations corresponding to better damage assessment performance with minimal

noise are selected. Since this damage assessment need not to assume prior the locations and extent of the damage, this guarantees the versatility of the method that can be applied to any structure before damage assessment.

Cawley and Adams (1979) proved that the change in the natural frequency of a structure due to damage is a function of the position vector of the damage and the reduction in stiffness caused by damage. Consequently, the ratio of the frequency changes is derived, which can then determine the damage locations. An alternative approach, which computes the changes in the natural frequencies due to damage, makes use of a sensitivity analysis. The basic principles of the method are described by Conraut and Hilbert (1953). The test results show that the proposed method can be used to detect, locate and roughly quantify damage in a structure. Friswell (1994) used a statistical method to reduce the effect of measurement errors and improve the performance of the method proposed by Cawley and Adams.

The damage assessment basing on the modal parameter of natural frequency is a popular trend, because the measurements at only one location on the structure can be used to localize and quantify the damages. The accuracy of the damage assessment is not sensitive to the measurement locations. However, the determination of the natural frequencies of the damaged structure may be difficult for higher modes, as the natural frequencies of different modes are spaced closely. The natural frequency change of a mode may not be accurately measured and determined. Therefore, the measured frequency change does not truely represent the effect of actual damages and this causes the inaccuracy of damage assessment.

Moreover, the change of frequency is not sensitive to the damages such that small severity of damage can not be determined by measuring the natural frequency changes of the structure.

Apart from using the change of natural frequencies for damage assessment, Pandey, Biswas and Samman (1990) present a new parameter called curvature mode shape, which is determined by the analytical finite element method, is investigated as a possible candidate for identifying and locating damage in a structure. The results pointed out that the curvature mode shapes are localized in the region of the damages.

Another approach for detecting the structural damage using the measured mode shapes also attracted much research effort. Allemang and Brown (1983) proposed to use the Modal Assurance Criterion (*MAC*) to detect the damage location. Lieven and Ewins (1988) used the parameter Coordinate Modal Assurance Criterion (*COMAC*) to localize damage site by the correlation of two sets of modes shapes before and after the occurrence of damage in the structure. This method refers to the full mode shapes.

The measurement of mode shapes is heavily contaminated with the measurement noise. However, the structural damage is sensitive to the change of mode shapes. It is beneficial to localize and quantify the damages basing on measuring the mode shapes changes. The effectiveness of damage assessment according to the mode shape changes depends on the measurement locations. Therefore, it is

advantageous for the verification on the effectiveness of health monitoring which is validated by receiving information at the sensor locations from sensor placement method in this project.

However, damage assessment basing on the mode shapes is also subjected to another problem of incomplete measurement. Since the measurement locations in the full finite element model due to physical constraints, the algorithmic approaches to enhance structural health monitoring capability with incomplete measurements are addressed by Zimmerman, Smith, Kim and Bartkowicz (1996). The results indicate that a reduction in the number of sensors reduces health monitoring performance and the damages can only roughly be localized.

Therefore, the effectiveness of damage assessment and health monitoring through the measurement depends on how many sensors are provided. Nevertheless, placing the sensors in the full finite element model is impossible due to the cost constraints and inaccessibility of some degrees-of-freedom of the structure. As a consequence, the algorithms of damage assessment with incomplete measurement or the modal expansion from incomplete measurement to the full finite element model are required to investigate the further development of health monitoring and damage assessment.

The modal expansion, which is also an algorithm to handle the problem of incomplete measurement is often desired to assess the modal response of the full structure at all degrees-of-freedom. The most common and least demanding reason

is for mode shape visualization. Other reasons include correlation of the measurement and analysis results at all degrees-of-freedom of the full finite element model of the structure. The full mode shape is also useful in predicting the response at unmeasured degrees-of-freedom for structural integrity and reliability assessments.

To account for uncertainties in the measurement and prediction, a new expansion technique base on Least Squares Minimization with Quadratic Inequality Constraints (*LSQI*) is proposed by Levine-West and Milman (1995). It has also been shown with actual data that the *LSQI* method is the only expansion method capable of locating the damage elements in a model. This makes the *LSQI* expansion method ideally suited for recursive model updating, damage detection and response prediction technique.

Afterwards, Shi, Law and Zhang (1998) verified that the elemental modal strain energy change ratio, which is sensitive to local damage, can be used as an indicator to locate structural damage sites successfully. An algorithm for quantifying damage extent was also developed based on this energy change.

Another algorithm dealing with the problem of incomplete measurement is required. Shi, Law and Zhang (in press) present a sensitivity based and statistical based method to detect structural damage using incomplete mode shapes. It is an extension of the work by Messina, Jones and Williams (1996). They proposed a Multiple Damage Location Assurance Criterion (*MDLAC*), which is a sensitivity

and statistical approach to locate a single damage in the structure. And Messina, Contursi and Williams (1997) extended this method to multiple damage detection. The damage sites are preliminary localized using incomplete measured mode shapes. The suspected damaged elements will be assessed again using the more accurate measured modal frequency information, and to determine the true sites and the extent of damage. In the following study, basing on Shi, Law and Zhang (1998). Moreover, this damage assessment method is beneficial to compare the effectiveness of health monitoring using the sensor locations from different sensor placement method.

Chapter 3

Basic theory for the sensor placement method

Section 3.1) Assumptions

The following assumptions are used to derive the formulations in this sensor placement method.

I. It is assumed that some rotational degrees-of-freedom are neglected in this sensor placement method. Furthermore, the degrees-of-freedom accessible for placing sensor are restrained to the translational degrees-of-freedom due to practical reasons. Therefore, some degrees-of-freedom, instead of the rotational or the boundary degrees-of-freedom, are included in this analysis and the term accessible degrees-of-freedom will apply in the following sections. This assumption can greatly reduce the computational cost and time.

II. Each considered element in a structure is assumed to have one unit change in its structural parameters with no *a prior* information about the damage configuration. Hence, the weighting on the sensitivities for a specify element is unity for comparison between all elements.

III. The sensors placed at the accessible degrees-of-freedom have the same ability to collect the damage information from each element. This means that the ability of damage detection at each sensor locations is the same.

IV. The contribution of the different vibration modes on the structural properties, such as the sensitivity, is the same under an uncoupled condition due to light damping. It is because each mode is assumed to be uncorrelated with other modes in a set of target mode and the contribution of each mode to the sensitivity would be similar.

V. Without loss of generality, the parameters of the sensitivities properties relating to the elements or degrees-of-freedom are assumed to be formulated linearly under the selected modes. Therefore, a linear model can be applied to estimate the parameter of the structural properties.

VI. For a small damage, the effect of a change of eigenvector with respect to damage in an element can be represented by the first order term of the eigenvector derivative. In the estimation of the physical parameters, the criteria for the sensor placement method are then based on this eigenvector derivative.

VII. In the application of the regression diagnostics techniques, the prediction matrix is applied for the determination of the consistent data points. The Fisher information matrix is then introduced in the parameters estimation.

and this matrix is assumed to be unique for the existence of the solution. Moreover, the component of the Fisher information matrix, such as the sensitivity matrix, should be full rank to provide uniqueness to the solution. Consequently, the number of rows of the sensitivity matrix has to be equal or greater than the number of columns.

VIII. It is assumed that the change of eigenvector with respect to a damage in an element is obtained from the analytical model without errors, and any error, such as the modeling error and measurement error, should be represented by a random error vector in the formulation of the parameter estimation. Furthermore, the random errors are also assumed to be uncorrelated and independent for simplicity.

IX. According to assumptions in the least-squares parameter estimation technique, the mean of the random error vector ε is zero and the random error vector ε has a common variance of $\sigma^2 I$.

Section 3.2) Sensitivity

Section 3.2.1) Derivation of sensitivity by means of Nelson's method

This project is mainly based on the change of eigenvector or mode shape with respect to the elemental parameter change. It is termed the eigenvector derivative or sensitivity, and it is a fundamental parameter representing the damage information emitted from elements or the ability to collect the damage information

at the degrees-of-freedom. The sensitivity derived by Nelson's method (Nelson, 1976) is used in this sensor placement method. The elemental parameter change can refer to any change of the structural properties generally. It can be regarded as a damage. This structural property of the eigenvector derivative is then used in this sensor placement method.

At first, for the purpose of establishing the sensitivity, the free vibrational response of a structural system is assumed to follow the harmonic motion without damping. And the stiffness and mass matrices of the structural system are symmetric. The characteristic equation for this system is then expressed as follows:

$$\begin{aligned} K\hat{\phi}_i - \lambda_i M\hat{\phi}_i &= (K - \lambda_i M)\hat{\phi}_i \\ &= 0 \end{aligned} \tag{3.1}$$

in which $\boldsymbol{K}$ and $\boldsymbol{M}$ are the stiffness and mass matrices of the structure, respectively; λ_i is the eigenvalue and $\hat{\phi}_i$ is the eigenvector for the *i-th* mode.

Taking the transpose of Equation (3.1) and using the property of symmetry matrices, we have Equation (3.2),

$$\begin{aligned} \left[(K - \lambda_i M)\hat{\phi}_i\right]^T &= \hat{\phi}_i^T\left(K^T - \lambda_i M^T\right) \\ &= \hat{\phi}_i^T\left(K - \lambda_i M\right) \\ &= 0 \end{aligned} \tag{3.2}$$

The left-hand-side and right-hand-side eigenvectors are required in Nelson's method to solve the non-symmetric structural system. This kind of eigenvectors satisfies the orthogonality condition in Equation (3.3). For simplicity, without the use of left-hand-side eigenvectors, the mass normalized eigenvectors, which satisfy the orthogonality condition in Equation (3.3), are used in the following analysis. The mass normalized eigenvectors ϕ can be evaluated by Equation (3.4).

$$\phi_i^T M \phi_i = I \quad \text{and} \quad \phi_i^T K \phi_i = \lambda_i \tag{3.3}$$

$$\phi_i = \frac{\hat{\phi}_i}{\sqrt{\hat{\phi}_i^T M \hat{\phi}_i}} \tag{3.4}$$

Taking the derivative of the characteristic equation in Equation (3.1) with respect to the element parameters, and replacing $\hat{\phi}_i$ by a mass normalized eigenvector ϕ_i, we have

$$\frac{\partial}{\partial D}(K - \lambda_i M)\phi_i = 0$$

$$(K - \lambda_i M)\frac{\partial \phi_i}{\partial D} = -\left(\frac{\partial K}{\partial D} - \lambda_i \frac{\partial M}{\partial D} - M\frac{\partial \lambda_i}{\partial D}\right)\phi_i$$

$$= f_i \tag{3.5}$$

Pre-multiplying the mass normalized eigenvectors with ϕ_i^T and substituting the result of Equation (3.2), the eigenvalue derivative can then be solved as follows:

$$\phi_i^T (K - \lambda_i M) \frac{\partial \phi_i}{\partial D} = -\phi_i^T \left(\frac{\partial K}{\partial D} - \lambda_i \frac{\partial M}{\partial D} - M \frac{\partial \lambda_i}{\partial D} \right) \phi_i$$

$$= 0$$

implying that

$$\frac{\partial \lambda_i}{\partial D} = \phi_i^T \frac{\partial K}{\partial D} \phi_i - \lambda_i \phi_i^T \frac{\partial M}{\partial D} \phi_i \tag{3.6}$$

By back substitution of the eigenvalue derivative into Equation (3.5), f_i can be solved and expressed as

$$f_i = -\left[\frac{\partial K}{\partial D} - \lambda_i \frac{\partial M}{\partial D} - \phi_i^T \left(\frac{\partial K}{\partial D} - \lambda_i \frac{\partial M}{\partial D} \right) \phi_i M \right] \phi_i \tag{3.7}$$

Equation (3.7) cannot be solved uniquely for the sensitivity. It is because the characteristic equation as Equation (3.1) is rank deficient and the sensitivity cannot be obtained from Equation (3.5). To overcome this difficulty, the sensitivity is expressed as the sum of the product of the mass normalized eigenvectors and the contribution coefficients for each degree-of-freedom as shown in Equation (3.8)

$$\left\{ \frac{\partial \phi_i}{\partial D} \right\} = \sum_{k=1}^{n} c_k \{\phi_k\} = [\phi]\{c\} \tag{3.8}$$

where n is the number of degree-of-freedom; c is the vector of contribution coefficients of eigenvectors; $\{\}$ and $[]$ represent column vector and two dimensional matrix, respectively.

Substitution of Equation (3.8) into Equation (3.5), and then pre-multiplying with $[\phi^T]$ on both sides and using the orthogonality condition as Equation (3.3), it gives

$$[\phi^T][K-\lambda_i M][\phi]\{c\} = [\phi^T]\{f_i\}$$

$$[(\lambda-\lambda_i)]\{c\} = [\phi^T]\{f_i\}$$

implying that

$$c_k = \frac{[\phi^T]\{f_i\}}{\lambda_k - \lambda_i} \qquad (i \neq k) \qquad (3.9)$$

where c_k is an arbitrary coefficient taken out from the *k-th* row and column entries of the set of characteristic equation.

The solution of the whole sensitivity is then separated into two parts to force the system of equations to have unique solution as shown in Equation (3.10). One part of the eigenvector derivative $\{V_i\}$ is the homogeneous solution of the system as given in Equation (3.8). Another part $c_i\{\phi_i\}$ corresponds to the particular solution due to rank deficiency with the *i-th* term taken out in the characteristic equation. This part can be expressed as a sum of all *n* eigenvectors except for the *i-th* term.

$$\left\{\frac{\partial \phi_i}{\partial D}\right\} = \sum_{k=1}^{n} c_k\{\phi_k\} + c_i\{\phi_i\}$$

$$= \{V_i\} + c_i\{\phi_i\} \qquad (3.10)$$

Taking derivative of the mass normalization orthogonality condition in Equation (3.2)

$$2\phi_i^T M \frac{\partial \phi_i}{\partial D} + \phi_i^T \frac{\partial M}{\partial D} \phi_i = 0 \tag{3.11}$$

By back substitution of Equation (3.10) into Equation (3.11),

$$2\phi_i^T M(V_i + c_i\phi_i) + \phi_i^T \frac{\partial M}{\partial D} \phi_i = 0$$

$$2\phi_i^T MV_i + 2c_i + \phi_i^T \frac{\partial M}{\partial D} \phi_i = 0$$

implying that

$$c_i = -\phi_i^T MV_i - \frac{1}{2}\phi_i^T \frac{\partial M}{\partial D}\phi_i \tag{3.12}$$

The coefficients c_i for the *i-th* degree-of-freedom are then substituted into Equation (3.10) to give the sensitivity with respect to element parameters. These element parameters can be normalized to be the percentage change of the element parameters, such as the stiffness or mass in Equation (3.13). The damage fraction is then taken into account in the formulation of sensitivity.

$$D = p \times property$$

$$dD = property \cdot dp \tag{3.13}$$

where D is the change of element parameter; the *property* are the element parameters or structural properties; p is the percentage change of the element parameter.

The eigenvector derivatives are then modified from Equation (3.10) by multiplying the element parameter and expressed as follows:

$$\left\{\frac{\partial \phi_i}{\partial D}\right\} \times property = (\{V_i\} + c_i\{\phi_i\}) \times property$$

$$\left\{\frac{\partial \phi_i}{\partial p}\right\} = (\{V_i\} + c_i\{\phi_i\}) \times property \tag{3.14}$$

Section 3.2.2) Implication of an eigenvector derivative

The sensitivity is defined as the change of eigenvector at a degree-of-freedom with respect to an element having a structural parameter change. This change can be regarded as a measure of the damage information generated from this element. When the damage information from an element is strong, the damage signal emitted form this element is easily collected by the sensors at these degrees-of-freedom generally. Therefore, the sensitivity is a structural property of a structure and is useful in this sensor placement method.

Section 3.3) Detectability

Section 3.3.1) Element Detectability

The sensitivity can be treated as the amount of damage information emitted from the elements, when they have a unit damage as Assumption II. Therefore, when a damage element can emits strong damage information, this damage element can be easily detected by placing the sensor at the degrees-of-freedom. It is called the detectable element. On the contrary, some damage elements produce much less damage information, and they are called undetectable element.

Actually, sensitivity may be positive and negative. A positive sensitivity value means that when the damage extent in an element increases, the eigenvector at a particular degree-of-freedom also increases. It means the opposite with a negative sensitivity value. However, these changes are all information on the damage element. In rating the effectiveness of each degree-of-freedom in collecting this damage information, their modulus values are used. Therefore, The ability of this damage element detected by the sensors can then be represented by the accumulative effect of the positive sensitivity with respect to each degree-of-freedom.

After the sensitivity at each degree-of-freedom takes up the absolute value, the sensitivities for all the accessible degrees-of-freedom are summed with respect to an element. It is called the Element Detectability under a particular mode. This Element Detectability can be treated as the damage information from an element

collected at the accessible degrees-of-freedom. The Element Detectability for each mode is then expressed as Equation (3.15),

$$\{\hat{x}_j\} = \sum_{i=1}^{l} \alpha_i \left| \frac{\partial \phi_i}{\partial p_j} \right| = \sum_{i=1}^{l} \left| \frac{\partial \phi_i}{\partial p_j} \right| \tag{3.15}$$

where α_i is the weighting factor for *i-th* degree-of-freedom and is equal to unity by the use of Assumption II. It means that the ability of getting the damage information by each sensor is the same; and l is the total number of accessible sensor locations or accessible degrees-of-freedom in a structure; $\hat{x}_j$ is element detectability for the *j-th* element.

Section 3.3.2) Total Detectability

In fact, the damage information collected not only depends on which accessible degrees-of-freedom the sensors are placed, but also on the number of target modes used in the analysis. Thus, the total damage information released from an element is found by summing the Element Detectability against the target modes, which is then called the Total Detectability of the element in the analytical model. The Total Detectability of an element according to the development of Cobb and Liebst (1997), is modified to express as Equation (3.16)

$$\{\bar{Y}_j\} = \sum_{k=1}^{m} \beta_k \hat{x}_{kj} \tag{3.16}$$

where m is the number of target modes; β_t is the modal contribution factor which is the contribution of each target mode to the Total Detectability for the *j-th* element; $\overline{Y}_j$ is the Total Detectability of the element in the analytical model.

The contribution of the different modes in a set of the target modes should be the same due to their uncorrelation property between the target modes. Thus the modal contribution factor for each mode is the same generally, and this contribution factor can be taken as unity for all target modes according to Assumption IV. In conclusion, the effect on the Element Detectability from each mode in a set of the target mode is independent of each other.

A high value of Total Detectability of an element means that there is a large change of the eigenvector or damage information under the target modes collected at the accessible degrees-of-freedom due to a damage in the element. It implies that this damage element can generate large total damage information under the target modes and it can be easily detected by placing sensors at the corresponding degrees-of-freedom.

The amount of damage information emitted from the elements can be measured by the parameter of Total Detectability of the elements. Also it is a measure of the ability of detecting the elements.

Section 3.4) Receptability

Section 3.4.1) Receptability of a degree-of-freedom

The eigenvector at a degree-of-freedom in a structure may be sensitive to the changes of different elements. These eigenvector changes can be interpreted as the damage information collected at a degree-of-freedom. The amount of the damage information received at a degree-of-freedom can then be used for health monitoring by placing a sensor at this degree-of-freedom. The amount of damage information collected is defined as Receptability of a degree-of-freedom. For each mode, it is the summation of the sensitivities or damage information emitted from the elements with respect to a degree-of-freedom as shown in Equation (3.17). The elements herewith refer to the detectable elements of interest. Details of the different types of element will be given later.

$$\{\hat{x}_i\} = \sum_{j=1}^{n} \alpha_j \left| \frac{\partial \phi_i}{\partial p_j} \right| = \sum_{j=1}^{n} \left| \frac{\partial \phi_i}{\partial p_j} \right| \tag{3.17}$$

where α_j is the contribution factor for the *j-th* target element and is equal to unity due to Assumption III; n is the total number of the detectable elements of interest; $\hat{x}_i$ is Receptability of a degree-of-freedom for the elements.

The absolute sign is also taken for the sensitivity at a degree-of-freedom with respect to the elements. A sensor at a degree-of-freedom collects the damage

information from the elements, which is assumed independent to that from sensors at other degrees-of-freedom. And the damage information emitted from one element would not be cancelled by that emitted from another element. Hence, for the Receptability of a degree-of-freedom, the sensitivity or damage information takes up a positive value before summation against the elements.

Section 3.4.2) Total Receptability of a degree-of-freedom

Again, the damage information from the elements received at a degree-of-freedom is different from different vibration modes included in the analysis. When more number of modes is included in the analysis, the damage information from the target elements collected at a degree-of-freedom would be logically large. And placing a sensor at this degree-of-freedom would monitor the elements efficiently. Therefore, the criterion of the sensor placement under the target modes should be based on the damage information collected at a degree-of-freedom. This criterion is termed as the Total Receptability of a degree-of-freedom. It is defined as the Receptability of a degree-of-freedom, which is the damage information or Receptability of a degree-of-freedom summed against the target modes, and it is shown as Equation (3.18).

$$\{\bar{Y}_i\} = \sum_{k=1}^{m} \beta_k \hat{x}_{ki} \tag{3.18}$$

where m is the number of the target modes; β_k is the modal contribution factor of *k-th* target mode on the damage information collecting at the *i-th* degree-of-freedom; $\overline{Y}_i$ is the Total Receptability of the *i-th* degree-of-freedom in the analytical model.

Similarly, the contribution of the different modes in a set of the target modes is the same due to Assumption IV. In conclusion, the effect of vibration mode on the Receptability of a degree-of-freedom is independent to each other.

The Total Receptability of the degree-of-freedom is a helpful criterion for sensor placement, because the amount of damage information on the elements collected at a degree-of-freedom can be judged from the value of the Total Receptability. If the Total Receptability of a degree-of-freedom for the elements is large, then there is a large amount of damage information emitted from the elements and collected at the corresponding degree-of-freedom. Thus, it indicates that this degree-of-freedom is a good sensor location to monitor these elements.

Section 3.4.3) Consistent element

Section 3.4.3.1) Inconsistent Total Detectability

As mentioned previously, the Total Receptability of a degree-of-freedom is a basic criterion for the sensor placement. A high value of the Total Receptability of a degree-of-freedom may be due to two reasons. One reason is that the damage information emitted from many damage elements is large. The second reason is

that the damage information released from a few of the damage elements is very large so that the damage information obtained at a degree-of-freedom dominates over those from other elements. This case is more common in practice for a large civil structure.

In the second case, although the Total Receptability of the degree-of-freedom is large, damage information emitted from some elements cannot be detected by a sensor placing at this degree-of-freedom. It is because the damage information from a few of the damage elements dominate over the other elements. Thus, this degree-of-freedom is only effective to detect a few of the damage element emitting dominating information, even when the Total Receptability of this degree-of-freedom is large.

This is a constraint on the application of the Total Receptability for the sensor placement method. A high value of the Total Receptability of a degree-of-freedom may not mean that placing a sensor at this degree-of-freedom can collect adequate damage information for monitoring all elements in a structure as previously explained. Therefore, the concept of consistent element should be applied on the basic criterion of the Total Receptability for selecting the sensor locations, so that this criterion would be more reliable to provide the complementary information on which damage elements contribute more damage information to the corresponding degree-of-freedom.

Section 3.4.3.2) Consistent element grouping

The consistent elements refer to a group of elements in which the ability of detecting damage in these elements are similar by placing a sensor at a degree-of-freedom. In other words, damage information emitted from the consistent elements is similar. A high value of the Receptability or Total Receptability of a degree-of-freedom for the consistent elements implies that these consistent elements can be monitoring effectively by placing a sensor at this degree-of-freedom. Therefore, placing a sensor at this degree-of-freedom would be more reliable to detect damages in the corresponding consistent elements.

Judging from another point of view, when the elements in a structure are inconsistent, and the Receptability or Total Receptability of a degree-of-freedom is large for these elements. Some damage in these elements may not be detected by a sensor at the corresponding degree-of-freedom. It is because a degree-of-freedom may not be sensitive to the damages in the inconsistent elements, as these damages have no dominating effect on this degree-of-freedom. Therefore, when the Receptability or Total Receptability of a degree-of-freedom is large, it does not imply that any damage element in the structure can be detected by a sensor at this degree-of-freedom. And this consistent element grouping can provide a reliability check or complementary information to the criterion of the sensor placement, such as the Receptability or Total Receptability.

Section 3.5) Linear model analysis

Section 3.5.1) Linear model on Total Detectability or Total Receptability

The Total Detectability or Total Receptability in the real model can be represented by a linear model after introducing a modeling error as shown in Equation (3.19) due to Assumption VI. This formulation is more realistic than the Total Detectability or Total Receptability of the analytical model shown in Equation (3.16) or Equation (3.18), respectively, as the modeling error included in these parameters can accurately represent the actual situation.

$$\{Y\} = [X]\{\beta\} + \{\varepsilon\} \tag{3.19}$$

in which Y is the column vector of the Total Detectability or Total Receptability in the real model; X is termed the sensitivity matrix, in the analytical model or finite element model of dimension $n \times m$; n is the element number or number of the accessible degrees-of-freedom; m is the number of target modes; β is the modal contribution vector of the target modes and ε is modelling error between the real model and the analytical model.

The error ε may be partially eliminated by model updating method, but it is difficult to obtain the parameters of the system from experiment. And the measurement error may then be introduced, as long as an experiment is conducted. Moreover, the Total Detectability or Total Receptability depend on the damage configuration on the structure, but this is absent with no *prior* information before

the analysis. Therefore, it is impossible to estimate the Total Detectability or Total Receptability of the real structure. For these parameters estimation, Total Detectability and total Receptability are taken as the simple summation of the damage information from the elements to estimate the ability of the elements being detected or the efficiency of the degree-of-freedom to monitor the elements, respectively.

In the linear model, the Total Detectability or Total Receptability can have different terms with similar meaning. And it is clearer to summarize the different terms first. The Total Detectability or Total Receptability Y formulated in Equation (3.16) or Equation (3.18) is in the analytical model. However, in the real model, there must be a random modelling error included in the formulation of the Y as Equation (3.19). Likewise, the Y in Equation (3.19) is in the original system after the introduction of measurement errors. afterwards, this Y is transformed into the estimation system in which the random error is minimized. The Total Detectability or total Receptability in the estimation system is called the best fit Total Detectability or Total Receptability $\hat{Y}$.

Section 3.5.2) Estimation of the best fit Total Detectability or Total Receptability

The Total Detectability and Total Receptability are expressed in the original system as Equations (3.16) and (3.18). The Total Detectability and Total Receptability are formulated as linear models passing though the origin.

However, the Total Detectability or Total Receptability in the original system contains error and cannot predict the structural properties about the damage configuration realistically. For the parameter estimation, the least-squares estimation is used to minimize the random error of the Total Detectability or Total Receptability as shown in Equation (3.20). This best fit Total Detectability or Total Receptability $\hat{Y}$ in the estimation system can reproduce the real situation more precisely, such that these parameters are more reliable for sensor placement.

$$\hat{Y} = Xb \tag{3.20}$$

where $\hat{Y}$ is the column vector of the best fit Total Detectability or Total Receptability in the estimation system obtained by least-squares estimation technique; X is sensitivity matrix of dimension $n \times l$; n and l are the number of the elements and the accessible degrees-of-freedom, respectively; b is an unbiased estimator for the transformation into the estimation system and is a column vector of dimension equal to the mode number.

According to the least-squares estimation technique, the Total Detectability or Total Receptability in the original and estimation systems have the following properties. The Y in the original system and $\hat{Y}$ in the estimated system are required to have a common covariance matrix $\sigma^2 I$ and their variances are constant and are assumed to be unity. The best fit Total Detectability or Total Receptability $\hat{Y}$ has a

mean $X\beta$. In addition, the random modelling vector ε has its mean equals zero and it also has a common variance $\sigma^2 I$.

In the Total Detectability or Total Receptability, Y and $\hat{Y}$ in the original and estimated system, respectively, have a relationship as shown in Equation (3.21).

$$\{Y\} = \{\hat{Y}\} + \{e\} \tag{3.21}$$

where Y and $\hat{Y}$ are the Total Detectability or Total Receptability in the original system and estimation system, respectively; e is the residual vector which reflects the lack of agreement between the original system and the estimation system.

However, the Total Detectability or Total Receptability can not be measured in the experiment but these predict the structural properties with a specific damage configuration. Since the damage configuration is unknown in the preliminary stage, it is impossible to predict the structural properties accurately with no *a prior* knowledge about the damage. Therefore, the best fit Total Detectability or Total Receptability is still an estimation in the least squares sense.

Section 3.5.3) Covariance matrix of unbiased estimator

Another parameter estimation is based on the minimum covariance matrix. According to the requirement of least-squares estimation technique, the unbiased

estimator for elements or degrees-of-freedom is indicated as Equation (3.22). It is an optimal condition for the estimator b, and it provides a minimization of the sum of residual under unconstrained condition.

$$b = [X^T X]^{-1} X^T Y \tag{3.22}$$

where b is the linear unbiased estimator.

For an efficient unbiased estimator, the covariance matrix would be as minimal as possible. A better estimation for the Total Detectability or Total Receptability is then provided.

$$\begin{aligned} P &= E\left[(\beta - b)(\beta - b)^T\right] \\ &= \sigma^2\left[X^T X\right]^{-1} \\ &= \left[X^T X\right]^{-1} \end{aligned} \tag{3.23}$$

where $E[\bullet]$ is the expectation value; b is the best unbiased estimator as Equation (3.22); β is the modal contribution vector; σ^2 is the variance of the error vector and is assumed to be unity; $\boldsymbol{P}$ is the inverse of the Fisher Information matrix or the covariance matrix.

Section 3.5.4) Use of prediction matrix

A prediction matrix can be established after the covariance matrix of the estimator is obtained. The use of prediction matrix is mainly for the consistency check on the elements, and therefore only the parameter of Detectability is used in the following formulation.

By back substituting Equation (3.22) into Equation (3.20), the best fit Total Detectability in the estimation system can be expressed as Equation (3.25).

$$\begin{aligned}\hat{Y} &= X\left[X^T X\right]^{-1} X^T Y \\ &= HY\end{aligned} \tag{3.25}$$

in which $\boldsymbol{H}$ is the prediction matrix and it can also be expressed as Equation (3.26).

$$\begin{aligned}H &= X\left[X^T X\right]^{-1} X^T \\ &= XPX^T\end{aligned} \tag{3.26}$$

where $\boldsymbol{P}$ is the inverse of Fisher Information matrix; $\boldsymbol{H}$ is the prediction matrix which is a symmetric and an idempotent matrix; $\hat{Y}$ is called the best fit Total Detectability, and the prediction matrix $\boldsymbol{H}$ maps Y into the estimation plane to become $\hat{Y}$. Thus, prediction matrix $\boldsymbol{H}$ may also be called the transformation matrix. However, the best fit Total Detectability $\hat{Y}$ cannot be evaluated as the Total Detectability Y is absent in the analysis.

The idempotent matrix has a properties of having its rank($\boldsymbol{H}$) equal to its trace($\boldsymbol{H}$). Moreover, the diagonal elements in the prediction matrix $\boldsymbol{H}$ must be positive and each diagonal element h_{ii} in the prediction matrix $\boldsymbol{H}$ is bounded by zero and one, such that $0 \le h_{ii} \le 1$. These properties are useful in the following analysis.

Moreover, according to the work of Chatterjee and Hadi (1988), the diagonal element h_{ii} in the prediction matrix $\boldsymbol{H}$ can be interpreted as the amount of leverage of *i-th* element. Or the diagonal element h_{ii} is the measure of leverage, which is the standardized measure of the distance between the Element Detectability and the centroid of the group of Element Detectabilities. And the actual value of Y is disregarded in this process.

Because of its interpretation, the diagonal terms h_{ii} in the prediction matrix $\boldsymbol{H}$ can be formulated as Equation (3.27) as stated in Rao and Toutenburg (1995). It is simplified in Equation (3.28). The consistency of the *i-th* element in an element group is then determined by Equation (3.27) or Equation (3.28), which is based on the corresponding Element Detectability. The amount of leverage is useful to determine the consistency of an element with respect to one or all degrees-of-freedom.

$$h_{ii} = \frac{\left(\sum_{j=1}^{l} \left| \frac{\partial \phi_j}{\partial p_i} \right| - E\left(\sum_{j=1}^{l} \left| \frac{\partial \phi_j}{\partial p_i} \right| \right) \right)^2}{\sum_{i=1}^{n} \left(\sum_{j=1}^{l} \left| \frac{\partial \phi_j}{\partial p_i} \right| - E\left(\sum_{j=1}^{l} \left| \frac{\partial \phi_j}{\partial p_i} \right| \right) \right)^2} \qquad (3.27)$$

$$h_{ii} = \frac{(\hat{x}_i - E(\hat{x}_i))^2}{\sum_{i=1}^{n} (\hat{x}_i - E(\hat{x}_i))^2} \tag{3.28}$$

where h_{ii} is the diagonal elements in the prediction matrix; $\hat{x}_i$ is Element Detectability; $E[\bullet]$ is expectation value; n and l are the number of the element and the number of the accessible degrees-of-freedom, respectively.

However, if the consistent elements are determined with respect to all accessible degrees-of-freedom, the consistent elements are referred to sensors on all accessible degrees-of-freedom. Obviously, it is impossible to place sensors on degree-of-freedom in a large civil structure. And the corresponding consistent elements are therefore meaningless. As l equals to one, the consistent element group is based on the damage information collecting by a sensor. It is more reasonable to evaluate the consistent element group for each degree-of-freedom, and determination of consistent elements is based on sensitivity. Hence, the determination of consistent elements depend on the sensor locations.

Section 3.6) Consistency check for elements

Section 3.6.1) Principle of determination of consistent elements

The check of consistent elements can overcome the limitation of the parameter of Total Receptability and make this parameter more reliable as previously

mentioned. The principle of consistent elements can then be demonstrated in the following paragraphs.

Figure 3.1 shows a simple example under one target mode for illustration. When there are m target modes included in the analysis, there will be m independent variables. And the regression line is replaced by m-dimensional regression space. Each element, which is represented by a black spot or data point in Figure 3.1, has its structural properties of the sensitivity X with respect to a degree-of-freedom and the Total Detectability Y under the target modes. Different elements have different properties, so the black spots are scattered. The regression line indicates a possible relationship between the sensitivity and Total Detectability of the system. Total Detectability of the system can then be estimated by using this relationship.

According to Figure 3.1, some data points are concentrated within a finite region as enclosed within a boundary. And some data points are scattered far away from the remaining elements. The structural property of these far away data points or elements are inconsistent with the remaining elements. These inconsistent elements emit extremely large or small damage information that is collected at a degree-of-freedom. It results in the unreliability in the criteria of Total Receptability to determine the ability of collecting damage information.

The principle of determination of consistent elements is to segregate the inconsistent elements from the remaining elements. And these inconsistent elements are to be eliminated from the remaining element group, until the

remaining elements become more consistent as required. The determination of consistent elements is based on the amount of leverage, as well as on the prediction matrix.

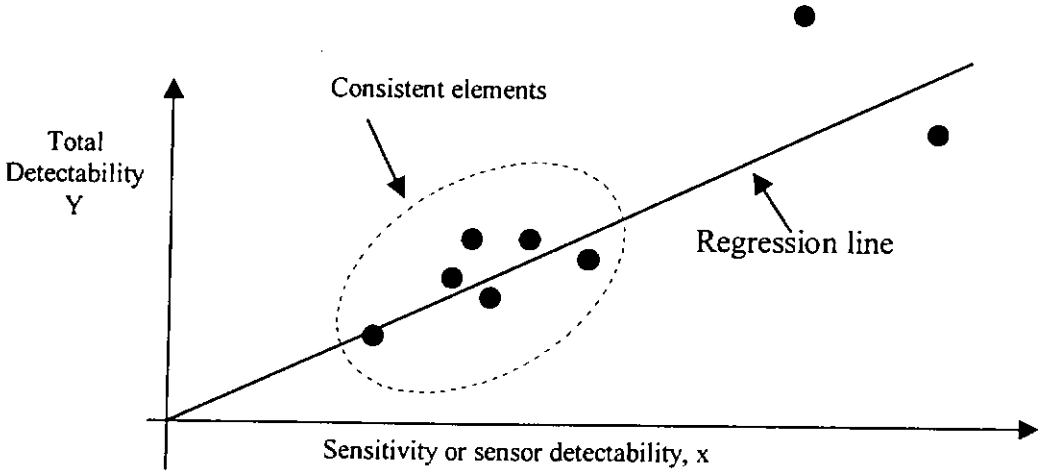

Figure 3.1 – Distribution of sensitivities in the linear model

Section 3.6.3) Criterion for determination of consistent elements

As previously mentioned, the consistency of the elements are based on sensitivity at a degree-of-freedom. Consistent elements are then determined by means of the damage information collected by a sensor at this degree-of-freedom.

The inconsistency of elements can be classified by the diagonal terms h_{ii} in the prediction matrix $\boldsymbol{H}$ given by Equation (3.27). Provided that a value of h_{ii} is larger than a certain threshold value, this corresponding *i-th* element is then classified as an inconsistent element. This threshold value is called the leverage point. It is because a large value of h_{ii} reflects that the data point of the *i-th* element is far

away from the centroid or the mean value of the remaining elements. Otherwise, the corresponding element is consistent.

Therefore, it is essential to establish a suitable threshold value or leverage point to determine the consistent elements. The value of this criterion should be based on the average value of the diagonal elements h_{ii} multiplying with a factor. The average value is equal to the summation of all diagonal elements h_{ii} divided by the total number of elements (Hoaglin, and Welsch, 1978). The total number of the diagonal elements h_{ii} is equal to the trace of the prediction matrix $\boldsymbol{H}$. And the trace of prediction matrix $\boldsymbol{H}$ is equal to the rank of the prediction matrix $\boldsymbol{H}$ due to the properties of idempotent matrix. As a result, the average value of the diagonal elements h_{ii} is the same as the rank of the prediction matrix over the total number of elements as shown in Equation (3.29). Moreover, the rank of the prediction matrix $\boldsymbol{H}$ is equal to the mode number in this study.

$$average \quad value = \frac{\sum_{i=1}^{n} h_{ii}}{n} = \frac{m}{n} \tag{3.29}$$

where m and n are the number of target modes and elements, respectively.

According to Belsley, et al. (1980), *2m/n* is taken as the required leverage point value to identify the potential consistency for all elements. When the *i-th* element is identified as inconsistent with the other remaining elements, the *i-th* element is

eliminated from the element group. The process is repeated until all elements in this group are consistent or no further elements are classified as inconsistent elements. The procedure or formulation of the determination on consistent elements is discussed in Chapter 4 in details.

The multiplying factor can control the amount of leverage point. Therefore, the multiplying factor will be adjusted to suit for different situations and requirements. When the structural property of the elements in a structure is very similar and higher consistency of the elements is required, the threshold value of the leverage point is reduced. On the contrary, when the property of the structural components is very varying, the threshold value should be larger to include more elements due to the limitation of Assumption VII. The value of leverage point should be about the average value as given in Equation (3.29).

Chapter 4

Methodology for the sensor placement method

Section 4.1) Introduction of proposed sensor placement method

The principle of the proposed sensor placement method is to select the sensor locations such that the interested elements are monitored relatively efficiently. It is necessary to maximize the damage information collected at a selected sensor location for damage in a set of interested elements. A set of target modes is included in the method, and the more sensitive sensor locations under the assumed damage configurations of the structure will be selected. The assumed damage configuration would include all interested elements which are to identify structural significant at the design stage.

The main components in the proposed method are shown in Figure 4.1. This method is mainly divided into two parts, which are the damage element classification and the sensor placement method. Damage element classification consists of the target mode identification process and damage element classification. The sensor placement method is subdivided into three parts. The first one is to maximize the Total Receptability relative from the analyzed elements, which are termed sensor placement ratio. The second one is minimization of the sensor number with the nearly same damage information

collection efficiency. The third one is consistency check on the analyzed elements to form consistent element group for each sensor locations. The details will be discussed in the later.

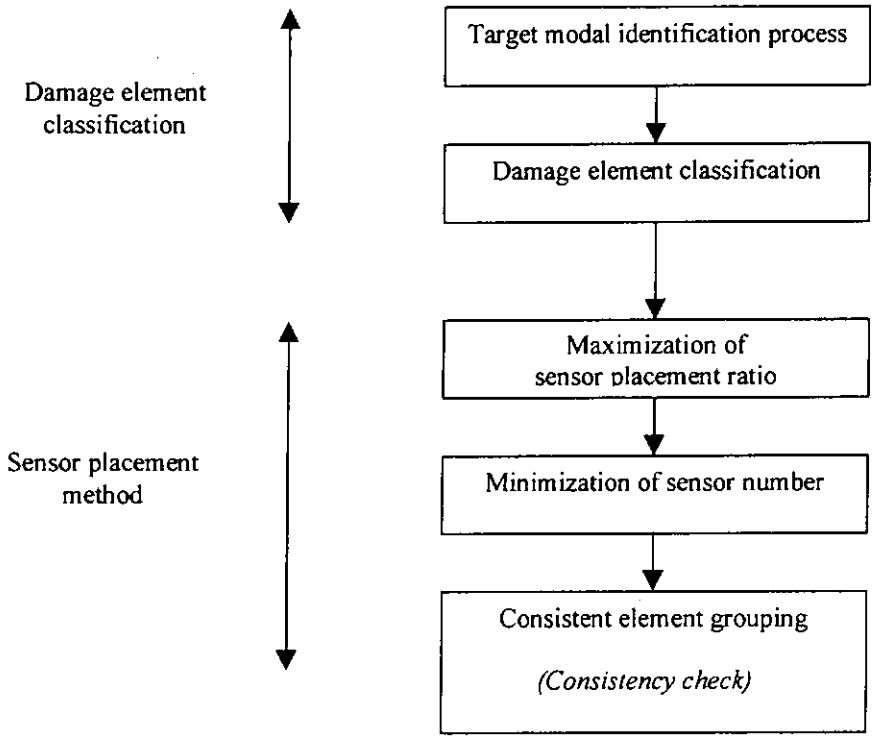

Figure 4.1 – Procedures of proposed sensor placement method

Section 4.2) Damage element classification

Section 4.2.1) Target mode identification process

According to the objective of this project, the basic aim of the target modes selection for the analysis is to increase the amount of damage information collected by the sensors, and emitted from the interested elements. The eigenvectors at the sensor locations under these target modes will then be relatively sensitive to the interested elements. The amount of damage information collected at the accessible

degrees-of-freedom can be measured by the magnitude of Element Detectability as the damage information, when the parameter of Total Detectability is not available at this stage. The target mode identification process is to maximize the Element Detectability from the interested elements relative to all elements. A Modal Criterion for target mode selection is then established, as the ratio of Element Detectability of the interested elements and that of all elements, which is expressed as Equation (4.1).

$$\text{Modal Criterion} = \left(\frac{\sum_{j=1}^{q} \sum_{i=1}^{l} \left| \frac{\partial \phi_i}{\partial p_j} \right|}{\sum_{k=1}^{n} \sum_{i=1}^{l} \left| \frac{\partial \phi_i}{\partial p_k} \right|} \right)_m \tag{4.1}$$

where $\sum_{k=1}^{n} \sum_{i=1}^{l} \left| \frac{\partial \phi_i}{\partial p_k} \right|$ is the summation of Element Detectability of all elements for each mode; and $\sum_{j=1}^{q} \sum_{i=1}^{l} \left| \frac{\partial \phi_i}{\partial p_j} \right|$ is the summation of Element Detectability of the interested elements for each mode; n and q are the element number of total elements and the interested elements, respectively; l is the number of the accessible degrees-of-freedom; m is the number of each mode considered in the analysis.

When the damage information under a particular mode emitted from the interested elements that is collected at the accessible locations is negligible, this mode is excluded from this analysis. And the Modal Criterion for this mode approaches zero. It implies that the corresponding mode does not contain sufficient damage

information emitted from the interested elements and collected at accessible degrees-of-freedom. When this criterion for a mode approaches unity, the information from this mode is adequate from the interested element. It is beneficial to be collected by the sensors. The Modal Criterion takes up limiting values of zero and unity. When the Modal Criterion of a mode is larger than a threshold value, this mode is selected as the target mode.

This threshold value is a dimensionless ratio, which depends on the type of structure and the number of interested element. In practice, the number of target mode is kept as a maximum. Therefore, the threshold value is more important to be set so as to retain as many numbers of modes as possible. Therefore, the threshold value is dependent of the required mode number, and it is determined basing on the type of selection and the number of interested elements.

Section 4.2.2) Damage element classification

According to Assumption II, all elements are assumed to have a unit damage in order to compare how much damage information would be emitted from the elements. The elements in a structure can be classified into two element groups in this analysis basing on the emission of damage information from the elements. They are detectable and undetectable elements. Basing on eigenvector sensitivity, the detectable elements are defined as these elements causing large eigenvectors changes at many degrees-of-freedom, when the damages occur in these elements or vice versa. Unfortunately, it is difficult to assess the damage in these undetectable

elements by using the eigenvector sensitivity, because any structural change occurred in the undetectable elements cause very little eigenvector change at any degrees-of-freedom of the structure. Therefore, no or less damage information from the undetectable elements will be collected at the accessible degrees-of-freedom. In view of the insensitive eigenvector changes due to the damage element, these elements should be excluded from the following analysis. These undetectable elements are most unlikely to be monitored by placing sensors at any accessible location of the structure. Exclusion of the undetectable elements is beneficial to reduce the computational effort and time in the analysis.

The classification of element into different groups is mainly based on the property of Total Detectability. When the Total Detectability of an element is larger than a threshold value, it is classified as detectable element which emits sufficient information about its damage. This threshold value is equal to the fraction of the maximum Total Detectability of elements under study.

In the process of damage element classification, it is essential to emphasize on which elements are valuable to the following sensor placement method. Hence those interested elements that are detectable elements, are called the analyzed elements. On the other hand, the elements which are not of interest but detectable, are called the non-analyzed elements.

Section 4.3) Sensor placement method

Section 4.3.1) Criterion of sensor placement ratio

As previously mentioned, the damage information from the considered elements collected at a degree-of-freedom can be represented by the Total Receptability. And each considered element is assumed to have unity damage according to Assumption II. There are different groups of the analyzed elements and the non-analyzed elements. The sensors have to be placed in locations such that they can collect the damage information emitted from the analyzed elements more efficiently than that from the non-analyzed elements. This requirement can be represented by a ratio of the Total Receptability between the analyzed and the non-analyzed elements with respect to each degree-of-freedom. It is called sensor placement ratio as given in Equation (4.4). The selection of sensor location is then based on the sensor placement ratio.

$$R_i = \sum_{ii=1}^{m} \left[\frac{\left(\sum_{k=1}^{r} \left| \frac{\partial \phi_i}{\partial p_k} \right| \times \beta_{ii} \right)^2}{\sum_{j=1}^{s} \left| \frac{\partial \phi_i}{\partial p_j} \right| \times \beta_{ii}} \times \frac{s}{r^2} \right] \tag{4.4}$$

in which R_i is the sensor placement ratio at a degree-of-freedom; r and s are element number of the group of analyzed elements and the group of non-analyzed elements, respectively; m is the number of the target mode in the analysis; β is modal contribution factor, which is assumed to be unity according to Assumption

IV; $\sum_{ii=1}^{m}\sum_{k=1}^{r}\left|\frac{\partial \phi_i}{\partial p_k}\right| \times \beta_{ii}$ and $\sum_{ii=1}^{m}\sum_{j=1}^{s}\left|\frac{\partial \phi_i}{\partial p_j}\right| \times \beta_{ii}$ are the Total Receptability at the *i-th* degree-of-freedom for the analyzed and the non-analyzed elements, respectively.

This ratio compares the damage information collected at a degree-of-freedom, and emitted from the analyzed elements with that from the non-analyzed elements. When this ratio is large, the damage information from the analyzed elements is generally larger than those from the non-analyzed elements received at the corresponding degree-of-freedom. Therefore, it is beneficial to allocate a sensor at this degree-of-freedom to monitor the analyzed elements effectively.

Average Total Receptability for the element groups is used to eliminate the effect of group size as shown in Equation (4.4). Consequently, the sensor placement ratio at the degree-of-freedom is independent of the size of the group, and is more reasonable to indicate the sensor effectiveness of collecting damage information from the analyzed element group.

The average Total Receptability at a degree-of-freedom from the analyzed elements in Equation (4.4) is squared. It is because the selection of sensor locations by a simple ratio may result in a degree-of-freedom by which the less damage information is collected from analyzed elements, with yet much lesser amount of information collected from the non-analyzed elements. Then the simple sensor placement ratio with respect to this degree-of-freedom as sensor location is large, but this degree-of-freedom is actually insensitive to both types of elements.

Therefore, the average Total Receptability from the analyzed elements is squared to amplify the damage information from the analyzed elements.

Section 4.3.2) Threshold value of sensor placement ratio

When the sensor placement ratio at a degree-of-freedom is larger than a threshold value, the corresponding degree-of-freedom is selected as the sensor location. This threshold value is again set as a fraction of the maximum sensor placement ratio of a set of degrees-of-freedom under study. The threshold value can be adjusted basing on the different types of structure.

When the sensor placement ratio at the *i-th* degree-of-freedom is greater than unity for each mode, the damage monitoring on the analyzed elements by placing a sensor at this degree-of-freedom is relatively effective.

Section 4.4) Minimization of the sensor number

Section 4.4.1) Limitation of sensor number

When the number of sensor location increases, the damage information collected at the sensor locations will be more sufficient naturally. However, the number of sensor location is limited in practice. Therefore, it is necessary to reduce the number of sensor location and yet maintain the efficiency of monitoring on the analyzed elements.

Section 4.4.2) Criterion on minimizing the sensor number

The criterion on minimizing the sensor number can be measured by the loss of the collected damage information after a sensor is deleted. When the loss of damage information is minimal due to elimination of a sensor in a candidate set. The total damage information collected by the remaining sensors will remain as maximal as possible, and this implies the remaining sensors can maintain the monitoring of the analyzed elements effectively.

Section 4.4.3) Formulation of sensor elimination process

The determinant of Fisher Information matrix is commonly used to quantify the collected information. According to the work presented by (Kammer, D.C., 1991), the determinant of the Fisher Information matrix is equivalent to the modal information of mode shape collected at the degrees-of-freedom of the selected sensor locations. On the other hand, in the proposed method the modal matrix is replaced by the sensitivity matrix under the same target modes to form the Fisher Information matrix. It should be noted that the sensitivities in the sensitivity matrix with respect to the degrees-of-freedom are summed for the analyzed elements only. Therefore, the determinant of the Fisher Information matrix represents the damage information emitted from the analyzed elements, such as $\left|X^T X\right|$. And then the collected damage information due to deletion of the *i-th* sensor can be represented by $\left|X^T(i)X(i)\right|$. The collected information by the *i-th* sensor is denoted by $x_i^T x_i$.

The loss of damage information due to elimination of an *i-th* sensor can be formulated as Equation (4.5).

Using the partition theorem stated in (Rao, and Toutenburg, 1995) and the properties of the prediction matrix, a more convenient form to represent the loss of damage information after elimination of an *i-th* sensor can be obtained as Equation (4.6). This form is used to determine which sensor at a degree-of-freedom collects the least damage information emitted from the analyzed elements.

$$\left|X^T(i)X(i)\right| = \left|X^TX - x_i^Tx_i\right| \tag{4.5}$$

$$\begin{aligned}\left|X^T(i)X(i)\right| &= \left|X^TX\right|(1 - x_i[X^TX]^{-1}x_i^T) \\ &= \left|X^TX\right|(1-h_{ii})\end{aligned} \tag{4.6}$$

where $x_i[X^TX]^{-1}x_i^T = h_{ii}$ by using the properties of prediction matrix $\boldsymbol{H}$ of dimension $l \times l$; and h_{ii} is the *i-th* diagonal element in the prediction matrix $\boldsymbol{H}$; $\boldsymbol{X}$ is sensitivity matrix of dimension $l \times m$; l and m are the number of accessible degree-of-freedom and target mode; $\left|X^TX\right|$ is the damage information emitted from the analyzed elements before the sensor elimination; $\boldsymbol{X(i)}$ is sensitivity matrix without the corresponding *i-th* row of dimension $(l\text{-}1) \times m$; $\left|X^T(i)X(i)\right|$ is the damage information collected by the remaining sensors; x_i is the *i-th* row of the sensitivity matrix $\boldsymbol{X}$ with $x_i^Tx_i$ representing the damage information collected at the *i-th* degree-of-freedom.

Section 4.4.4) Criterion of the least loss of damage information

The amount of the collected damage information at *i-th* degree-of-freedom can be related to the corresponding diagonal element h_{ii} in the prediction matrix as shown in Equation (4.6). (1-h_{ii}) can be regarded as a fraction loss of damage information $\left|X^T X\right|$ retained due to an *i-th* sensor elimination. If the value of h_{ii} is small, then the fraction is close to unity. It means that the loss of damage information due to deletion of the *i-th* sensor is the least. Therefore, it should eliminate a sensor at a degree-of-freedom collecting the least damage information, the damage information collected by the remaining sensors $\left|X^T(i)X(i)\right|$ can be maintained as maximal.

Consequently, the criterion for the sensor elimination can be based on the least value of the diagonal elements h_{ii} in each cycle. In other words, the magnitude of diagonal element h_{ii} can be interpreted as the amount of damage information collected by the *i-th* sensor in the remaining sensors.

It should be noted that the loss of collected damage information becomes significant, after a certain large number of sensors are deleted from the candidate set. The decreasing curve of collected damage information due to sensor elimination is expected to be descending gently at the beginning of this process. However, when the number of remaining sensor reaches a critical number, the decreasing curve goes down rapidly. For example, the h_{ii} value increases to be just

below a critical value after a few cycles of the sensor elimination process. The sensor elimination process should be terminated. The critical value should depend on the particular h_{ii} value. Therefore, the optimal sensor number is maintained as minimal as possible, before this h_{ii} value for the remaining sensors in corresponding sensor elimination cycle reaches the critical value. As a result, the adequate damage information emitted from the interested elements can be maintained. The critical value for the minimal sensor number should be on further study.

Since the above criterion for sensor number minimization is based on the least loss of damage information, the effects of linear independence on selection of sensors is neglected in the proposed method. Therefore, the sensors will be placed symmetrically on the structure and the damage information collected by the corresponding sensors lacks of linear independence. For example, for two symmetrical interested element groups, the sensor locations with respect to these two Target Groups may be different by receiving the same or symmetric damage information.

Section 4.4.5) Procedures of the sensor deletion process

The minimization of the sensor number is a backward elimination process basing on the criterion of least loss of the damage information as represented by the smallest diagonal element h_{ii} in the prediction matrix. The number of available sensor is known given in practice. The degrees-of-freedom having the least value

of the diagonal element h_{ii} is eliminated. A new prediction matrix is evaluated by the inversion matrix lemma as stated in (Chatterjee, and Hadi, 1988). This process is repeated, until the number of remaining sensor locations is slightly greater than the number of available sensors, since further reduction of sensors will be conducted in the consistency check for the elements. However, the minimum sensor number remained in a group must be greater than or equal to the number of target modes due to Assumption VII.

Section 4.5) Consistency check

Section 4.5.1) Introduction of consistent elements grouping

As previously mentioned, the high value of Total Receptability of a degree-of-freedom may not imply that this degree-of-freedom is sensitive to all damage elements. The following consistent element grouping will provide the additional information that a particular degree-of-freedom collects approximately the same damage information from the elements with a reliable measure. These elements are called consistent elements with respect to this degree-of-freedom. Different degrees-of-freedom have different consistent element groups, and these consistent elements refer to the analyzed elements. Therefore, when the Total Receptability of degree-of-freedom is large, this degree-of-freedom is sensitive to these consistent elements. A sensor can be then allocated on an optimal location to monitor the corresponding consistent element group effectively.

Section 4.5.2) Criterion of the consistent elements grouping

As mentioned in Chapter 3, the consistent elements can be determined from the diagonal elements h_{ii} in the prediction matrix $\boldsymbol{H}$ which is due to its interpretation as the amount of leverage in the group. When this diagonal element h_{ii} is less than the leverage point, the *i-th* analyzed element is regarded as a consistent element with respect to a particular degree-of-freedom.

This criterion of leverage point can be adjusted in accordance with different types of structures and requirements. And this leverage point should be taken as the product of a multiplying factor and the average value of diagonal elements h_{ii}. Therefore, the multiplying factor controls the value of the leverage point to satisfy the required consistency of the elements under different situations.

Section 4.5.3) Model updating process for elimination of inconsistent elements

As mentioned previously, the consistent elements are determined from the prediction matrix. The sensitivity matrix forming the prediction matrix is of dimension $r \times m$, where r and m are the number of the analyzed elements and mode number, respectively. Moreover, the sensitivities in the sensitivity matrix are with respect to a degrees-of-freedom which satisfies the criterion of sensor placement ratio.

Since this elimination process is mainly based on the prediction matrix ***H*** for the remaining analyzed elements, updating the Fisher Information matrix after an inconsistent element eliminated is necessary by means of matrix inversion lemma as Equation (4.8) in an iterative approach. The damage information of an inconsistent *i-th* element is deleted from the Fisher Information matrix formulated as Equation (4.7). And the sensitivity matrix ***X(i)*** which exclude the damage information emitted from the *i-th* inconsistent element are multiplied with the updated Fisher Information matrix as shown in Equation (4.9) to form an updated prediction matrix H'. The diagonal element in this new H' gives a measure of the consistency of the remaining analyzed elements. This backward elimination process is repeated, until no remaining analyzed elements are classified as the inconsistent elements, or the number of remaining elements in the prediction matrix is greater than or equal to the number of the target modes due to Assumption VII.

$$[X^T(i)X(i)] = [X^T X - x_i^T x_i] \tag{4.7}$$

$$[X^T(i)X(i)]^{-1} = [X^T X - x_i^T x_i]^{-1}$$

$$= [X^T X]^{-1} + \frac{[X^T X]x_i^T x_i [X^T X]}{\left(1 - x_i [X^T X]^{-1} x_i^T\right)}$$

$$P_{n-i} = P_n + \frac{P_n x_i^T x_i P_n}{(1 - x_i P_n x_i^T)} \tag{4.8}$$

where $P_{n-i} = [X^T(i)X(i)]^{-1}$ and $P_n = [X^T X]^{-1}$

$$H' = X(i)\left[X^T(i)X(i)\right]^{-1}X^T(i) = X(i)P_{n-i}X^T(i) \tag{4.9}$$

where ***X(i)*** is the sensitivity matrix without the corresponding *i-th* row in the sensitivity matrix ***X***; P_{n-i} is the inverse of the Fisher Information matrix excluding the damage information emitted from an *i-th* inconsistent element; x_i is the *i-th* row vector in the sensitivity matrix ***X***, which includes all the analyzed elements in structure; ***H*** is the prediction matrix for the analyzed elements before elimination of dimension $r \times r$; r is the number of analyzed element; and H' is the updated prediction matrix for the analyzed elements after elimination.

After the elimination process, a group of consistent elements is established for a selected degree-of-freedom. Another elimination process is repeated as Equations (4.7) to (4.9) for another degree-of-freedom. It is noted that all of these degrees-of-freedom which satisfy the criterion of sensor placement ratio is only computed in this iterative process to reduce computational effort.

Chapter 5

Verification basing on damage information

Section 5.1) Introduction

The proposed sensor placement method will be verified by comparing the results with other sensor placement methods, such as the Effective Index Method presented by (Kammer, 1991) and the Co-linearity Matrix Method addressed by (Cobb and Liebst, 1997). However, the basic principles of these sensor placement methods are different. The Effective Index Method evaluates the sensor locations to obtain the linear independent information of the eigenvectors. The proposed method and the Co-linearity Matrix Method are based on the sensitivity with respect to damage in element as the damage information. As a result, the comparison of the results among these methods would not be on the same basis. The Effective Index Method is therefore modified with the sensitivity to damage as the linear independent information.

Moreover, these sensor placement methods except the proposed method are also based on the linear independent information at the selected sensor locations. However, it is difficult to evaluate the linear independent information with the damage information, because the information about the damage elements is always different under different damage configurations. The damage elements are not

where u_s is the measured mode shape by the sensors; ϕ_s is the modal matrix of the measured eigenvectors partitioned to the sensor locations of dimension $l \times m$. l and m are the number of sensor locations and target modes, respectively; q_m is the column vector of the selection matrix; ε is the column vector representing the stationary Gaussian white noise in the measurement.

When the best estimate of the modal states is obtained, an optimal condition should have been achieved that the covariance matrix of the errors is minimum. For an efficient unbiased estimator, the covariance matrix of the error is expressed as Equation (5.2).

$$\begin{aligned} P &= \sigma^2 \left[\phi_S^T \phi_S\right]^{-1} \\ &= \left[\phi_S^T \phi_S\right]^{-1} \\ &= Q^{-1} \end{aligned} \tag{5.2}$$

in which $\boldsymbol{P}$ is the covariance matrix of the estimator or inverse of the Fisher Information matrix; $\boldsymbol{Q}$ is the Fisher Information matrix; and σ^2 is the variance of the stationary Gaussian white noise, which is assumed to be unity in the formulation.

Therefore, maximizing $\boldsymbol{Q}$ can lead to minimizing the covariance matrix $\boldsymbol{P}$. According to Assumption VIII in Chapter 3, the measurement noise ε in each

known before the sensor placement analysis. Thus, the methods basing on linear independent information may not be suitable to evaluate the sensor locations for damage detection.

Section 5.2) Effective Index Method

Section 5.2.1) Introduction

As previously mentioned, the principle of the Effective Index Method (Kammer 1991) is to maintain as much linearly independent information as possible. The sensors at the selected degrees-of-freedom can collect independent information of the eigenvectors. This means that the information of the mode shape collected is unique and the collected information would not be duplicating that from another sensor under an optimal sensor configuration. Therefore, an optimum set of sensor locations are those that obtain the linear independent information of eigenvectors under a given set of target modes.

Section 5.2.2) Fisher Information matrix

The collected information of the eigenvectors by the sensors is formulated by measurement equation as Equation (5.1) according to (Kammer 1991).

$$u_s = \phi_s q_m + \varepsilon \tag{5.1}$$

linear independent information. Moreover, the terms in each row of F_E can be formulated as Equation (5.7).

$$F_E = [\phi_s \psi] \otimes [\phi_s \psi] \lambda^{-1} \tag{5.6}$$

$$H_D = \left[\sum_{j=1}^{k} F_{E1j} : \sum_{j=1}^{k} F_{E2j} : \ldots : \sum_{j=1}^{k} F_{Esj} \right]^T \tag{5.7}$$

in which F_{Eij} represents the *j-th* term in the *i-th* row of the matrix F_E; $\otimes$ denotes a term by term multiplication.

The column vector H_D as shown in Equation (5.7) refers to the effective independence distribution of the *i-th* candidate set of sensors. This independence distribution vector H_D can be alternatively formulated as the diagonal elements of the matrix $\boldsymbol{H}$ as shown in Equation (5.8) by using the condition of Equation (5.5).

$$\begin{aligned} H &= \phi_s \psi \lambda^{-1} \psi^T \phi_s \\ &= \phi_s A_0^{-1} \phi_s \\ &= \phi_s [\phi_s^T \phi_s]^{-1} \phi_s^T \end{aligned} \tag{5.8}$$

H_D represents the effective independence of the *i-th* sensor location in the modal matrix ϕ_s. Therefore, when the value of the diagonal elements in the matrix $\boldsymbol{H}$ approaches unity, the corresponding sensor location will collect more linearly

sensor is assumed to be uncorrelated and independent. The Fisher Information matrix can also be expressed as Equation (5.3).

$$Q = \frac{1}{\sigma^2}\phi_s^T\phi_s$$

$$= \frac{1}{\sigma^2}A_0 \tag{5.3}$$

Therefore, a suitable norm of A_o can be maximized to minimize the covariance matrix. The norm of A_o can be represented by its trace or the determinant of the Fisher Information matrix.

Section 5.2.3) Fractional contribution of sensor locations

The characteristic equation in Equation (5.4) is used to solve the eigenvalue λ and the eigenvectors ψ of the matrix A_o satisfying the orthonormal condition in Equation (5.5).

$$[A_o - \lambda I]\psi = 0 \tag{5.4}$$

$$\psi^T A_o \psi = \lambda \tag{5.5}$$

Matrix F_E, which represents the fractional contribution from the sensor locations that receive the independent information of eigenvectors, is expressed as Equation (5.6). When F_E equals to unity, the corresponding degrees-of-freedom yield the

independent information. Therefore, sensor locations can be selected as those degrees-of-freedom having the larger value of the diagonal elements in the matrix ***H***.

Section 5.2.3) Modification of the Effective Index Method

The principle of Effective Index Method is based on collecting the linearly independent information of the eigenvectors as previously mentioned. The other sensor placement methods are based on the change in mode shapes due to damage. The Effective Index Method is modified to base on the sensitivity for comparison in this study. The modal matrix of measured eigenvectors is therefore replaced with the sensitivity matrix ***X*** in the measurement equation of Equation (5.1). And the matrix ***H*** or the prediction matrix stated in this thesis as shown in Equation (5.9) can be formed from the sensitivity matrix ***X***.

$$H = X\left[X^T X\right]^{-1} X^T \qquad (5.9)$$

where ***H*** is the prediction matrix stated in this study; ***X*** is the sensitivity matrix of dimension $l \times m$. l and m are the number of the accessible degrees-of-freedom and target modes, respectively.

It is assumed that each of the interested elements has unity damage. These interested elements are referred to the element of interest or those which are of great significance to the service life of the structure.

Section 5.3) Co-linearity Matrix Method

Section 5.3.1) Introduction

The method is based on examining the eigenvector sensitivity in the finite element model. No *a priori* knowledge of the damage location or extent is assumed and no damage locations are specified in particular. Two parameters of the sensitivity are explored. First one is the magnitude of the sensitivity due to a structural stiffness change. A large value implies that the corresponding element is sensitive under a particular damage configuration. The second property is that damage in different elements may produce similar changes at selected locations. These damage elements are difficult or impossible to distinguish from the collected information. These two properties are called the detectability and co-linearity, respectively. Moreover, this sensor placement method is divided into two main parts. One is sensor location prioritization and the other is the damage localization. The sensor locations are then chosen so that the collected damage information is maximized and linearly independent.

Section 5.3.2) Sensor location prioritization

Given that there are m measured modes, the detectability as defined in last paragraph or eigenvector derivative at the *l-th* degree-of-freedom due to the changes in the elements of the structure is expressed as Equation (5.10).

$$D_{\phi l} = \sum_{k=1}^{n}\sum_{i=1}^{m}\left|\left[\frac{\partial \phi}{\partial p}\right]_{l\times k}\right|_i = \sum_{k=1}^{n}\sum_{i=1}^{m}|X|_i \tag{5.10}$$

where $D_{\phi l}$ is the column vector of the detectability at the *l-th* degree-of-freedom; X is termed the sensitivity matrix of dimension $l \times n$. l and n are the number of the accessible degrees-of-freedom and the element number, respectively. And then the column vector $D_{\phi l}$ is then sorted in descending order.

Initially, the sensor locations are prioritized on the basis of maximizing the detectability. A threshold value is set basing on the measurement uncertainty and the finite element modeling errors. Values of $D_{\phi l}$ below this threshold value indicate that the eigenvectors of the target modes at the *l-th* degrees-of-freedom are unaffected by the structural damage elements. A co-linearity check is then made to determine which degrees-of-freedom collect similar damage information emitted from the elements. When the co-linearity $S_{\phi ij}$ is unity in the co-linearity matrix as given in Equation (5.11), it indicates that the damage information at the *i-th* and *j-th* degrees-of-freedom is dependent. And these degrees-of-freedom are grouped in the same symmetric sensor group, which means that these locations receive similar damage information. On the other hand, when the co-linearity in the co-linearity matrix is zero, the damage information collected at the two corresponding degrees-of-freedom are independent.

$$S_{\phi ij} = \left[\frac{1}{m} \sum_{i=1}^{m} \left[XX^T \right] \right]_{i \times j} \tag{5.11}$$

in which $S_{\phi ij}$ is the co-linearity of information collected between *i-th* and *j-th* degree-of-freedom. It is a square matrix with a dimension of the accessible degrees-of-freedom.

Also, a threshold value $S_{\phi ij}$ smaller than unity is set on the basis of measurement uncertainty and the finite element modeling errors. When the co-linearity is above this threshold value, it implies that the damage information collected at the two degree-of-freedom is indistinguishable from each other under the *m* target modes, and these two degrees-of-freedom should be in the same symmetric sensor group. Those above the threshold value represent the recommended degrees-of-freedom for placing sensors. When an element in the column vector $D_{\phi l}$ is maximum, this *l-th* degree-of-freedom is most sensitive to all elements in a structure. As a result, one sensor location is selected from each symmetric sensor group ranked according to the maximal detectability in each group.

Section 5.3.3) Damage localization

The accessible degrees-of-freedom as sensor locations are obtained by the sensor location prioritization process. The damage localization process determines the possible extent of damage which can be isolated to the individual element. The two structural parameters of detectability and co-linearity are also used, and eigenvalue

derivatives are also used to evaluate the detectability and co-linearity. The detectability in terms of the eigenvalue change due to the change in the *k-th* element is shown as Equation (5.12). Similarly, the detectability in terms of the eigenvectors change due to damage in the *k-th* element is given in Equation (5.13).

$$D_{\lambda k} = \sum_{i=1}^{r} \left| \left\{ \frac{\partial \lambda}{\partial p_k} \right\}_i \right| \tag{5.12}$$

$$D_{\phi k} = \sum_{l=1}^{s} \sum_{i=1}^{r} \left| \left[\frac{\partial \phi_l}{\partial p_k} \right]_i \right| = \sum_{l=1}^{s} \sum_{i=1}^{r} \left| X^T \right| \tag{5.13}$$

where $\left\{ \frac{\partial \lambda}{\partial p_k} \right\}$ is a column vector of the eigenvalue derivative; X is also called the sensitivity matrix of dimension $n \times l$. n and l are the element number and the number of the accessible degrees-of-freedom, respectively; s and r are the number of degrees-of-freedom and target modes, respectively.

The co-linearity in the co-linearity matrices S_λ and S_ϕ are given in Equation (5.14) and (5.15), respectively.

$$S_{\lambda jk} = \left[\left\{ \frac{\partial \lambda}{\partial p} \right\} \left\{ \frac{\partial \lambda}{\partial p} \right\}^T \right]_{jk} \tag{5.14}$$

$$S_{\phi k} = \left[\frac{1}{r} \sum_{i=1}^{r} \left[X^T X \right] \right]_{jk} \tag{5.15}$$

The element at the intersection of the *j-th* row and *k-th* column of the co-linearity matrices S_λ and S_ϕ indicate the correlation of damage information of the eigenvalue and eigenvector from the *j-th* and *k-th* damage elements. When elements with their corresponding components in D_λ and D_ϕ are below the modeling and measurement uncertainty threshold level, they are declared undetectable elements. Thus, damage in an undetectable element cannot be identified. The elements in the co-linearity matrices S_λ and S_ϕ which are above the threshold value are detectable, but they emit different and distinguishable damage information. Therefore, the damage elements can be distinguished and then localized, as long as the two structural parameter of detectability and co-linearity satisfy the two conditions as discussed above.

5.4) Simulated structure for illustration

Section 5.4.1) Structural properties and form of simulated structure

A simple symmetric three-storey plane steel frame is shown in Figure 5.1 for the purpose of illustration. There are forty-five Euler-Benoulli beam elements. In this simulated structure, two types of elements are only modeled as the column and beam elements. And this structure contains only two types of stiffness of the column and beam elements so as to simplify this illustration. The structural properties of the beam and column elements are shown in Table 5.1.

Table 5.1 – Section properties of three-storey plane steel frame

	Section area (m^2)	I_{yy} (m^4)	I_{xx} (m^4)
Beam elements	284.6×10^{-6}	1.88×10^{-9}	2.185×10^{-8}
Column elements	142.4×10^{-6}	2.35×10^{-10}	12.1515×10^{-9}

Since this simple simulated structure has no rotation at the floor level, when the floor is modeled by a ten times stiffer beam elements, this structure can represent the typical low-rise buildings and is classified as a shear type of structure. On the other hand, a high-rise building behaves as a cantilever. It is relatively simple in the eigenanalysis. Therefore, this simple structure can simply simulate the complicated structure.

Since the stiffness of the beam elements are relative larger than those of the column elements, it is expected that the eigenvector changes at many degrees-of-freedom are less sensitive to the damages in the beam elements. Therefore, it is difficult to detect the damages in such kind of elements according to the general sensor placement methods which is based on the eigenvector sensitivity. In view of this difficulty, the beam elements are then selected as interested elements for monitoring with the element number ranging from 31 to 45. This selection can emphasize on the effectiveness of the proposed method. If the damages really occur in the column elements, it is easier to detect these damages due to their relatively high sensitivities.

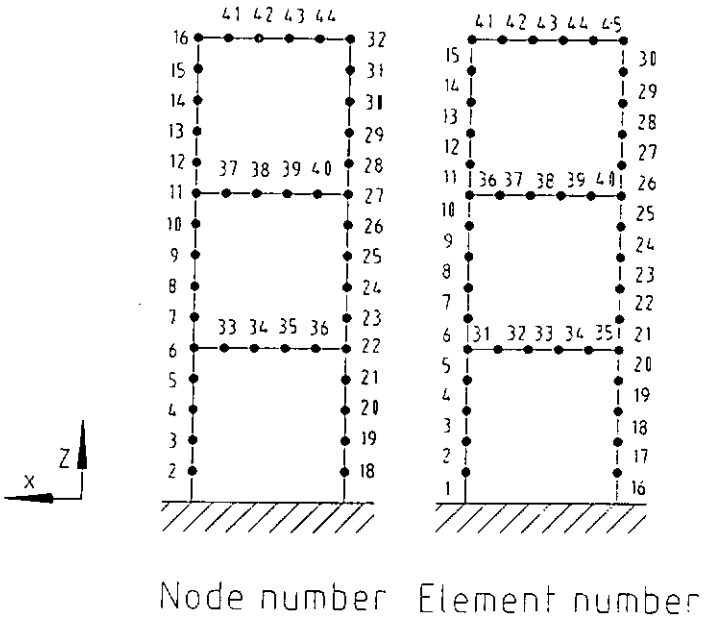

Figure 5.1 – Evaluation view of three-storey plane steel frame

It should be noted that the corresponding finite element model consists of forty-four nodes with forty-two unconstrained nodes each with x and z displacements and two constrained nodes. However, the column nodes and beam nodes have very small contribution to vibration modes in the z-direction and x-direction respectively. The accessible degrees-of-freedom include only the horizontal translation in x-direction for column nodes and the vertical translation in z-direction for beam nodes. In addition, all rotational degrees-of-freedom are ignored in this sensor placement method due to Assumption I. Therefore, each node has only one active degree-of-freedom for placing a sensor. And the accessible degrees-of-freedom are denoted by the corresponding node number in the following discussion.

Section 5.4.2) Vibrational properties of simulated structure

Free vibration analysis is conducted on the three-storey plane steel frame with no damping. The first thirteen modes are used in the analysis. The first three modes are global mode and the others are local modes. The natural frequencies of the structure are listed in Table 5.2. And the mode shapes for each mode are shown on Figure 5.2.

Table 5.2 – Natural frequencies of three-storey plane steel frame

Mode	Frequency	Mode	Frequency	Mode	Frequency	Mode	Frequency
1	4.51	5	71.94	9	99.49	13	225.48
2	13.32	6	84.38	10	108.30		
3	20.56	7	85.29	11	112.81		
4	62.97	8	95.70	12	121.29		

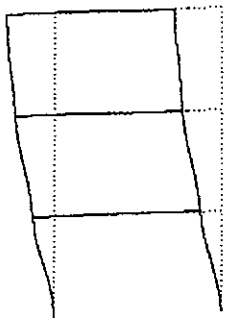

Mode 1

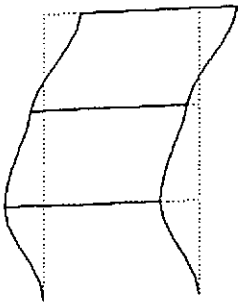

Mode 2

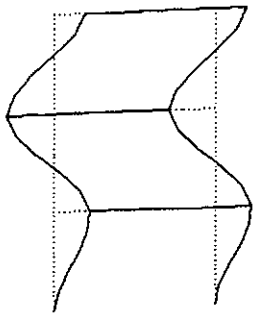

Mode 3

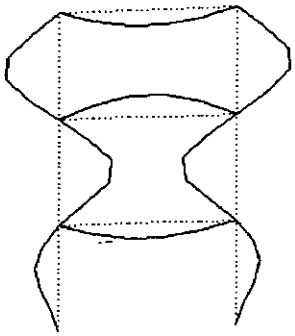

Mode 4

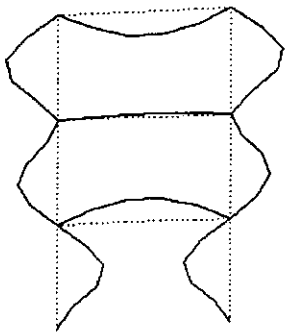

Mode 5

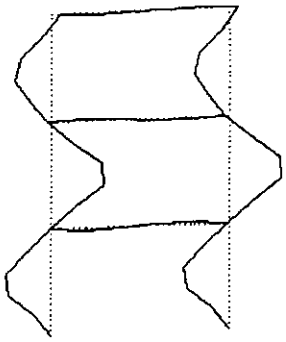

Mode 6

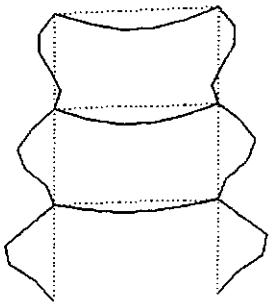

Mode 7

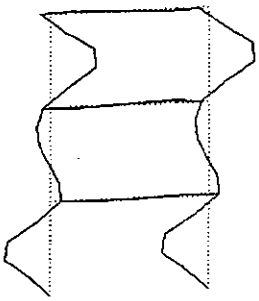

Mode 8

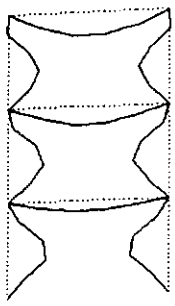

Mode 9

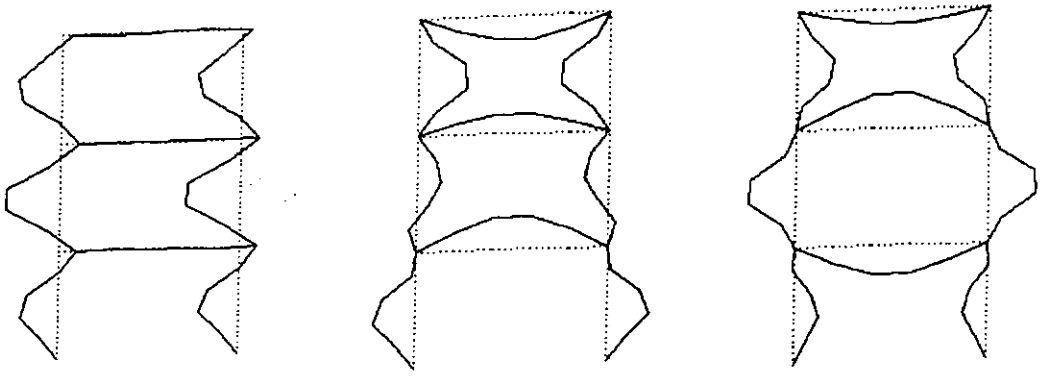

Mode 10 Mode 11 Mode 12

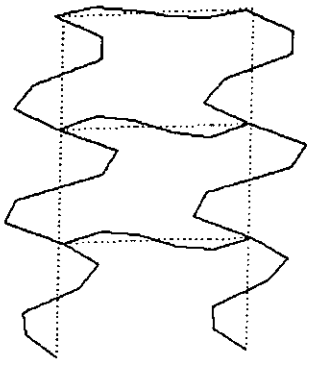

Mode 13

Figure 5.2 – Mode shape of three-storey plane steel frame

Six target modes are identified from modal identification process for the analysis, which are modes 4, 5, 9, 11, 12 and 13. These target modes are beneficial to the

interested beam elements. The vibrational amplitudes of the translation in *z*-direction of beam nodes are generally large under these target modes as shown in Figure 5.2. It is concurrent with the engineering sense.

Section 5.5) Results from proposed sensor placement method

Section 5.5.1) Threshold values

In the proposed sensor placement method, the threshold values for the different criteria in different processes are bellow:

Threshold for Modal Criterion	0.17×max(Element Detectability)
Threshold for undetectable element	0.3×max(Total Detectability)
Threshold for Sensor Placement Ratio	0.45×max(sensor placement ratio)
Threshold for leverage point	$2m/n$

It should be noted that the determination of the threshold values in different processes depends strongly on the engineering judgement. Therefore, basing on different situations and problems handled by different engineers, the threshold values can be different. Therefore, it is difficult to be implemented as an automatic process, as the different threshold values are required to suit the different situations and types of structure.

The threshold values in the different processes in the proposed method are strongly related to the different types of structures and different situations. For example, the

stiffnesses of the structural elements in the structure are the variables with a wide range. The ratio of the threshold values for the undetectable elements should then be large enough to include more elements for analysis. Moreover, the ratio of the threshold values for sensor placement ratio depends on how many sensors be available and how effective monitoring can be carried out by the selected sensors. This is on an engineering basis. Finally, the threshold for leverage point is based on the study presented by Belsley, Kuh and Welsch (1980). The value adopted is adequate to obtain a high consistency of the elements in the same group.

Section 5.5.2) Undetectable elements

Undetectable elements in the group are identified in the damage element classification process. And the interested group of elements excluding the undetectable elements are called analyzed elements as previously stated. The analyzed elements number are from 32 to 34, 37 to 39 and 42 to 44. The undetectable elements are those at the joints on the beam elements.

The above result contradicts with the general view that the elements at a joint are easier to be monitored when there is damage in the element. The changes of eigenvectors at the element ends would affect eigenvectors at many adjacent degrees-of-freedom through the joint connection. In fact, the damage is assumed to be small in the proposed method and the beam elements are ten times stiffer than the column elements. Thus, as the mode shapes at these elements are basically small and the changes of the eigenvectors at end of the beam elements are also

small. And they have small effects on other elements. With this small damage information, the beam elements next to the joints are therefore difficult to be detected.

Section 5.5.3) Sensor locations from proposed method

The required number of sensors is limited to ten. The given number of sensor is adequate, as there are only fifteen interested elements selected for monitoring. The sixteen degrees-of-freedom satisfying the criterion of sensor placement ratio is ranked in descending order. They are referred to the corresponding node number as listed in Table 5.3. It should be noted that these degrees-of-freedom satisfying the criterion are relatively sensitive to damages in the analyzed elements.

Table 5.3 – Sensor placement ratio for each sensor location

Node	Sensor placement ratio	Node	Sensor placement ratio
39	1.694	44	0.810
38	1.694	41	0.810
43	1.407	33	0.786
42	1.407	36	0.786
34	1.298	14	0.766
35	1.298	30	0.766
37	1.021	13	0.764
40	1.021	29	0.764

The number of sensor location is minimized basing on the least loss of information due to sensor deletion. The number of resulting sensor location is greater than the required number of ten, because further reduction of the number sensor locations is required in the process of consistency check. The remaining sensor locations are listed in Table 5.4.

Table 5.4 – Sensor locations remained according to the least loss of information

Optimal node	39	38	43	42	34	35	37	40	44	41	33	36	14	13	29

Table 5.5 – Consistent elements with respect to each sensor locations

	Consistent elements (✓)								
Node	32	33	34	37	38	39	42	43	44
13		✓		✓	✓	✓	✓		✓
14		✓		✓	✓		✓	✓	✓
29		✓	✓		✓	✓		✓	✓
33	✓		✓	✓		✓	✓		✓
34	✓		✓	✓		✓	✓		✓
35	✓		✓	✓		✓	✓		✓
36	✓		✓			✓	✓	✓	✓
37	✓		✓	✓			✓	✓	✓
38	✓		✓		✓	✓	✓		✓
39	✓		✓		✓	✓	✓		✓
40	✓		✓	✓	✓		✓		✓
41	✓		✓	✓		✓	✓		✓
42	✓		✓	✓		✓	✓		✓
43	✓		✓	✓		✓	✓		✓
44	✓		✓			✓	✓	✓	✓

Table 5.6 – Finalized sensor locations from proposed sensor placement method

Finalized sensor locations	39	38	43	42	34	35	37	40	44	14

Finally, the analyzed elements are assembled into consistent groups with respect to each of the remaining degrees-of-freedom as shown in Table 5.5. The consistent elements in a group are checked in the table. The results indicate that damage in the group of consistent elements can be effectively detected by the corresponding degree-of-freedom. It is noted that after the above selection process, each consistent element contributes nearly the same and close to average Receptability at a degree-of-freedom, and a damage in any such element contributes relatively large change in the mode shape at this degree-of-freedom. The degrees-of-freedom selected as sensor locations should be able to monitor all analyzed element effectively and reliably.

Table 5.5 shows that any degree-of-freedom can monitor changes at element 44 while only five degrees-of-freedom can monitor the condition of element 43. Degree-of-freedom of node 37 is selected for the latter because of its higher sensor placement ratio among the five degrees-of-freedom as shown in Table 5.3. the other locations are selected in a similar way. In the selection of the last location, degree-of-freedom of node 14 is selected to replace degree-of-freedom of node 41 which is higher in the list of sensor placement ratio, since degree-of-freedom of node 14 is the best degree-of-freedom capable to monitor element 33 as shown in Table 5.5. The finalized sensor locations are listed in Table 5.6 to monitor all the analyzed elements in Table 5.5.

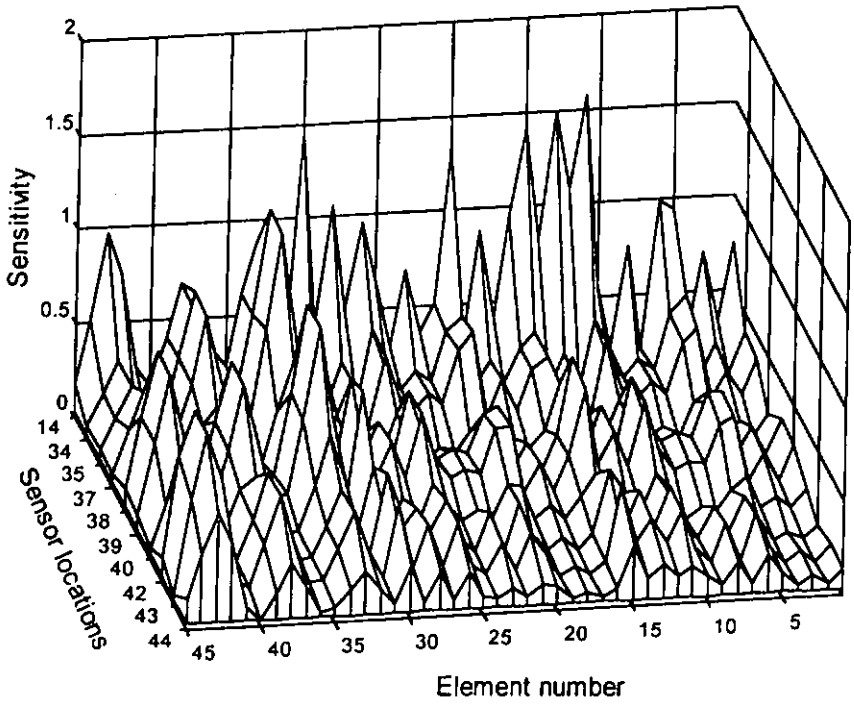

Figure 5.3 – Distribution of sensitivities at finalized sensor locations

The distribution of sensitivities at the finalized sensor locations against all elements is plotted in Figure 5.3. Each finalized sensor location is sensitive to the particular analyzed elements, as the peak values are always found at the analyzed elements in the figure. Moreover, it should be noted that the sensor locations are most likely to be on the beam elements. It is concurrent with the engineering sense that when the beam elements are selected for monitoring, most of the sensors should be placed on the beam to collect the adequate damage information from such elements.

Section 5.6) Results from other sensor placement methods

Section 5.6.1) Sensor locations from Effective Index Method

The Effective Index Method is modified basing on damage information as discussed previously. The minimization of sensor number by Effective Index Method is then based on the linearly independent damage information. The analysis is based on the same target modes as for the proposed method. The sensor locations are tabulated in Table 5.7 according to their Effective Independence Index (EFI) in descending order. The value of EFI shows the contribution of linearly independent information at the corresponding degrees-of-freedom. When the value of EFI is high the information collected is more linearly independent.

Table 5.7 – Linearly independent distribution by Effective Index Method

Sensor locations	EFI
3	0.668
4	0.664
8	0.577
25	0.500
10	0.463
33	0.723
26	0.463
5	0.480
41	0.591
15	0.436

Section 5.6.2) From Co-linearity Matrix Method

The Co-linearity Matrix Method is performed on the damage information under the same target modes. The symmetric sensor groups from the Co-linearity Matrix Method are determined from the co-linearity matrix, but the sensor grouping may be different by using different ways of searching the co-linearity in the co-linearity matrix as Equation (5.11). No reference is found in the original literature. Two methods of searching the co-linearity are used in this study. The symmetric sensors grouping by methods (i) and (ii) are given in Tables 5.8 and 5.9, respectively.

Table 5.8 – Linearly independent information by Co-linearity Matrix Method (i)

Sensor locations	Symmetric sensor group
4	2, 3
5	
11	6, 16, 22, 27, 32
10	7
8	9
14	12, 13, 15
19	18, 20
21	
23	26
24	25
30	28, 29, 31
34	33, 35, 36, 37, 38, 39, 40
43	41, 42, 43, 44

Method (i) identifies the element in the matrix which has the value above the threshold. The elements along the first row are inspected, and those above the threshold are identified. The degrees-of-freedom corresponding to the row number and the column number of the identified elements are grouped into a symmetric sensor group. These degrees-of-freedom are deleted from the co-linearity matrix. The process is repeated for another symmetric sensor group, until all the degrees-of-freedom are selected. This method has the disadvantage of having less co-linear degrees-of-freedom in the sensor group, and the sensors may not provide fully independent damage information.

Table 5.9 – Linearly independent information by Co-linearity Matrix Method using method (ii)

Sensor locations	Symmetric sensor group
38	39
4	3
30	13, 14, 16, 20, 29, 32
34	35
19	33, 27, 11
8	9
43	42
24	25
22	6
28	21

Method (ii) is similar to method (i). The element in the first column is identified. Instead of inspecting the elements along the row of the element, all elements that lie on the corresponding row and column of this element having the largest co-linearity are checked against the threshold value. Those above the threshold value are identified. The rest of the procedure is the same as Method (i). This method ensures high co-linearity between the information collected at two degrees-of-freedom.

One sensor location is then selected from each symmetric sensor group. However, the number of symmetric sensor group is greater than the required sensor number, the selection of sensor location from which symmetric sensor group is by engineering judgement. The sensor locations from the different methods are tabulated in Table 5.10.

Table 5.10 – Summary of sensor locations from different sensor placement methods

Proposed method	14	34	35	37	38	39	40	42	43	44
Effective Index Method	3	4	5	8	10	15	25	26	33	41
Co-linearity Matrix Method (i)	4	5	8	10	14	19	23	24	30	34
Co-linearity Matrix Method (ii)	4	8	19	22	24	28	30	34	38	43

Section 5.6.3) Implication of symmetrical sensor placement

The three-storey steel plane frame is geometrically and structurally symmetric. The damages are assumed to occur in all the elements. Therefore, when the sensors are symmetrically placed in a structure, the collected damage information at symmetrical sensors from all symmetrical elements should intuitively be the same.

In the Effective Index Method, the final sensor locations are not placed in symmetry, except nodes 10 and 26. The collected information by each of these sensors are nearly independent.

In the Co-linearity Matrix Method, the selected sensor locations by both methods are symmetric in most cases, and each sensor in the different sensor groups may collect the same damage information. The geometric symmetrical sensor locations are more obvious in method (i). For example, sensor groups of 2, 3, 4 and 18, 19, 20 are symmetric in geometry. It implies that two sensors from these two sensor groups collect the same information. On the other hand, the sensor locations from method (ii) are seldom in symmetry. Therefore, sensor locations from method (ii) provide more linearly independent damage information than those from method (i).

Section 5.7) Comparison and discussion

Section 5.7.1) Comparison of sensor locations

The minimization of sensor numbers in the proposed method is to maintain as much damage information as possible after sensor elimination. However, this minimization process ignores the linear independence on sensor locations. Thus, the finalized sensor locations listed in Table 5.5 are geometrically symmetric. This shortcoming also occurs in the Co-linearity Matrix Method (i) seriously.

The advantage of the proposed method is that the sensor locations are close and adjacent to the analyzed elements, which can monitor the analyzed elements directly. On the contrary, sensor locations determined from the other two sensor placement methods are distributed over the structure. For a large civil structure with many structural components, the sensor locations determined from the other sensor placement methods may be allocated far away from the target elements. And damages in these target elements are difficult to be detected by the corresponding sensors. But, according to the proposed sensor placement method, sensors at the selected locations can effectively detect damages in the target elements or the analyzed elements.

Section 5.7.2) Comparison of eigenvector changes due to unity damage

According to this proposed method, the sensor location selection is aimed at maximizing the collection of damage information emitted from the analyzed

elements. In other words, if the analyzed elements have a unity damage, the eigenvectors change at these sensor locations are comparatively large. The damages in these elements are then easily detected due to the large mode shape changes at the selected locations.

As an example for illustration, a unit damage occurs in elements 38 and 42, and the eigenvector changes at the sensor locations from different sensor placement methods are ranked in descending order and they are plotted in the Figures 5.4 and 5.5. The eigenvector changes at the sensor locations from the proposed method are larger than those from the Effective Index Method, when the damages are in the analyzed elements. It is because the Effective Index Method is mainly based on the linearly independent information and does not guarantee the collection of more damage information.

On the other hand, the Co-linearity Matrix Method using methods (i) and (ii) generally give slightly less eigenvector changes, when the damages occur in the beam elements. The sensor locations according to the Co-linearity Matrix Method are located away from the beam elements. The damage information collected by the corresponding sensors are then slightly less.

This example indicates that the proposed method is more efficient to monitor the damages in the analyzed elements than other methods.

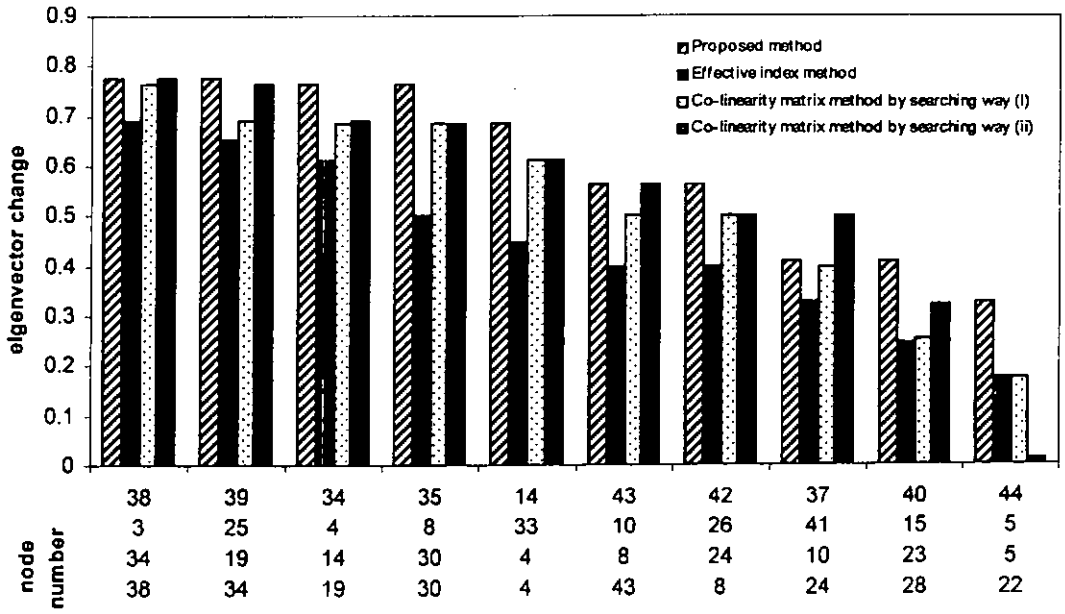

Figure 5.4 – Eigenvector change at sensor locations due to damage element 38

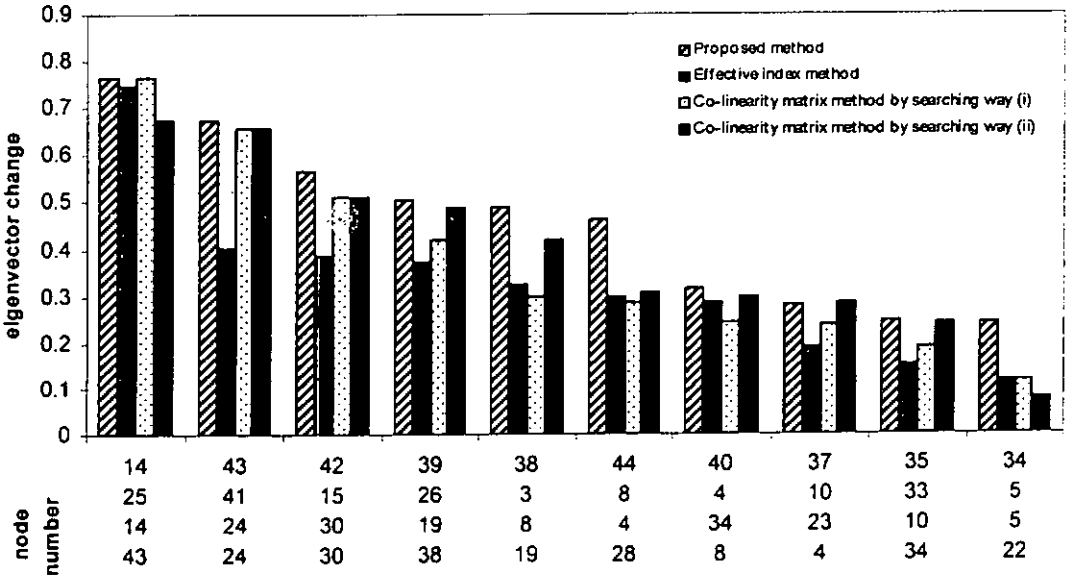

Figure 5.5 – Eigenvector change at sensor locations due to damage element 42

It should be noted that the node number in *x*-axis of Figures 5.4 and 5.5refers to the sensor placement methods in the same order that is in the legend.

Section 5.7.3) Discussion on damage in different types of elements

The changes of eigenvectors due to damage in different types of elements are plotted in Figure 5.6 using the proposed method. The types of elements include the undetectable, non-analyzed and analyzed elements. And they are chosen randomly.

It is evident from Figure 5.6 that the eigenvector changes due to damage from the analyzed elements are generally much greater than those from the non-analyzed and undetectable elements. Sensors at the selected locations are relatively efficient to detect the damage in the analyzed elements with larger eigenvector change or damage information.

It is also noted that the eigenvectors change at the sensor locations due to damage in the undetectable element is very small. Therefore, the process of element classification is considered necessarily to classify elements which are impossible to be detected.

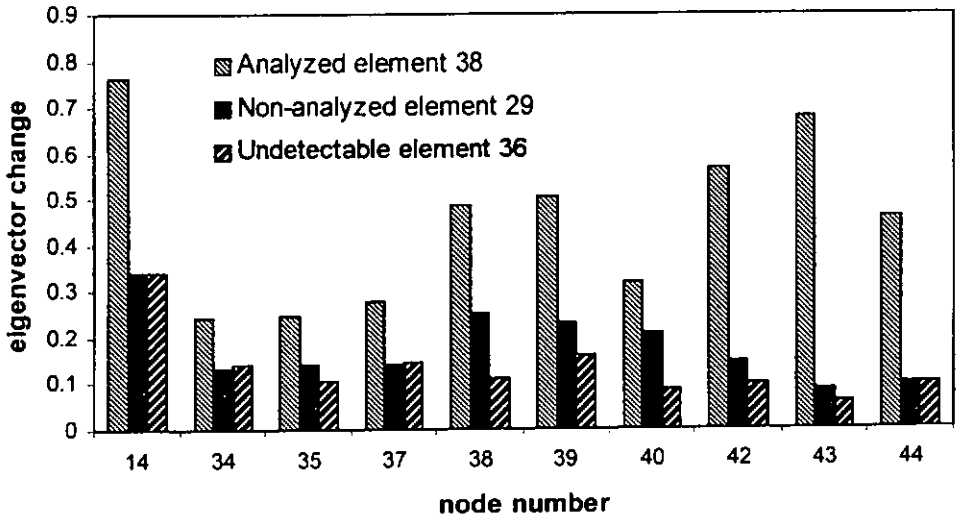

Figure 5.6 – Eigenvector change due to different elements in proposed method

Section 5.7.4) Discussion on consistent element grouping

Table 5.5 is studied again from a different point of view. The sensors can be grouped in symmetric sensor groups to monitor the same consistent elements. For example, all the sensors are in a symmetric sensor group for monitoring element 44. And all the sensors except sensor 13, 14 or 39 are assembled into a symmetric sensor group to monitor either elements 32, 34, 42 and 44 or when all of them have a damage. Theoretically, one sensor in the symmetric sensor group can monitor the whole group of consistent elements effectively, and collects similar damage information emitted from the corresponding consistent elements. The final sensor locations shown in Table 5.6 should have some duplicated damage information for the consistent elements, but it does not implies that the sensors from the proposed

method is poor in the performance of damage assessment. This will be discussed in details in Chapter 5.

Chapter 6

Verification basing on damage assessment

Section 6.1) Introduction

Verification of the proposed method is further conducted by comparing with other sensor placement methods using experimental results. The damage localization is mainly basing on the Multiple Damage Location Assurance Criterion (*MDLAC*) (Shi, et al. 1998) by using incomplete modal information. And the damage quantification is based on the sensitivity approach.

Although it is common knowledge that the measured mode shape is contaminated with large measurement noise, compared with the measured natural frequencies, the damage assessment would still be based on the mode shapes. It is because sensors from the sensor placement methods can only collect incomplete modal information. The effectiveness of damage assessment for each sensor placement method is then judged using different incomplete modal information collected at different sensor locations.

Firstly, the comparison on damage assessment is made on the simulated structure shown in Figure 5.2. The damage on this simulated structure is assumed to occur in a particular element with unity extent as Assumption II.

Secondly, the comparison would be based on the measured mode shapes of a test structure with multi-damage states. This test structure is a five-storey plane steel frame to be described later.

Section 6.2) Damage assessment using incomplete mode shapes

Section 6.2.1) Damage localization using *MDLAC*

The method is originally developed by (Messina, et al. 1998), which requires the change of natural frequencies in the measurement and the theoretical frequencies changes for damage localization and quantification. The *MDLAC* approach is further modified (Shi, et al. 1999) making use of incomplete mode shape information to localize the damage sites. The basic algorithm of *MDLAC* using natural frequencies or incomplete mode shapes is similar.

The *MDLAC* method combines the change of incomplete mode shapes from the analysis with those from measurement at the corresponding sensor locations to form the correlation parameter of *MDLAC*. The analytical mode shape changes are calculated from the sensitivity under the damage configurations with first order formulation. If this correlation parameter is close to unity, it means that the analytical eigenvectors under an assumed damage configuration is nearly the same as those from the measurement. And the assumed configuration models actual damage. This assumed damage element is then recognized as a damage site. It is formulated on the same basis as the Modal Assurance Criterion (*MAC*) in (Ewins

1984) for quantifying correlation of the correspondence between related vectors as Equation (6.1).

$$MDLAC(\{\delta p_j\}) = \frac{\left|\{\Delta\Phi\}^T \cdot \{\delta\Phi(\{\delta p_j\})\}\right|^2}{(\{\Delta\Phi\}^T \cdot \{\Delta\Phi\}) \cdot (\{\delta\Phi(\{\delta p_j\})\}^T \cdot \{\delta\Phi(\{\delta p_j\})\})} \tag{6.1}$$

where $\{\Delta\Phi\}$ is the measured mode shape change vector with a dimension equals to the product of the number of measured modes and the number of sensor locations; $\{\delta\Phi\}$ is a column vector of the change of analytical mode shape at the same degrees-of-freedom due to damage elements $\{\delta p_j\}$ and it is a function of the eigenvector change with the damage as variable; and $\{\delta p\}$ is a column vector of damage extent distribution in the elements.

In the calculation of each set of *MDLAC* value, only one element is assumed to have a unit damage. In other words, other elements in the vector $\{\delta p\}$ are equal to zero except the *j-th* element. It is assumed that the damage information from each element has linearly independent contribution to the eigenvector changes at the sensor locations. In this context, the interaction between the damage elements causing the eigenvector change is ignored and the eigenvector change would be mainly due to individual *i-th* damage element. The potential damage elements can then be approximately localized with the largest *MDLAC* values, because this damage configuration produces the analytical eigenvectors that match with the measurements. It should be noted that the *MDLAC* with incomplete modal

information is directly derived from the damage information collected at the sensor locations without introduction of any errors.

The sensitivity of the *k-th* mode shape due to damage at *j-th* element is given by Equation (6.2) according to (Shi, et al. 1999), which forms the expression of the theoretical eigenvector changes under the different damage configuration as Equation (6.3).

$$\frac{\partial\{\phi_k\}}{\partial p_j} = \sum_{r=1}^{n^*} \frac{-\{\phi_r\}^T \cdot [K_j]\{\phi_k\}}{\lambda_r - \lambda_k}\{\phi_r\} \qquad (r \neq k) \tag{6.2}$$

in which $\{\phi_k\}$ and λ_k are the analytical mode shape at *k-th* mode and the *k-th* analytical eigenvalue, respectively; and n^* is the number of analytical modes used in the calculation. It is noted that n^* should be equal to the total degrees-of-freedom of the system. Hence only a limited number of modes of the system are used in practice.

Section 6.2.2) Damage quantification using *MDLAC*

For any combination of damage elements, the theoretical eigenvector changes can be expressed as a linear combination of the sensitivities, which is expressed in Equation (6.3).

$$\begin{aligned}\{\delta\Phi_1\} &= \frac{\partial\{\Phi_1\}}{\partial p_1}\delta p_1 + \frac{\partial\{\Phi_1\}}{\partial p_2}\delta p_2 + \cdots + \frac{\partial\{\Phi_1\}}{\partial p_L}\delta p_L \\ &\vdots \\ \{\delta\Phi_m\} &= \frac{\partial\{\Phi_m\}}{\partial p_1}\delta p_1 + \frac{\partial\{\Phi_m\}}{\partial p_2}\delta p_2 + \cdots + \frac{\partial\{\Phi_m\}}{\partial p_L}\delta p_L\end{aligned} \tag{6.3}$$

When m modes are used together to localize the damage elements, the analytical eigenvector change at the sensor locations as Equation (6.3) can be rewritten in the matrix form as Equation (6.4) or in the compacted form as Equation (6.5).

$$\{\delta\phi\} = \begin{Bmatrix}\delta\phi_1 \\ \vdots \\ \delta\phi_m\end{Bmatrix} = \begin{bmatrix}\frac{\partial\{\phi_1\}}{\partial p_1} & \cdots & \frac{\partial\{\phi_1\}}{\partial p_L} \\ \vdots & \ddots & \vdots \\ \frac{\partial\{\phi_m\}}{\partial p_1} & \cdots & \frac{\partial\{\phi_m\}}{\partial p_L}\end{bmatrix}\begin{Bmatrix}\delta p_1 \\ \vdots \\ \delta p_L\end{Bmatrix} \tag{6.4}$$

$$\{\delta\phi\} = [X]\{\delta p\} \tag{6.5}$$

where the *{}* denotes the column vector; *[]* denotes the two dimensional matrix; and $\boldsymbol{X}$ is the sensitivity matrix.

Since the linear assumption as Assumption VI embodied in Equation (6.3) means that changing the corresponding damage element vector $\{\delta p\}$ by a constant does not change the *MDLAC* correlation parameter as Equation (6.1), the absolute value of damage extent is absent from this equation. The actual damage extent cannot be determined directly. Since the column vector of measured eigenvector changes

$\{\Delta\Phi\}$ is known from the measurement, an absolute damage scaling coefficient C can be estimated by Equation (6.7) so that it provides the actual value of damage extent of the test structure.

If a linear analytical model is the true modal of the damage, the theoretical eigenvector changes given by Equation (6.5) would be identical to the measured changes. Therefore, the analytical eigenvector changes in Equation (6.5) are replaced by the measured eigenvector changes, and the true distribution of $\{\delta p_j\}$ is input to calculate the absolute values of damage extent as given in Equation (6.6). And the Equation (6.6) can be rewritten as Equation (6.7) for the *k-th* mode.

$$\{\Delta\phi\} = C \cdot [X]\{\delta p\} \tag{6.6}$$

$$C_k = \frac{\Delta\phi_k}{x_k^T\{\delta p\}} \tag{6.7}$$

in which x_k^T is a row vector of the sensitivity matrix $\boldsymbol{X}$; C is a vector of scaling coefficients to determine the absolute amount of the damage.

In principle, the scaling coefficient vector C should be the same for the modes. However, due to Assumption VI and the effects of errors in the measurement, a more reliable value of the scaling coefficient is determined by averaging the estimated coefficient C_k from all target modes used in the analysis. The damage extent can then be expressed as the combination of the two terms $C\{\delta p\}$. The

damage element distribution can be any number, or scale of same proportion for all damage elements, because different scale in $\{\delta p\}$ does not affect the percentage change. Therefore, the percentage change of damage extent can be determined by Equation (6.8).

$$\text{Percentage change} = \frac{C\{\delta p\}}{property} \times 100\% \tag{6.8}$$

The *property* is a parameter which affects all components in the stiffness matrix of the element. The elastic modulus E is adopted in this study, because it only affects directly the structural stiffness including the axial and bending stiffnesses.

Section 6.3) Damage localization with simulated three-storey frame

The simulated structure is a three-storey plane steel frame as shown in Figure 5.2. This structure is assumed to have a unit damage in the analyzed elements 38 or 42. The incomplete modal information from sensor locations selected by different sensor placement method is then used to calculate the damage location using the *MDLAC*. Results of the damage assessment of this structure are compared with the true location. The sensor locations from each sensor placement method are repeated in Table 6.1.

Table 6.1 – Summary of sensor locations from different sensor placement methods

	Sensor locations									
Proposed Method	14	34	35	37	38	39	40	42	43	44
Effective Index Method	3	8	14	19	24	30	33	34	37	41
Co-linearity Matrix Method (i)	4	5	8	10	14	19	23	24	30	34
Co-linearity Matrix Method (ii)	4	8	19	22	24	28	30	34	38	43

When *MDLAC* value based on the incomplete modal information is close to unity, the collected information from the sensor locations can be used to estimate the damage location accurately. The analyzed elements 38 and 42 are assumed to be the damage locations with unit damage one at a time. Under this circumstance, the "measured" eigenvector changes in Equation (6.1) are determined theoretically from the structural system under the given damage configuration. Measurement error is not present in this comparison.

The results of damage localization by *MDLAC* for the group of potential damage elements are plotted in Figures 6.1 and 6.2, respectively, with the *MDLAC* values normalized with respect to the largest value of the group. The *MDLAC* value for element 38 from the proposed method is the largest among the other sensor placement methods as shown in Figure 6.1. And the *MDLAC* values for element 42 from the proposed method are also larger than other methods in Figure 6.2. Both the Co-linearity Matrix Method (i) and (ii) give *MDLAC* values for element 42 close to zero. In general, the ranking of *MDLAC* values for elements 38 and 42

from the proposed method is higher than those from other methods as shown in Table 6.2. It means that the proposed method is more effective in damage localization, when the damage elements are analyzed elements.

Table 6.2 – Ranking of the MDLAC values for damage element 38 and 42

	Proposed method	Effective Index Method	Co-linearity Matrix Method (i)	Co-linearity Matrix Method (ii)
Element 38	6	7	8	7
Element 42	3	4	9	7

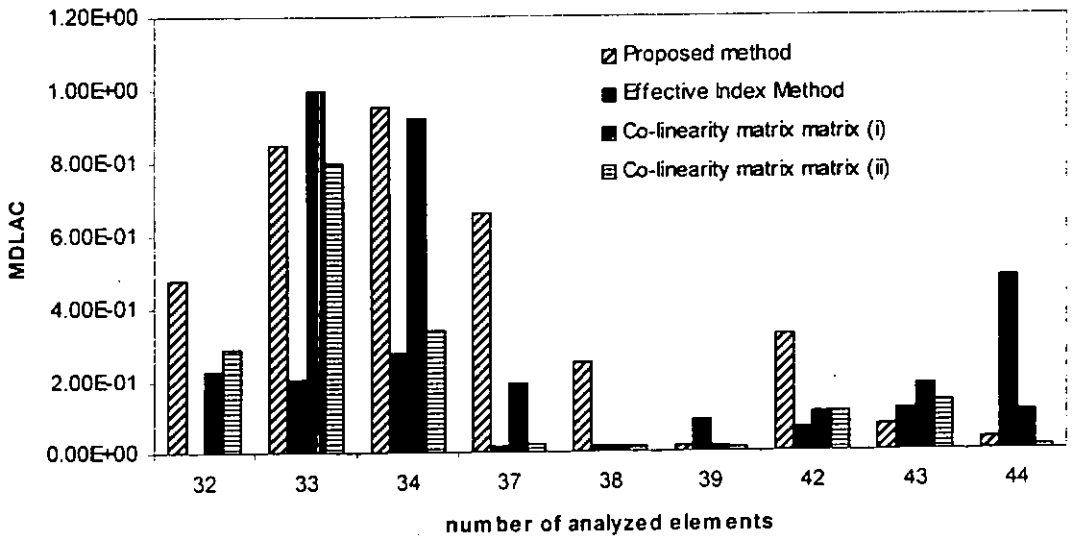

Figure 6.1 – Damage localization of *MDLAC* due to damage element 38

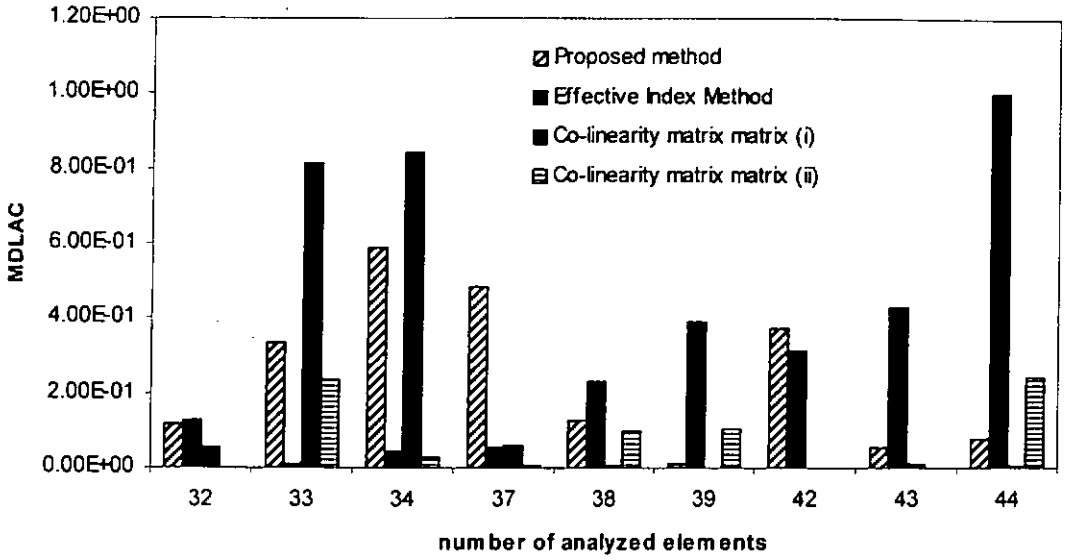

Figure 6.2 – Damage localization of *MDLAC* due to damage element 42

Section 6.4) Experimental verification on five-storey steel frame

Section 6.4.1) Test structure

Further comparison of different sensor placement methods is based on the effectiveness of damage localization and quantification with real multi-damage states. The effectiveness of using different Target Groups in the proposed method is investigated. In addition, the effectiveness of different sensor placement methods is also compared.

This test structure is a five-storey plane steel frame as shown in Figure 6.3. It consists of two columns and five horizontal interconnecting beams. The connections between the beams and columns and at the bottom joint with the

supporting plate can be considered rigid. The column members are flat steel bars with a cross-sectional dimension of 4.45mm thick and 32mm wide. The beam members are Tee-beams with 31.3mm wide × 3.8mm thick flange with a total high of 30.25mm. The whole frame measures 2 metres high and 0.59 metres wide. The motion of the frame is confined in the *x-z* plane. The finite element model of this structure consists of seventy-two nodes and seventy-five Euler-Bernoulli beam elements. There are seventy unconstrained nodes and two constrained nodes at the ground supports. However each unconstrained nodes has only one accessible degree-of-freedom. The column nodes and beam nodes have the accessible degrees-of-freedom in *x*- and *z*-direction, respectively. The cross-sectional areas of the column and beam elements are $142.4\times10^{-6}\,m^2$ and $230.03\times10^{-6}\,m^2$, respectively. The second moments of inertia of the elements in the plane of bending are $2.35\times10^{-10}\,mm^4$ and $23.5\times10^{-9}\,mm^4$, respectively.

Since the assessment is based on the eigenvector changes due to damages, the eigenvectors at all the accessible degrees-of-freedom under the multi-damage states are measured in the experiment. The measured eigenvector changes due to damage in each damage state can then be determined in the experiment. Comparison on the damage assessment using different methods would be based on a subset of this set of measurement as incomplete modal information.

Hammer testing on the structure has been performed by the authors, and mode shapes and modal frequencies have been obtained. However, checking on the inconsistencies of the results reveals that the structure is under forced excitation by

air current from exhaust vents of the air-conditioning system in the laboratory. The experimental results are discarded. The comparison study in this Chapter is based on the experimental work performed by another research student Miss P.S. Mak.

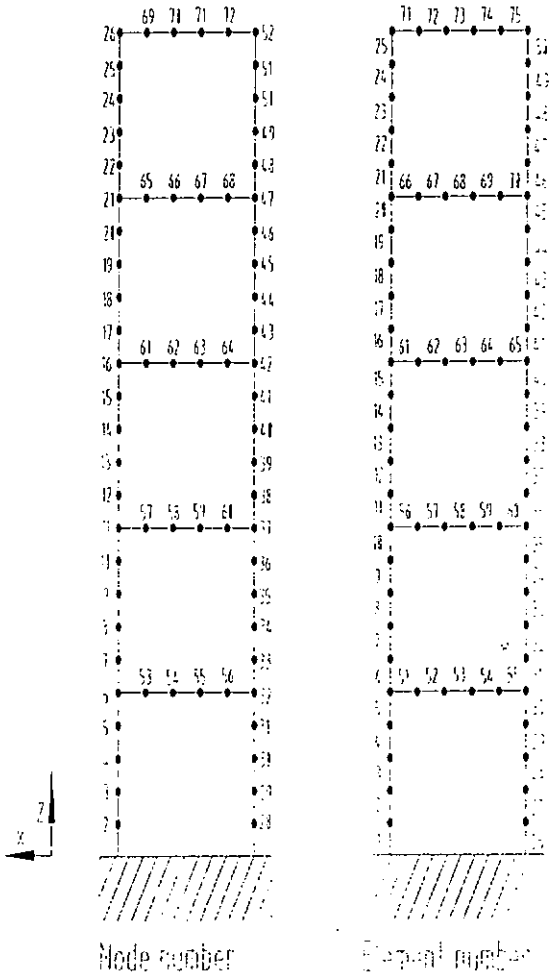

Figure 6.3 – Evaluation view of five-storey plane steel frame

Section 6.4.2) Setup of the experiment

The setup of the experiment is illustrated in Figure 6.4. The random force generated from the exciter is controlled by a signal generator. The force is applied to the bottom plate supporting the steel frame as shown in Figure 6.5, which would be transmitted indirectly to the steel frame. The natural frequencies of the random force covers from 2Hz to 100Hz for identifying the lower five modes which are global modes, and from 30Hz to 316Hz for identifying the remaining higher modes which are local modes of the steel frame.

Seven B&K 4372 accelerometers are placed on the accessible degrees-of-freedom of the steel frame in each measurement, and the acceleration responses at these degrees-of-freedom are digitized directly. Eleven sets of measurements are required to record the all responses at the accessible degrees-of-freedom. In each measurement , a reference sensor is fixed on a degree-of-freedom having larger responses and six moving sensors record the responses at other degrees-of-freedom. Signal from each sensor is then normalized and combined to obtain the full mode shapes.

The signals are sampled with the software package GLOBALAB together with a Data Translation A/D Card DT2829 at a frequency of 249.75023 Hz and 2012.0724Hz for the two sets of lower mode and higher mode measurements respectively. The frequency resolution for the first set of measurement would be 0.061 Hz when a 4096 data is used in the subsequent Fast Fourier Analysis. The

second set of data is decimated further at a ratio of 1 to 4, and the resulting frequency resolution in the Fourier spectrum is 0.0614 Hz. Spectral analysis and modal analysis are performed on these digitized signals. And the mode shapes and the modal frequencies are obtained for different modes.

It should be noted that small pieces of lumped masses are placed at the accessible degrees-of-freedom of the structure as shown in Figure 6.5. The weight of each mass is the same as that of the accelerometer, so that it counteracts the variation of structural mass of the system due to changing locations of the accelerometer in different sets of measurement. Therefore, the distribution of the mass of system is the same for different sets of measurement.

After completion of the data collection on the state with no damage in the frame, the procedures described in the last few paragraphs are repeated for the following damage states: (a) with single damage in element 6; (b) with two damages in elements 6 and 23; and (c) with three damages in elements 6, 23 and 53. It is noted that element 6 is located at the column just above first level. Element 23 is at the column between the fourth and fifth levels. Element 53 is located at the middle of the beam at first level.

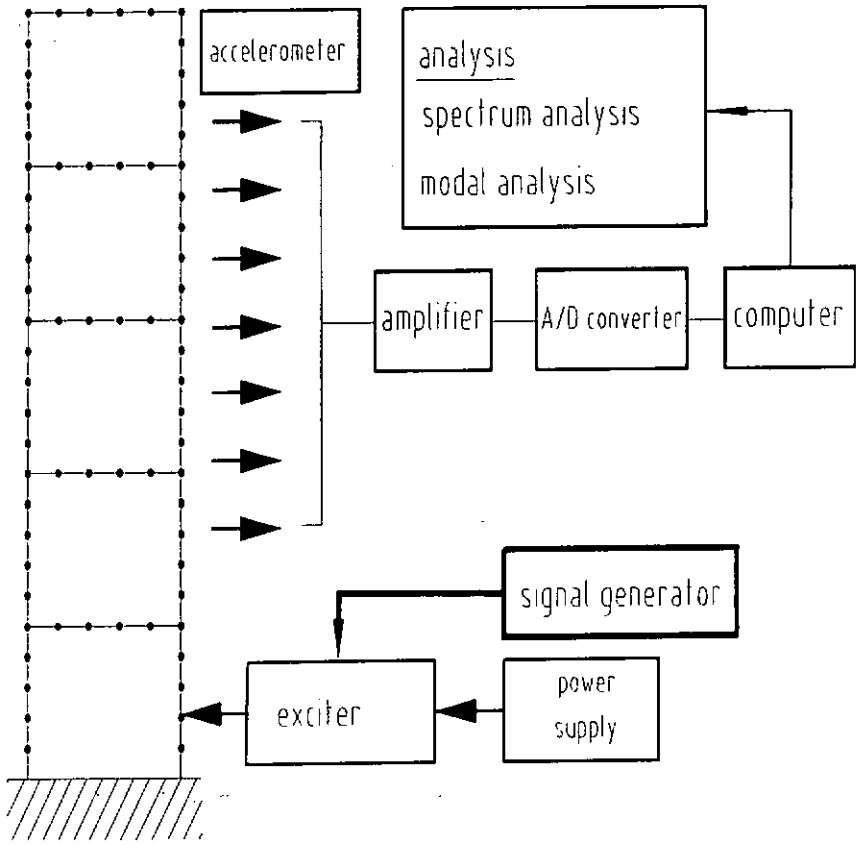

Figure 6.4 – Experimental setup to measure complete mode shapes

Figure 6.5 – Photograph of experimental setup

Section 6.4.3) Identification of eigenvalues and eigenvectors of the damages stages

The modal frequencies for the four different states of the structure are listed in Table 6.3 together with those from the analytical model of the structure. The mode shapes for the first five global modes and four local modes in the initial state are shown in Figure 6.7. Moreover, the eigenvectors of the different damaged states are also measured.

Table 6.3 – Natural frequencies for different damage states

Damage states	Global modes (Hz)					Local modes (Hz)			
No damage	4.207	12.439	20.304	26.829	31.463	145.956	154.123	181.877	188.939
First damage	4.146	12.439	20.243	26.707	31.402	145.895	154.062	181.877	188.939
Second damage	4.146	12.439	20.243	26.707	31.402	145.649	153.877	181.877	188.939
Third damage	4.146	12.439	20.243	26.707	31.402	nil	153.816	181.816	188.816

The measured mode shapes and natural frequencies of the undamaged structure may have slight differences from the analytical results. The mode matching is then applied for determining the mode shapes in the initial state and the corresponding natural frequencies are then identified for these modes. It should be noted that the mode matching is the correlation between the two corresponding mode shapes, such as the measured and the analytical mode shapes.

When many damage elements exist in the structure, the mode shapes of the damaged structure change with a great extent from those of the undamaged

structure. The identification of mode shapes in the damage state is then made use of the natural frequency. The natural frequency of the damaged structure changes and peaks in the frequency response function of this structure also shift. However, the natural frequencies of the modes in the damage and undamaged structures are similar. Therefore the eigenvectors for each mode of the damaged structure are then identified as those having a similar natural frequency in a previous damaged state.

The natural frequency changes due to many damages in a structure may shift up or down. In reference with the observation from (Cobb and Liebst 1997), the natural frequency change of the flexible structure generally shifts down when damaged. In the measurement of the steel frame, the natural frequencies of the damaged structure also slightly reduce when damaged. It should be noted that the natural frequency changes in global modes are negligible. Since the small damages on the structure are only allowed. These small damages do not influence the overall performance of the structure and also the natural frequencies in the global modes. The sequence of the eigenvector changes of the structure under multi-damage states are displayed in Figure 6.8 for the local mode of 188.939Hz.

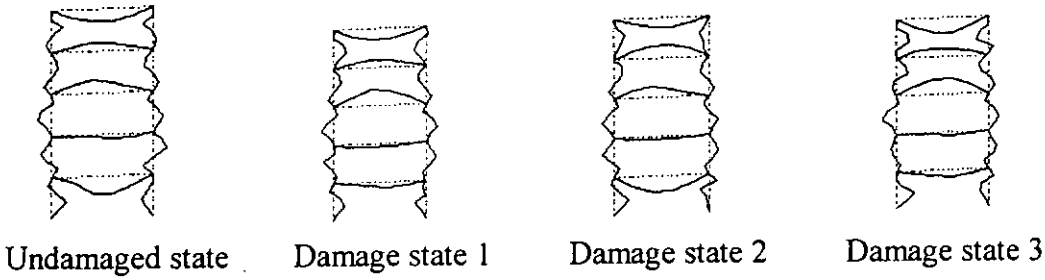

Figure 6.6 – Eigenvector change at 188.939Hz mode for multi damage states

According to Figure 6.6, the overall view of mode shapes under multi-damages states change gradually. However, the amplitude of vibration of the structure varied locally with a great extent. Therefore, the damage elements influence the mode shapes locally. And the comparison of monitoring from different sensor locations is beneficial to base on eigenvector changes, since the information collected at different sensor locations is locally sensitive to the damage elements.

From another point of view, the identification of modes can be carried out by the use of correlation between two damage states. The correlation of the experimental and analytical modes of the initial state is obtained by mode matching and by inspection of the Modal Assurance Criterion (*MAC*) as shown in Table 6.4. for multi-damage states, the *MAC* can act as a guidance for identification of modes. According to Table 6.4, most of the modes have the higher *MAC* values greater than 0.9. Poor correlation is found at two occurrences between the local modes from the second damage state and the analytical modes with the *MAC* smaller than 0.7.

Table 6.4 – Correlation of mode shapes between different damage states

State of Structure	Modal Assurance Criterion (*MAC*)								
Analytical requencies(Hz)	4.364	12.987	21.163	28.139	32.791	150.37	159.905	198.752	204.115
No damage	0.998	0.993	0.997	0.998	0.995	0.726	0.952	0.868	0.876
Single damage	0.999	0.995	0.996	0.997	0.993	0.815	0.969	0.918	0.793
Two-damages	1	0.997	0.998	0.999	0.996	0.661	0.946	0.661	0.883
Three-damages	0.999	0.995	0.998	0.996	0.994	Nil	0.951	0.847	0.791

There is a natural frequency of the local mode missing in Table 6.3 and 6.4, because the mode shapes of the structure having three damage elements are unsuccessful to be matched. It may be because the number of damage elements on a structure is large so that the eigenvector changes of the damaged structure are unpredictable and complicated for visual identification.

In conclusion, the mode shapes of the structure change significantly due to damages such that the mode matching between measurement and analysis in two damage states is difficult. And damage is insensitive to the natural frequency in the global modes. This suggests a potential difficulty in identifying local modes in a complex structure when there are several damages in it, or when the damages are large causing large changes in the mode shapes.

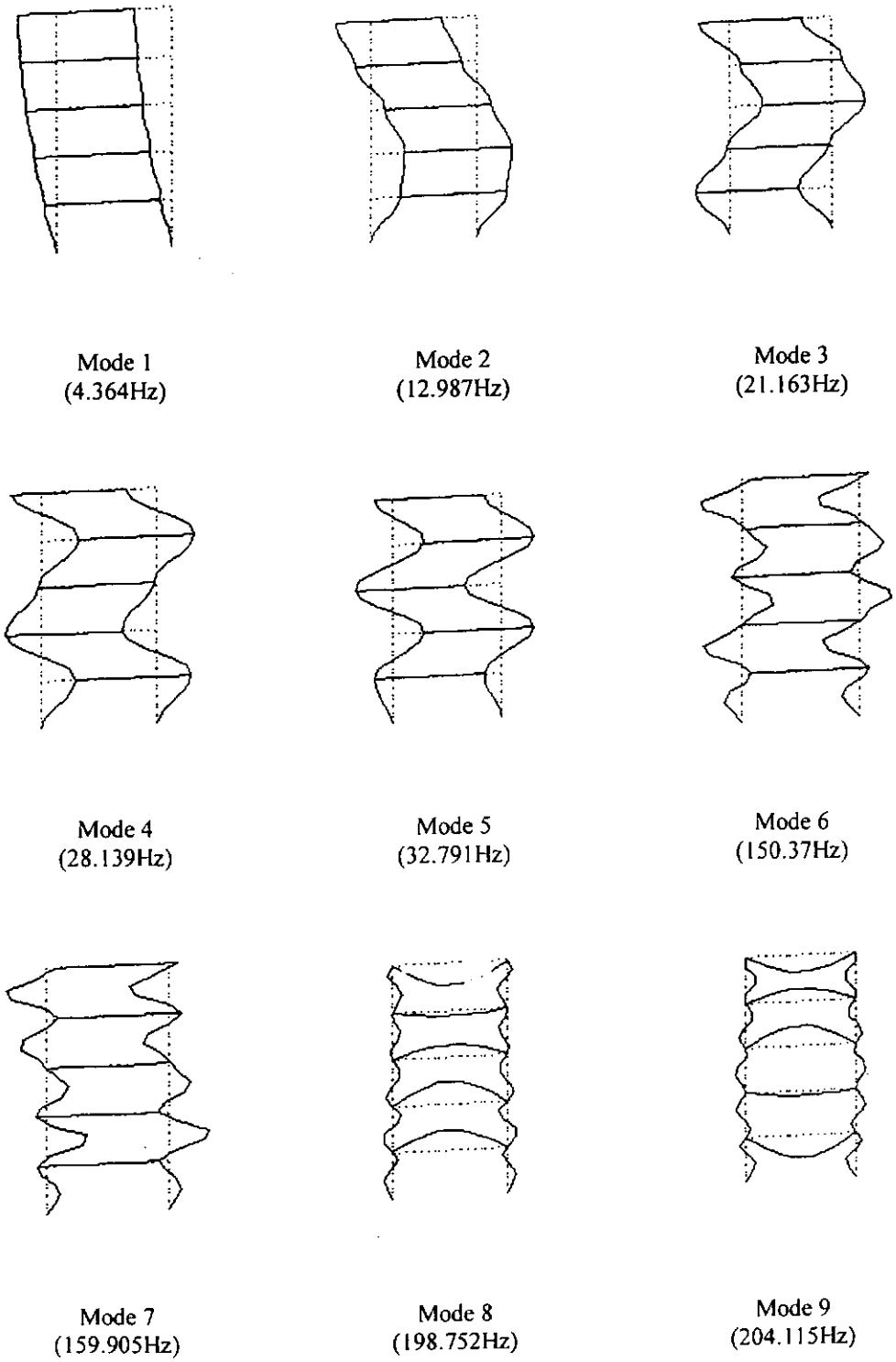

Figure 6.7 – Mode shapes of undamaged five-storey plane steel frame

Section 6.4.4) Damage in the test structure

In the experiment, damage in an element is created with a saw cut of 1.0mm width and of different depth located at mid-length of the element. The depth of the cut in elements 6, 23 and 53 are 8mm, 4mm and 6mm respectively on both sides of the member. The cut for element 53 is in the flange.

Damage in an element has been defined most generally as a scalar reduction in the stiffness of the element. The exact damage extent of an element in the present study is determined as a fractional reduction of its elemental stiffness matrix. The elemental mass matrix is assumed unaffected by the existence of the saw cut. An equivalent member of uniform cross-section is reconstructed from the cracked member with the same volume of material. The original thickness is retained, and the width of the equivalent element is calculated due to damage. The damaged stiffness matrix $\boldsymbol{K}^d$ of the element in its local coordinate system is then evaluated basing on this reduced equivalent width.

The damaged stiffness matrix K^d is then represented by the product of a reduction ratio μ and the analytical stiffness matrix $\boldsymbol{K}$ of the undamaged element as formulated in Equation (6.9). Multiply both sides of Equation (6.9) by the inverse of the analytical stiffness matrix, the eigenvalue equation can be obtained as Equation (6.10). The ratio μ can then be determined by taking the determinant of the left-hand-side of Equation (6.10) equals to zero. The fundamental mode of the solution yields the reduction coefficient.

$$K^d = \mu K \tag{6.9}$$

$$K^{-1}\left(K^d - \mu K\right) = 0$$

$$\left(K^{-1}K^d - \mu I\right) = 0 \tag{6.10}$$

$$\left|K^{-1}K^d - \mu I\right| = 0 \tag{6.11}$$

where K^d is the stiffness matrix of a damage element in its local coordinates; $\boldsymbol{K}$ is the analytical stiffness matrix of an element without damage; μ is the reduction ratio of percentage change of the undamaged stiffness matrix, which can be interpreted as the damage extent.

The damage extents for the damage elements are obtained from Equation (6.11) and they are tabulated in Table 6.5 as percentage change. The damage extent of element 6 is the largest among the three damage elements. It is approximately twice of that of element 23. Damage extent of element 53 is the smallest. Though the saw cut is longer than that in element 23, it is created in the flanges which does not has a significant reduction on the bending stiffness. Moreover, the beam element is stiffer than the column element. So the percentage change due to 6mm cut is also small.

Table 6.5 – True damage extent of damage elements in five-storey steel frame

Element number	Percentage change (%)
Element 6 (first damage state)	0.625%
Element 23 (second damage state)	0.298%
Element 53 (third damage state)	0.278%

Section 6.5) Verification of the test structure

Section 6.5.1) Verification in the multi-damage states with the proposed method

The damage sites are at elements 6, 23 and 53. These damage elements are also detectable in the proposed method. Target modes should be selected for each Target Group of interested elements. However, in this present study, all the vibration modes obtained from the experiment are used. The natural frequencies of these vibration modes are shown in Table 6.3.

Firstly, in the proposed method, the comparison on damage assessment is based on different interested element assembled into a Target Group. For each of the Target Groups, the sensor locations are evaluated with the proposed method using different threshold values for the corresponding criteria, which are given below. These threshold values are the same for different Target Groups for the same comparison.

Threshold for undetectable element	0.1×max(Total Detectability)
Threshold for sensor placement ratio	0.25×max(sensor placement ratio)
Threshold for leverage point	$2m/n$

These sensors which are based on the proposed method are placed around the analyzed elements and monitor these elements effectively, when these analyzed elements are assembled into a Target Group. So selection of different Target Groups means that different selected elements are concerned for the health monitoring. These elements are then classified as the consistent elements with respect to a sensor location, which are monitored by the corresponding sensor efficiently and reliably, because the sensitivity parameter of the corresponding sensor with respect to these elements is high.

Afterwards, the effects of multi-damage states on the damage assessment are also included in the verification analysis. Finally, the efficiency in damage assessment using the different sensor placement methods is also investigated by using corresponding incomplete modal information.

Six Target Groups of interested elements have been identified for the comparison, and they are shown in Figure 6.8. The bolded lines coincide with the columns or beams in the frame denote the target elements. These element groups are selected to include a single or more damage elements. Target Groups 1, 2 and 3 include elements 6, 23 and 53 respectively. Target Group 4 includes both elements 6 and 23. Target Group 5 is an anti-symmetric group of elements to Target Group 4.

Target Group 6 includes all three damage elements. Groups 1, 2, 3, and 4 are used in the study of the first damage state. Groups 1, 2, 4 and 5 are used for the second damage state to study the efficiency of sensors for groups with or without both damage elements, and the efficiency of sensors for the anti-symmetric Group 5. Groups 3, 4, and 6 are used for the third damage state to study the efficiency of sensors from Groups 3 and 4 which do not include all damage elements, and from Group 6 which includes all damage elements.

Each sensor location is therefore related to a group of consistent elements. Groups of ten sensors selected to monitor all the consistent elements in each Target Group are listed in Table 6.6. The number of selected interested elements is about fifteen to twenty in each Target Group. Thus, ten sensors are also effective to monitor the interested elements. Since only one degree-of-freedom is accessible at a node in the x-z plane of the frame, node numbers are again given as the sensor locations. It should be noted that the number of interested elements must not be less than the number of target modes due to Assumption VII. Otherwise, the analysis of the proposed method cannot proceed.

Table 6.6 – Sensor locations for corresponding Target Groups

Target Group No.	Number of Interested Element In Target Group	Sensor Location (Node Number)	Consistent Element Number
1	11-25	13, 18, 19, 22, 23, 24, 39, 40, 45, 50	11, 13, 15, 16, 18, 20, 21, 22, 23, 24, 25
2	1-15	2, 3, 5, 8, 9, 13, 34, 35, 39, 40	1, 2, 3, 5, 6, 7, 8, 10, 11, 13, 15
3	51-65	8, 34, 35, 53, 54, 56, 57, 60, 61, 64	51, 52, 53, 54, 55, 57, 58, 59, 62, 63, 64
4	1-25	2, 5, 8, 11, 15, 16, 37, 42, 44, 50	1, 2, 4, 5, 6, 7, 9, 10, 11, 12, 14, 15, 16, 17, 19, 20, 22, 25
5	26-50	11, 16, 18, 24, 28, 31, 34, 37, 41, 42	27, 29, 30, 32, 34, 36, 37, 39, 40, 41, 42, 44, 47, 49, 50
6	1-25, 51-55	2, 3, 12, 18, 29, 33, 35, 45, 53, 57	1, 2, 3, 5, 6, 7, 8, 10, 11, 13, 15, 18, 21, 22, 23, 24, 25, 51, 52, 53, 54, 55

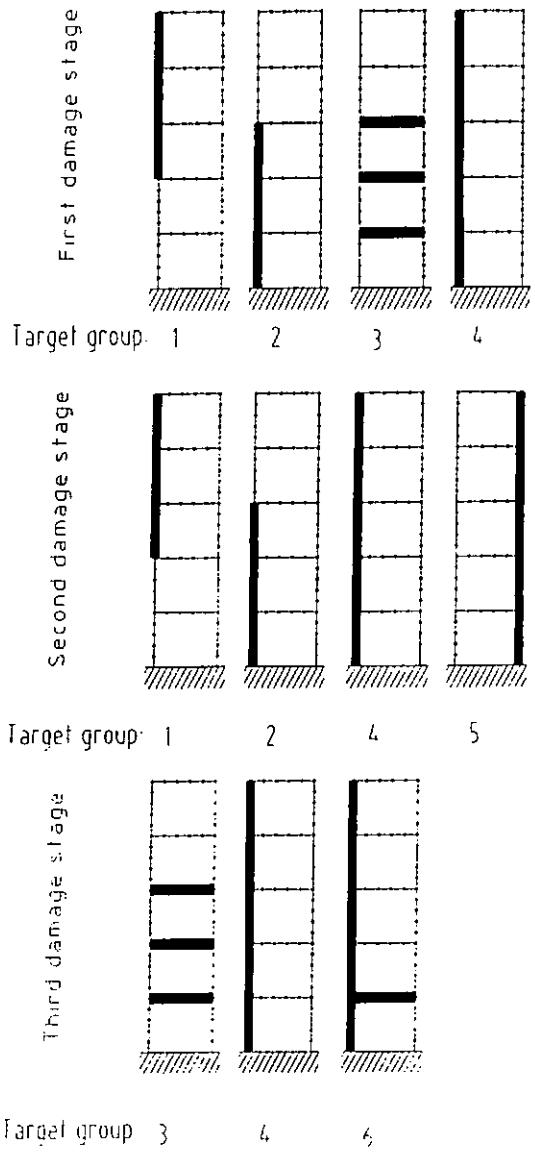

Figure 6.8 – Different target elements in five-storey plane steel frame

Section 6.5.2) Verification in the multi-damage states with other methods

The sensor locations obtained from the Effective Index Method and Co-linearity Matrix Method by methods (i) and (ii) are listed in Table 6.6. The comparison on damage assessment with these methods is based on the ability of different sensor locations collecting the modal information.

Table 6.6 – Summary of sensor locations from different sensor placement methods

	Sensor locations									
Effective Index Method	6	11	16	23	34	39	47	52	54	70
Co-linearity Matrix Method (i)	3	7	8	17	18	23	29	30	39	49
Co-linearity Matrix Method (ii)	3	11	16	18	29	34	39	41	54	58

Section 6.5.3) Comparison using different Target Groups with proposed method

Section 6.5.3.1) Effects of different Target Groups on damage localization

The effectiveness of damage localization for different Target Groups can be judged by using the ranking order of the *MDLAC* values of the damage element. For a Target Group, the MDLAC value of a true damage element has a relatively high ranking order. This Target Group is then beneficial to localize the damage element. The *MDLAC* values of all the consistent elements in the six Target Groups are computed and averaged over the number of modes, and the *MDLAC* values for different damage elements are ranked.

The ranking of *MDLAC* values of elements 6, 23 and 53 for different Target Groups in the third damage states are shown in Table 6.7. The ranking of these *MDLAC* values is compared with the different Target Groups in the proposed method. It should be noted that Table 6.7 shows the ranking order in each Target Group of analyzed elements only. The ranking basing on all 75 elements of the steel frame are shown in Table 6.8. The ranking of these *MDLAC* values is compared for all the sensor placement methods described previously. Values shown in bracket are the results of localization including the consideration of different target modes. The number of target modes is based on the target mode identification for each analysis of each Target Group. The *MDLAC* values are also plotted in Figures 6.10 to 6.13 for illustration. The following observations are related to the localization results.

Table 6.7 – *MDLAC* ranking for damage elements of each Target Group

		Order in the ranking of *MDLAC*					
	Number of Consistent Element in the group	First damage State	Second damage State		Third damage State		
Damage Element		6	6	23	6	23	53
Target Group 1	15	-	-	4	-	-	-
Target Group 2	15	6	8	-	-	-	-
Target Group 3	15	-	-	-	-	-	5 (3)
Target Group 4	25	14	14	15	9 (9)	20 (21)	-
Target Group 5	25	-	-	-	-	-	-
Target Group 6	30	-	-	-	14	21	15

Note: Values shown (•) denote results with the inclusion of Target Mode selection.

Table 6.8 – *MDLAC* ranking based on all 75 elements

	Order in the ranking of *MDLAC*					
	First damage State	Second damage State		Third damage State		
Damage Element	6	6	23	6	23	53
Target Group 1	68	65	24	-	-	-
Target Group 2	25	49	43	-	-	-
Target Group 3	12	-	-	4	46	28
Target Group 4	49	50	52	41	73	11
Target Group 5	-	33	49	-	-	-
Target Group 6	-	-	-	49	67	52
EIF Method	70	65	52	65	62	39
Co-linearity Method (i)	11	8	12	26	47	49
Co-linearity Method (ii)	56	48	49	37	28	71

In the first damage state, the effectiveness of sensors for different Target Groups on localizing damage in element 6 are ranked in the descending order of 2, 3, 4 and 1 as shown in Figure 6.9. It is noted that element 6 is a consistent element in both Groups 2 and 4. The high *MDLAC* value for Group 3 is due to the fact that element 6 is directly connected to element 53, which is also a consistent element of this group.

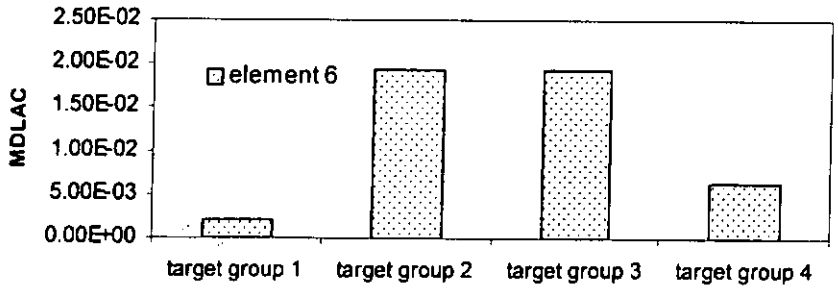

Figure 6.9 – *MDLAC* values with different Target Groups in first damage state

In the second damage state, sensors for Target Group 1 are effective to localize damage in element 23, while damage in element 6 does not show up distinctly good performance in all groups under consideration as shown in Figure 6.10. The element 23 is a consistent element in Group 1. Element 6 is a consistent element for Groups 2 and 4, and both Figure 6.10 and Table 6.7 indicate sensors for Group 2 is more efficient in the localization than that for Group 4.

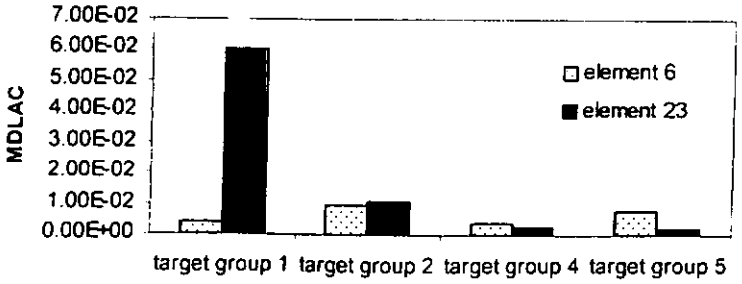

Figure 6.10 – *MDLAC* values with different Target Groups in second damage state

It is noted that the sensors for Target Groups 4 and 5 are symmetrical on the steel frame, as the interested elements in the two groups are also geometrically symmetric. The element 6 is not a consistent element in Group 5, but in Group 4.

The damage information generated from an element and collected by symmetrical sensors should not be the same, and therefore sensors for Groups 4 and 5 have different performances in the damage localization for damage element 6.

In the third damage state, sensors for Target Group 3 are distinctly effective to localize damage in element 53 as shown in Table 6.7, and damage in element 23 cannot be localized using any group of sensors according to Figure 6.11. It is noted that element 53 is a consistent element for Groups 3 and 6 but not Group 4.

The localization of elements 6, 23 and 53 as discussed above are supported by their ranking of the *MDLAC* based on all elements of the structure as shown in Table 6.8. The selected sensor locations according to the proposed method are relatively effective to localize the damage elements based on some Target Groups. All the corresponding Target Groups indicate that the damage elements are ranked in the upper third of the group.

There is significant improvement in the *MDLAC* for Target Groups 3 and 4 in the third damage state when target modes are considered. The *MDLAC* value for elements 23 and 53 increase by approximately four times for Group 3 as seen in Figures 6.12 and 6.13, and that for element 6 almost triples for Group 4. The ranking of element 53 for Group 3 advances from the fifth place to the third place in Table 6.7 while no significant improvement occur in the other cases. Inspection of the target modes for these two groups shows that the modal information from modes 3 to 5 at the selected sensor locations contains few damage information

from element 53, while modes 8 and 9 contains few damage information from element 6 and 23 at the selected sensors.

Therefore, it is necessary to select the target modes to make the interested elements sensitive to the damage, when the total number of target mode is kept constant. When the number of modes increases in the analysis, the collected damage information also increases to benefit the analysis. This can be supported by the value of percentage change for different number of target modes according to Table 6.9, which will be discussed later.

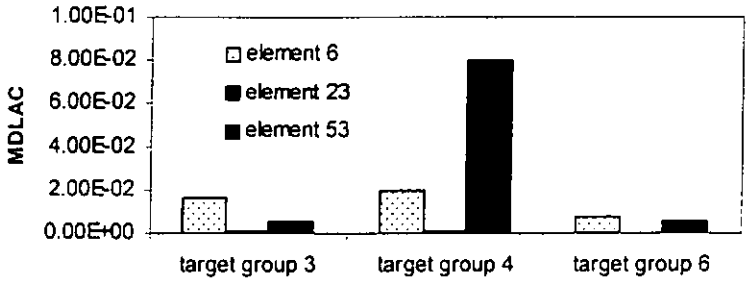

Figure 6.11 – *MDLAC* values with different Target Groups in third damage state

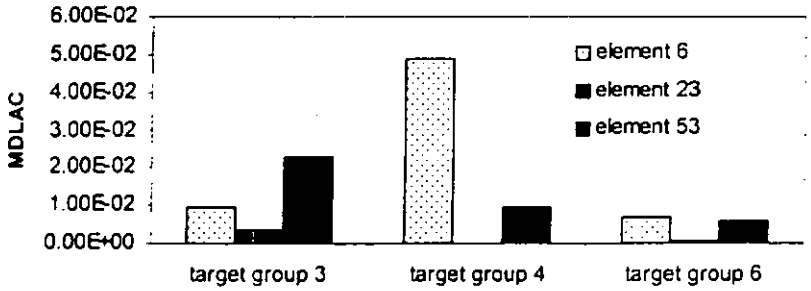

Figure 6.12 – *MDLAC* values with different Target Groups in third damage state (based on target mode)

The *MDLAC* approach in damage localization assumes that the information from individual damage element for the calculation of the correlation parameter is independent. This possible interaction of the damage information from several elements affects the *MDLAC* values resulting in less accurate damage localization result. This argument is supported by results from Tables 6.11 to 6.12 where damage localization and quantification in the first damage state are more accurate in general than those in the multi-damage states.

Section 6.5.3.2) Effects of different Target Groups on damage quantification

The effectiveness of damage quantification using the different sensor placement methods will be gauged basing on the difference between the true damage extent and the calculated values from corresponding incomplete modal information. The calculated damage extent of these elements is identified and they are given in Table 6.9.

In the first damage state, sensors for Target Group 2 give more accurate damage extent for element 6 than the sensors for other groups. This is consistent with the localization result as discussed before.

Table 6.9 – Damage quantification in different damage states

	Identified Percentage Reduction in Stiffness (%)					
	First damage State	Second damage State		Third damage State		
Damage Element [true damage %]	6 [0.625]	6 [0.625]	23 [0.298]	6 [0.625]	23 [0.298]	53 [0.278]
Target Group 1	0.15	0.05	0.02	-	-	-
Target Group 2	0.30	0.05	0.03	-	-	-
Target Group 3	0.06	-	-	0.01 (0.007)	0.002 (0.003)	0.002 (0.003)
Target Group 4	0.14	0.05	0.02	0.31 (0.014)	0.15 (0.007)	0.14 (0.006)
Target Group 5	-	0.43	0.02	-	-	-
Target Group 6	-	-	-	0.01	0.002	0.002
EIF Method	0.06	0.04	0.02	0.05	0.02	0.02
Co-linearity Method (i)	1.17	0.34	0.16	0.06	0.02	0.02
Co-linearity Method (ii)	0.52	0.35	0.17	0.05	0.02	0.02

Note: Values shown (•) denote results with the inclusion of Target Mode selection.

In the second damage state, sensors for Target Group 5 give very close to true damage extent for element 6. Damage in one leg of the frame generates damage information which is collected by sensors at a set of symmetric degrees-of-freedom on both legs. Both sets of sensors should have the same effectiveness. However, the presented result indicates that the damage information collected on the other side of the frame would be much better than that collected on the same side of the damage. This damage information would most probably be beneficial in the first few modes which are the global modes of the structure with dominating horizontal

vibration in the columns. The result is consistent with the ranking of element 6 in the group of all elements in Table 6.8 which shows a much higher ranking of *MDLAC* for sensors from Group 5 than Group 4. However, this result somewhat deviates from the prediction of the Consistent Element Method since element 6 is not a consistent element in Group 5.

Target Group 4 gives estimates on the damage extent of the elements 6, 23 and 53 in the third damage state which are all approximately half of the true values when all measured modes are used. This good prediction is not consistent with the localization result in Tables 6.7 and 6.8, but it is noted that elements 6 and 23 are consistent elements in Group 4.

For the quantification with different number of target modes, the calculated damage extent with a small number of target modes is much less than those with all nine target modes. And it cannot quantify the true damage accurately. Therefore, it may be concluded that the accuracy of damage quantification improves with more damage information included in the analysis.

Section 6.5.3.3) Effects of damage sequence on damage assessment

In damage localization, Target Group 4 is selected under all three damage states. The *MDLAC* values of damage element 6 for Target Group 4 are then plotted for three damage states in Figure 6.13. Basing on the sensors from the Target Group 4.

the effectiveness of damage localization of element 6 decreases in second damage state, and then increases with the highest *MDLAC* values in the third state.

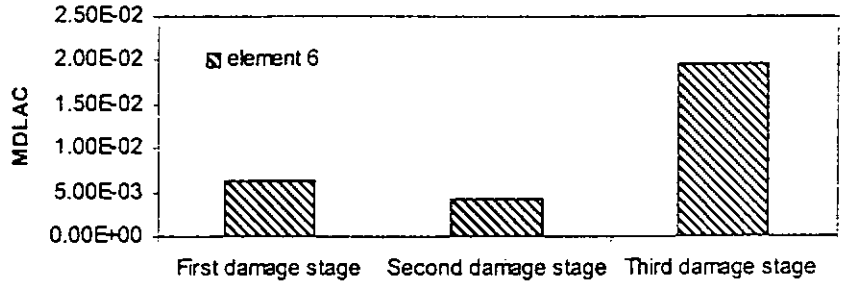

Figure 6.13 – *MDLAC* values with Target Group 4 for all three damage states

For the same Target Group 4, the percentage change of damage element 6 for all three damage states are shown in Figure 6.14. The sensors for Target Group 4 can quantify the damage element 6 most precisely in the third damage state. It is evident that the damage assessment of element 6 is most beneficial in the third damage state with Target Group 4. Moreover, the results of damage localization and quantification are consistent for these multi-damage states.

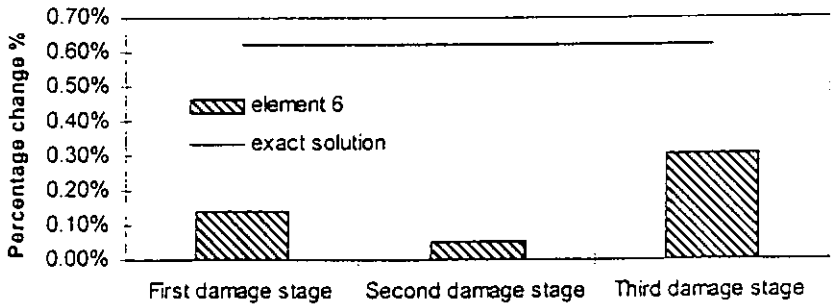

Figure 6.14 – Damage extent with Target Group 4 for all three damage states

For Target Group 2, the *MDLAC* value of damage element 6 is comparatively larger in the first damage state, according to Figure 6.15. This indicates that the effectiveness in localization of element 6 is reduced for multi-damage states.

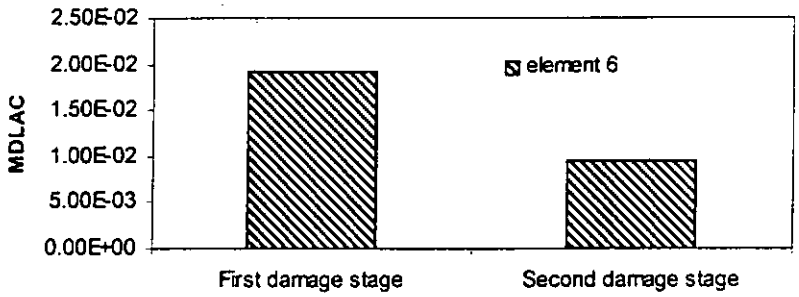

Figure 6.15 – MDLAC values with Target Group 2 for all three damage states

Also, in the damage quantification according to Figure 6.16, the percentage change of element 6 for Target Group 2 becomes less accurate for multi-damage states.

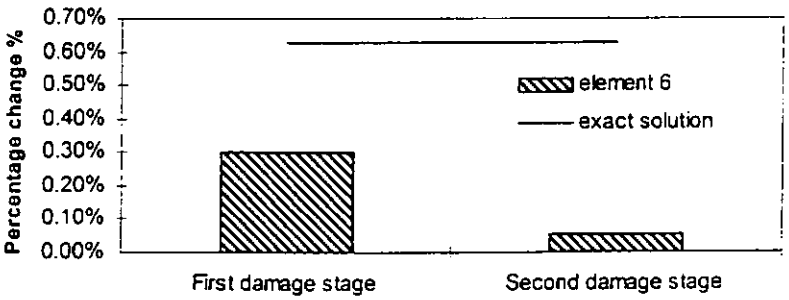

Figure 6.16 – Damage extent with Target Group 2 for all three damage states

Form the above results, the damage localization and quantification are also worse in performance in the second damage states. It should be concluded that the damage configurations influence the effectiveness of the damage assessment. And

the effectiveness of damage assessment not only depends on the sensor locations, it also depends on damage configuration.

It should be reminded that, under multi-damage states, there is an interaction of the damage information from the several elements, because the damage information from an element can interfere with those from another element. The damage information collected at a degree-of-freedom is then coming from two damage elements. In other words, when a sensor obtains this combined damage information from two elements to localize and quantify a damage in an element, the effect of another damage elements is inevitable taken into account for the assessment of this element. It may therefore worsen the accuracy of the damage assessment for this element under multi-damage states. And it is difficult to cope with this problem at this stage.

Section 6.5.4) Comparison between the different sensor placement methods

The *MDLAC* values obtained from other methods are plotted in Figures 6.17 to 6.19 for comparison, and the ranking of the *MDLAC* from other methods are also shown in Table 6.8. The damage quantification results are shown in Table 6.9.

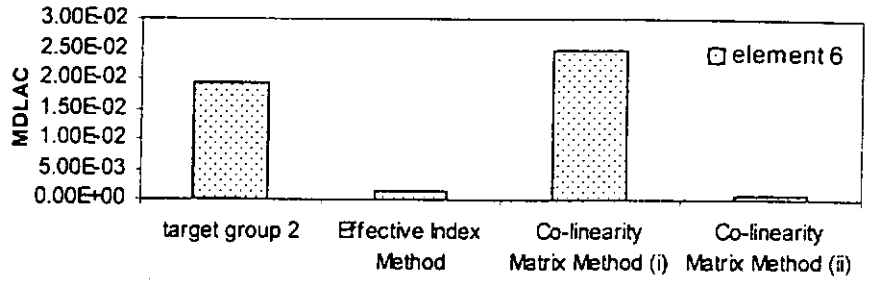

Figure 6.17 – *MDLAC* values with different methods in first damage state

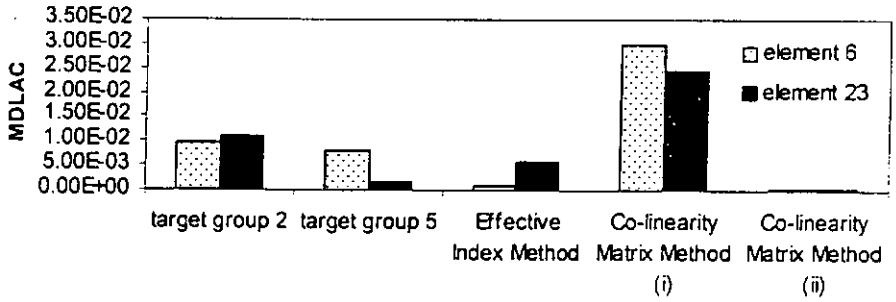

Figure 6.18 – *MDLAC* values with different methods in second damage state

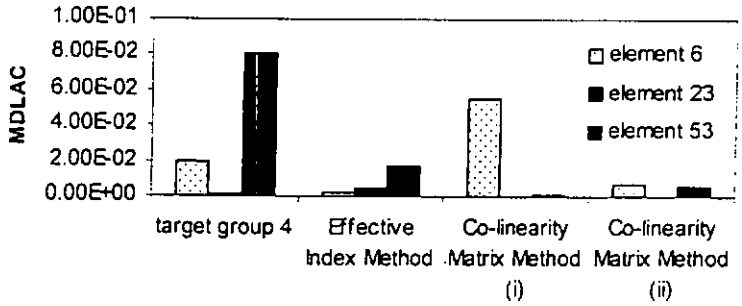

Figure 6.19 – *MDLAC* values with different methods in third damage state

Both the *MDLAC* values and their ranking in the group show that Co-linearity Matrix Method (i) give the best results in localization and quantification in general. Both methods (i) and (ii) give an estimated damage which is about half of the true values in the second damage state, while method (i) can localize the damage

elements 6 and 23 with a very high ranking at the 8th and the 12th position in the group of all elements. It also ranks element 6 in the 11th place for the first damage state. Method (ii) gives a close to true damage extent in the first damage state. The Effective Index Method fails to indicate anything significant in all three damage states.

Co-linearity Matrix Method (i) is better than Method (ii) in both the damage localization and the quantification. This indicates that co-linearity of measured information may not be an essential requirement for damage detection, and the amount of damage information collected would be a controlling factor in damage assessment.

Section 6.5.5) Summary on the effectiveness of the method in damage assessment

When a few of the damage elements are localized on a structure, it is favourable to have the damage element included in the Target Group as the interested elements. The results reported herein indicate that the damage identification is also effective, when the interested elements in the Target Group is adjacent to the damage.

The effectiveness in damage localization and quantification of the symmetric Target Groups 4 and 5 is similar, when the structure and the damage are geometrically and structurally symmetric. However, for the damage quantification of damage elements 6 and 23, the damage detection by the sensors for Group 5 is better than that for Group 4. This gives evidence that the co-linearity in the

collected information from different sensors is not a requirement for sensor placement.

The sensor locations basing on Target Group 4 is beneficial to localize and quantify the damage in elements 6, 23 and 53 in the third damage state. However, they are less effective than other Target Groups in damage assessments under both the first and second damage states. Some evidences are found showing that the damage configuration as well as the sensor locations can influence the effectiveness of the damage assessment.

Measurement errors effect the identification of mode shapes particularly in the higher modes bringing adverse effects in the *MDLAC* values and hence in the damage detection results. It is because the pattern of eigenvector and eigenvalue change is difficult to predict. There is no comprehensive tool for identification of mode shapes with multi-damage correctly in the present stage.

The proposed method with Target Groups provides an efficient monitoring of the damage elements in general. And, for a particular Target Group, the damage assessment from the proposed method is better than the Effective Index Method in most cases. The Co-linearity Matrix Method is relatively beneficial in monitoring the damage elements in some circumstance.

Chapter 7

Application on Tsing Ma Bridge

Section 7.1) Background of Tsing Ma Bridge

Section 7.1.1) Introduction

A new airport and new town developments are located on the north of the Lantau Island in Hong Kong. The important part of the transportation network between the new facilities and the existing urban areas is the Lantau Fixed Crossing. In this transportation network, the long suspension Tsing Ma Bridge is the main structure carrying a dual three-lane highway. Since the Tsing Ma Bridge is built in a typhoon region carrying both highway and railway, the bridge would suffer from the dynamic wind and traffic loading. This kind of loading easily induces damages, such as fatigue, crack and fracture on this structure. Therefore health monitoring for this kind of structure plays an essential role to ensure a safe linkage between the new airport and the urban areas.

No *a priori* knowledge of the damage location is assumed, and contributions from all structural components, which are assumed to be damaged, are counted towards the sensitivity at a DOF in the work of (Cobb and Liebst, 1997). This does not take into account of the high sensitivities from a few of the potential damage elements. This results in that all sensors will then localize particularly for a few of highly

sensitive elements with little consideration from other interested elements in general. Intuitively, it therefore results in some of the damaged elements of interest would be difficult to detect with the sensors selected basing on the criteria of sensitivity. This problem becomes worse particularly for a large civil structure, because a large number of structural components normally contain a few highly sensitive elements. And it is impossible to place the sensors on all degrees-of-freedom of the large civil structure. In addition, for efficient monitoring, the selection of these sensor locations on the structure should depend on the different damaged elements. A set of sensor locations cannot be expected to monitor all different damage elements at the same time. So an effective sensor placement method should include the possible damage configuration into consideration.

Since the performances of the EFI method has been shown to be very poor in the previous comparisons, the comparison of the sensor placement methods on the Tsing Ma Bridge is made only between the proposed method and the Co-linearity Matrix Method. The health monitoring by different sets of sensors is illustrated in the following for different sensor placement methods. Method (i) of the Co-linearity Matrix Method is conducted in the following analysis.

Section 7.1.2) Main features of the Tsing Ma Bridge

The Tsing Ma Bridge, linking the Tsing Yi Island to Ma Wan Island, has a main span of 1377m between the Tsing Yi Tower and the Ma Wan tower. It is the longest double-deck suspension bridge in the world. The upper deck has two

carriageways each of three lanes for road traffic and the lower deck has two rail tracks and two sheltered emergency lanes.

The height of both towers is 206m. The two main cables are 36m apart and they are accommodated by the four saddles located at the top of the tower legs. The 355.5m Ma Wan side span and the main span are suspended from the main cables by suspenders, and the 300m Tsing Yi side span is supported by a series of concrete piers. The two main anchorages are gravity structures resting on the underlying bed rock located on each side of Tsing Yi and Ma Wan Island. The bridge deck is a hybrid steel structure continuous throughout its length and it consists of Vierendeel cross-frames supported on two longitudinal trusses with stiffened steel plates. The evaluation view of the Tsing Ma Bridge is shown in Figure 7.1.

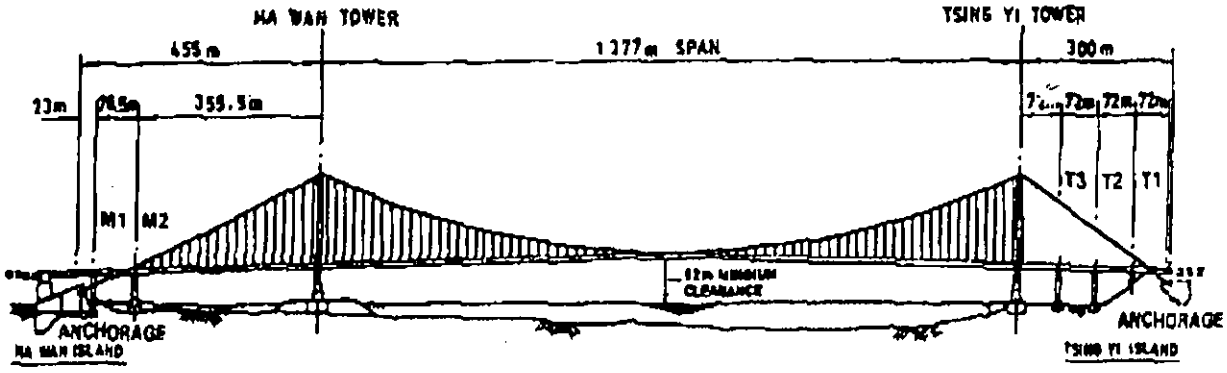

Figure 7.1 – The evaluation view of Tsing Ma Bridge

Section 7.1.3) Finite element modelling of Tsing Ma Bridge

The Tsing Ma Bridge consists of many types of structural components, such as towers, piers, cables, suspenders, longitudinal trusses, cross beams, bridge deck and bearings. For the monitoring process with the proposed method, an appropriate dynamic finite element model of the bridge is therefore required to determine the natural frequencies and mode shapes of the bridge analytically. The towers are then modeled by Timoshenko shear beam elements including the shear effects in the finite element model, which is appropriate for the thick elements. And the other one dimensional elements, such as the longitudinal trusses and cross beams, are modeled by the Euler-Benoulli beam elements. The components of cable are also modeled as the Euler-Benoulli elements.

Since the structural details of the bridge decks comprise a huge sum of components, the deck of long span bridges in the global dynamic analysis is commonly modeled by a single equivalent beam according to Report addressed by Lau (1992). The tremendous computational effort on the global analysis can be then avoided. The sectional properties of the equivalent beam are derived by imposing an appropriate unit displacement or rotation in one of the 12 degrees-of-freedom in turn, when others are equal to zero in the three-dimensional finite element model. The equivalent structural properties include the cross-sectional area, the shear areas in two directions, the second moments of inertia about the two axes, the torsional constant, the centroid, the shear center, the mass per unit length, and the mass moment of inertia.

Table 7.1 – Different Tsing Ma Bridge components in finite element model

Element No.	Structural component	Location
1-119	Bridge decks	(1-26) Main span at Ma Wan side (27-103) Main span (104-119) Main span at Tsing Yi side
120-335	Transverse beams	(120-173) Transverse beams at Ma Wan side (174-335) Main transverse beams
336-458	Left cable	(336-362) Left cable at Ma Wan side (363-439) Main left cable (440-458) Left cable at Tsing Yi side
471-593	Right cable	(471-497) Right cable at Ma Wan side (498-574) Main right cable (575-593) Right cable at Tsing Yi side
606-700	Left suspenders	(606-624) Left suspenders at Ma Wan side (625-700) Main left suspenders
701-719	Right suspenders	(701-719) Right suspenders at Ma Wan side (720-795) Main right suspenders
796-842	Ma Wan tower	(796-831) Tower leg (832-842) Tower beam
861-896	Tsing Yi tower	(861-896) Tower leg (897-907) Tower beam

The number of elements of the Tsing Ma Bridge in the finite element model is 1024. The main structural components denoted by the element number in the finite element model are given in Table 7.1. And the total number of nodes of the finite element method is 777.

Section 7.2) Sensor locations on Tsing Ma Bridge from different methods

Section 7.2.1) Sensor locations from Co-linearity Matrix Method

The sensor locations from Co-linearity Matrix Method applied on the Tsing Ma Bridge are tabulated in Table 7.1 according to the Report presented by Kong (1998). The 6 target modes used in this analysis include 1, 4, 6, 7, 8 and 9. The maximal number of sensors placing on the Tsing Ma Bridge is limited to 40. The sensor numbers are given as ---y. Table 7.2 where --- and y denote the node number and the degree-of-freedom in the translational direction, respectively. For example, *x*, *y* and *z* mean the longitudinal, vertical and lateral directions, respectively. All rotational degrees-of-freedom are excluded from the analysis according to Assumption I.

Table 7.1 – The sensor locations from Co-linearity Matrix Method

Sensor locations
286y, 290y, 291y, 295y, 296y, 300y, 301y, 305y, 306y, 310y, 311y, 315y, 316y, 320y, 321y, 325y, 326y, 330y, 331y, 334y, 336y, 339y, 341y, 344y, 346y, 349y, 351y, 356y, 491y, 494y, 501y, 515y, 520y, 525y, 526y, 530y, 531y, 535y, 540y, 545y

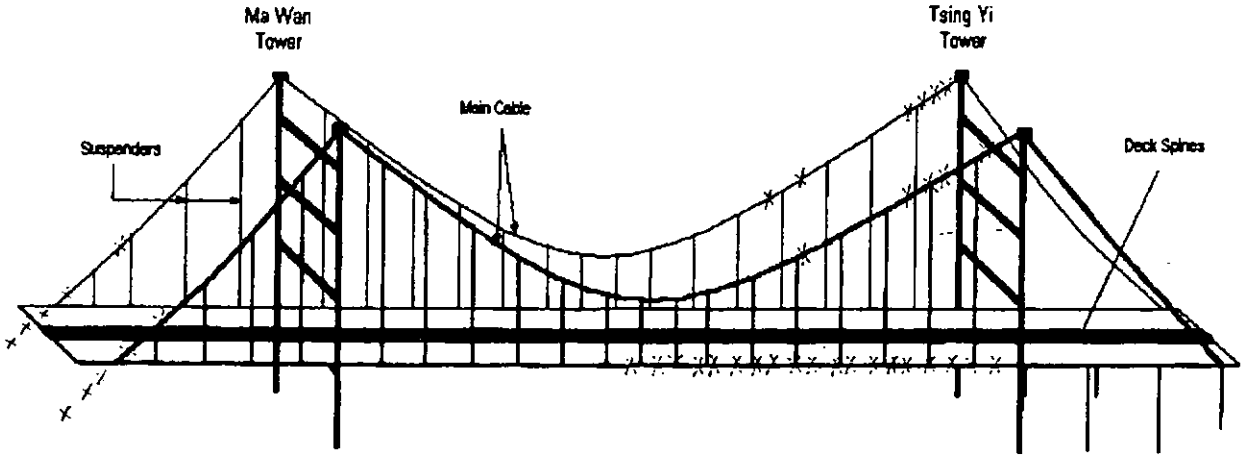

Figure 7.2 – Sensor locations on Tsing Ma Bridge from Co-linearity Matrix Method

The approximated sensor locations on the Tsing Ma Bridge is also shown in Figure 7.2 for illustration. All sensors are placed on the Tsing Ma Bridge in the vertical direction. Most of the sensor locations are congested on one side of the transverse beam are half of the main span on the Tsing Yi side. The remaining sensors are

placed on the cables at the very beginning of the Ma Wan side and near the Tsing Yi Tower.

Section 7.2.2) Sensor locations from proposed method for interested elements

Section 7.2.2.1) Introduction

The sensor locations evaluated from the proposed method can consider the different groups of potential damage elements for monitoring one at each time. These potential damage elements refer to the interested elements as previously described. The set of sensor locations would be different for different groups of interested elements.

In this study, the proposed sensor placement analysis of the Tsing Ma Bridge is divided into four cases for consideration of four different element groups. The interested element groups consist of deck spines at Ma Wan side-span, main deck spines, the cables and the suspenders. However, the deck spines on Tsing Yi side are excluded from the analysis. It is because the continuous deck spines supported by a series of piers, and they are very stiff compared with the other suspended elements. Elements of the towers are also excluded from the analysis due to the same reason. It means that these elements are undetectable basing on the criteria of sensitivity in the proposed method.

The threshold values for different criteria are the same for the different interested element groups so that the comparison is made on the same basis.

Section 7.2.2.2) Target Group of deck spines on Ma Wan side

In the first case, the interested elements include the deck spines on the Ma Wan side-span. The total interested element number is 27. The target modes are from 1 to 20. And the maximum number of given sensor is limited to 40. The sensor locations are shown in Table 7.3. The corresponding sensor locations on the Tsing Ma Bridge is approximately indicated in the Figure 7.3.

Table 7.3 – The sensor locations from proposed method for deck at Ma Wan side

Sensor locations
26z, 32z, 37z, 110z, 111z, 112z, 115z, 116z, 117z, 120z, 121z, 122z, 125x, 127x, 130x, 132x, 135x, 137x, 140x, 140z, 141z, 142z, 142x, 145x, 145z, 146z, 147x, 147z, 150z, 151z, 152z, 155z, 156z, 157z, 161z, 162z, 165x, 167x, 167z

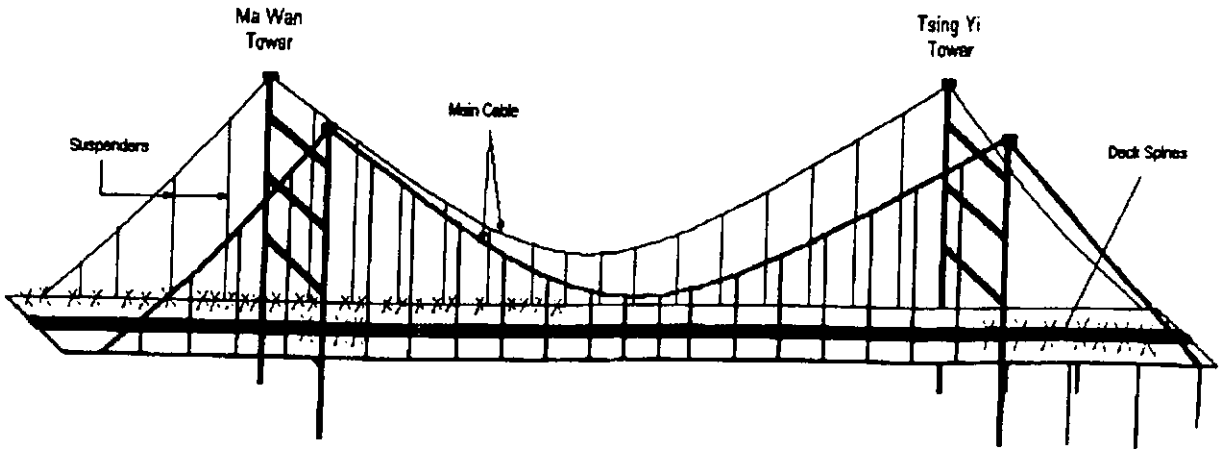

Figure 7.3 – Sensor locations on Tsing Ma Bridge for deck at Ma Wan side

According to Figure 7.3, many sensors are placed in the lateral direction and the other sensors are placed in the longitudinal direction. Most of the sensor are crowded on one end of the transverse beam from the beginning of Ma Wan side-span to middle of the main span. And a few of the sensor locations are located on the central deck spines on Tsing Yi side-span and on the main span close to Ma Wan Tower.

Section 7.2.2.3) Target Group of deck spines on main span

In the second case, the interested elements include the deck spines at the main span. The total number of interested elements is 77. The target modes are from 1 to 20. The 40 sensor locations are displayed on the Table 7.4 and plotted on the Figure 7.3.

Table 7.4 – The sensor locations from proposed method for main deck spines

Sensor locations
272y, 277y, 282y, 287y, 292y, 297y, 302y, 307y, 312y, 317y, 322y, 327y, 332y, 337y, 342y, 347y, 352y, 408y, 413y, 418y, 423y, 428y, 433y, 438y, 502y, 507y, 512y, 517y, 522y, 527y, 532y, 537y, 542y, 547y, 552y, 557y, 562y, 567y, 572y, 577y,

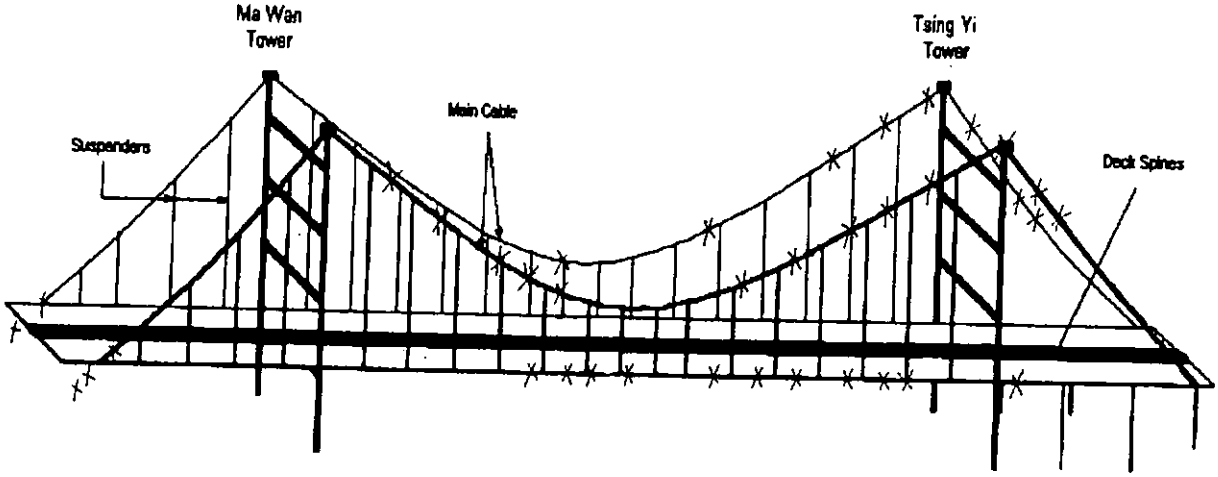

Figure 7.4 – Sensor locations on Tsing Ma Bridge for main deck spines

According to Figure 7.4, all sensors are placed on the Tsing Ma Bridge in the vertical direction. Most of the sensors are allocated along the main cables evenly. And the remaining of the sensors are also placed evenly on the one end of the transverse beam in the main span from near mid-span to the Tsing Yi Tower.

Section 7.3) Discussion on sensor locations from different methods

The Co-linearity Matrix Method gives most sensors on one end of the transverse beam from near mid-span of the main span to the Tsing Yi Tower. It is then questionable from engineering sense for these sensor locations to effective monitor all components of the Bridge, when the sensor number is usually limited in practice. Intuitively, the effective health monitoring of Tsing Ma Bridge is confined to the elements on one half of the Bridge on Tsing Yi side, when most of the sensors localize around these elements. Moreover, the sensor locations evaluated from the Co-linearity Matrix Method may not flexible for monitoring

different components of the structure, because this method can evaluate only one set of sensor locations to monitor the whole structure.

The sensor locations from the proposed method distribute evenly on the Tsing Ma Bridge for the interested elements of the main span. For the interested elements of the deck spine at Ma Wan side-span, the sensors are densely allocated surrounding the interested elements, and some sensors are placed on the deck spine of Tsing Yi span. The results indicate that the ratio between the interested element number and the sensor number influence the sensor locations. When the ratio is large, the sensors will be distributed evenly over the interested elements.

In conclusion, the proposed method can evaluate the sensor locations which are around the selected interested elements. And it is strongly believed that a particular set of sensor locations cannot effectively monitor all elements of the large civil structure. The potential damage elements or interested elements should be account for in the early stage of health monitoring account. The proposed method is flexible for the consideration of different elements in a large civil structure to be monitored.

Chapter 8

Conclusions and recommendations

Section 8.1) Conclusion on damage information collected

A sensor placement method is proposed to evaluate the sensor locations which are sensitive to the selected potential damage elements or interested elements basing on the eigenvector sensitivity. A large sensitivity is also interpreted as a large amount of damage information to benefit the damage assessment. However, the interested elements may not emit similar damage information so that damages in these elements may not be detected by the selected sensors in a large civil structure. Therefore a group of consistent elements should be determined through a backward elimination and sequential replacement approach for the reliability of health monitoring.

As previously mentioned, the collected damage information is an indicator of effectiveness of health monitoring. A comparison between the sects of sensor locations basing on different sensor placement methods is performed on their ability to collect maximal damage information. The different sensor placement methods include the proposed method, Co-linearity Matrix Method (i) and (ii) and the Effective Index Method. It should be noted that the Co-linearity Matrix Methods (i) and (ii) are different in searching approach in the co-linearity matrix.

The comparison results show that the sensors according to the proposed method can collect relatively large damage information compared with those according to the Effective Index Method. And the total collected damage information basing on the proposed method and the Co-linearity Matrix Method are similar. Hence the sensor locations basing on the proposed method is in general more effective than those from existing methods.

The damage information emitted from different types of elements, such as the analyzed elements, non-analyzed elements and undetectable elements, is quantified. And the selected sensor locations can collect the maximal damage information from the analyzed elements. On the contrary, the damage information from the non-analyzed elements is relatively insufficient at the corresponding sensor locations. And there is much less contribution of damage information from the undetectable elements at the sensor locations. This shows that the damage element classification process successfully classifies the detectable and undetectable elements. And also the analysis of sensor placement ratio can determine which sensor location is relatively sensitive to the analyzed elements.

Section 8.2) Conclusion on damage localization and quantification

After the comparison of the indicator of effectiveness health monitoring, a more practical consideration arises as to how well the corresponding sensors localize and quantify the damage elements. This is studied with a simulated structure and a test structure by means of Multiple Damage Location Assurance Criterion (*MDLAC*).

The incomplete modal information at the corresponding sensor locations are used to localize and quantify the damage elements. For the damage quantification, the damage extent is defined by means of the first eigenvalue of the stiffness matrix of the damaged element.

Comparison with the Effective Index Method in the simulated three-storey plane frame indicates the better performance of the proposed method in localizing the damage by using the *MDLAC*. And the damage localization using sensors from the proposed method has slightly improvement over the Co-linearity Matrix Methods (i) and (ii).

The comparison on accuracy in damage localization and quantification are also performed on the five-storey plane steel frame experimentally. Instead of placing the sensors close to the potential damage elements which is a traditional approach, the proposed method requires the input of the potential damage elements to determine the sensors locations. The proposed method with the use of initial Target Group of potential damage elements provides an effective means of sensor placement for damage detection. The results show that the Target Group should include the potential damage element to be monitored, or elements in the Target Group should be located near the potential damage elements.

Effective Index Method is found not suitable for sensor placement for damage assessment, where the sensor locations are selected basing on the linear independence of the mode shapes.

Section 8.3) Conclusion on sensor locations on Tsing Ma Bridge

As previously mentioned, the sensitivity of different components of a large civil structure usually varies much. Most of the sensors will be localized on the degrees-of-freedom in which are near highly sensitive elements. The proposed method will result in having sensor locations distributed around our interested elements. It is applied to the Tsing Ma Bridge to check on its performances in a large civil structure.

It is strongly believed that a particular set of sensor locations cannot effectively monitor all elements of a large civil structure. The potential damage elements or interested elements should be account for in the early stage of health monitoring. It would be flexible to consider different groups of elements in a large civil structure to be monitored. The results from the proposed method on the Tsing Ma Bridge show that the sensor locations for different Target Groups distribute around this group of elements. On the other hand, the sensor locations from the Co-linearity Matrix Method on the Tsing Ma Bridge are localized on the degrees-of-freedom which are near to some of the highly sensitive elements of the whole structure. Intuitively, it is ineffective to monitor all elements of the Tsing Ma Bridge using one set of sensors. Different sets of interested elements for monitoring should be input in the sensor placement method for different sets of sensors for an effective damage monitoring.

Section 8.4) Recommendation

The linear independence of potential damage information collected by sensors is found not a requirement for the sensor selection in the proposed method. The amount of useful information collected would be a significant factor in the sensor selection for damage assessment, because the amount of damage information directly relates to the damage location and extent. In other words, a damage element can emit much amount of damage information, this damage is highly possible to be detected

Moreover, it should be reminded that the basic principle of the *MDLAC* method is the correlation between the analytical and measured eigenvectors, and the number of the sensor should be as large as possible so that the actual damage configuration matches with that from the analysis of the *MDLAC* method. The damage location and extent can then be correctly predicted by means of the *MDLAC* method. However, according to the comparison on the damage assessment by the *MDLAC* method, the accuracy of the damage assessment is relatively poor basing on the some sensor placement methods in the first damage state. It is believed that the sensor number used in the analysis is too small. The sensor number is ten for collecting the damage information from fifteen elements in which the damages may occur. Therefore, the increase of the ratio between the sensor number and the monitored element number may improve the accuracy of the damage assessment by the *MDLAC* method. After the accuracy of the damage assessment has been improved, the other issues on the damage assessment, such as different sensor

locations, different damage elements, complicated structural type and symmetrical effects of damage information, become critical for the investigation later.

Basing on the *MDLAC* method for the multi-damage states, the damages are also difficult to be localized and quantified precisely by the general damage assessment methods, because the damage information from an element can interfere with those information from other elements collected at a degree-of-freedom. This interaction of the damage information from different elements is not easy to resolve. It means that a sensor collects the total damage information from different elements and is unable to distinguish the damage information emitted from the corresponding elements. In other words, when a sensor obtains this total damage information from different elements to localize and quantify a damage in an element, the effect of other damage elements is inevitably taken into account for the assessment of this element. Therefore, it is impossible to assess the damage in this element accurately. The further research works should therefore be necessary to enhance the accuracy of identification of the damage locations and extents under multi damage-states so that the comparison on the damage assessment by the different sensor placement methods could lead to a more enlightening conclusion. Moreover, in the proposed method, after the accuracy of damage assessment method under multi-damage states is improved, the relationship among the number of damages, the accuracy of the damage assessment and the sensor locations can be successfully predicted.

Furthermore, the inaccuracy of the results from damage assessment of tested

structure may be due to different sources of errors in the measurement of eigenvector changes and modeling error in sensor placement algorithm. In the measurement of the eigenvector changes at the degrees-of-freedom, these errors include the effect of noise in the collected signal. Moreover, matching the measured modes with those from the analysis by means of frequency response function results in some inaccuracies, especially when the natural frequencies in the local modes are densely spaced. Finally, the errors in the computational model of the tested structure also cause discrepancies between the results of damage assessment and the actual damage configuration. These errors can be due to incorrect input parameters, incorrect modeling techniques, unmodeled dynamics, or small non-linearity. Therefore, for the further study on the damage assessment, it is recommended to remove all possible errors in the damage assessment analysis such that the damage configuration can be correctly evaluated for the real structure. And remedial work can be immediately implemented to prevent the damages from developing further.

Finally, the actual damage analysis for a large civil structure is also required for the further research works. The effectiveness of damage assessment on a large civil structure is then compared for the different sensor placement methods basing on the simulated structure. And the damages are then assumed to occur at certain locations with certain extents in the computer modeling. Moreover, the implementation of the proposed method on a large civil structure should be carried out for further verification using the field test data.

References

1. Adelman, H.M., and Haftka (1986) "Sensitivity analysis of discrete structural sytems" *AIAA Journal*, vol. **24**, No. 5, 823-832.
2. Allemang, R.J. and Brown, D.L. (1983) "A correlation coefficient for modal vector analysis" *Proceedings of the 1st International Modal Analysis Conference*, Vol. **1**, 110-116.
3. Baruh, H., and Choe, K. (1988). "Sensor Placement in Structural Control" *AIAA Journal*, Paper 88-4056.
4. Belsley, D.A., Kuh, E. and Welsch, R.E. (1980). *Regression diagnostics: identifying influential data and sources of co-linearity,* John Wiley & Sons.
5. Cawley, P. and Adams, R.D. (1979) "The location of defects in structures from measurements of natural frequencies" *Journal of strain analysis*, vol. **14**, No. 2, 49-57.
6. Chen, J.C and Garba, J.A. (1985). "Structural analysis model validation using modal test data" *Joint ASCE/ASME Mechanics Conference*, Albuquerque, NM, 109-137.
7. Chatterjee, S. and Hadi, A.S. (1988). *Sensitivity analysis in linear regression,* John Wiley & Sons.
8. Cobb, R.G. and Liebst, B.S. (1997) "Sensor placement and structural damage identification from minimal sensor information" *AIAA Journal*, vol. **35**, 369-374.
9. Courant, R. and Hilbert, D. (1953). *Methods of mathematical physical.*
10. Ewins, D.J. (1984) "*Modal Testing: Theory and Practice*". Research Studies Press Ltd. John Wiley & Sons Inc.

11. Flanigan, C.C. and Botos, C.D. (1992) " Automated selection of accelerometer locations for modal survey tests".

12. Fox, R.L. and Kapoor, M.P. (1968) "Rate of change of eigenvalues and eigenvectors" *AIAA Journal*, vol. **6**, 2426-2429.

13. Guyan, R.J. (1965) "Reduction of stiffness and mass matrices" *AIAA Journal*, vol. **3**, No. 2.

14. Hoaglin, D.C. and Welsch, R.E. (1978) "The hat matrix in regression and ANOVA" The *American Statistician*, vol. **32**, No. 1, 17-22.

15. Levine-West, M.B. and Milman, M.H. (1995) "Mode shape expansion techniques for model error localization and damage detection" *Design Engineering Technical Conferences*, vol. **3**, Part C, 1279-1284.

16. Lieven, N.A.J. and Ewins, D.J. (1988) "Fault detection in structures from changes in their modal parameters" *Proceedings of the 7th International Modal Analysis Conference*, Vol. **1**, 87-94.

17. Kammer, D.C. (1991) "Sensor placement for on-orbit modal identification and correlation of large space structures" *Journal of Guidance, Control and Dynamics*, vol. **14**, No.2, 251-259.

18. Kammer, D.C. (1992a) "Effect of noise on sensor placement for on-orbit modal identification of large space structure" *Journal of Dynamic System, Measurement, and Control*, vol. **114**, 436-443.

19. Kammer, D.C. (1992b) "Effect of model error on sensor placement for on-orbit modal identification of large space structure" *Journal of Guidance, Control, and Dynamics*, vol. **15**, No. 2, 334-341.

20. Kashangaki, T.A.L. (1992) "Mode Selection for Damage Detection using the Modal Sensitivity Parameter", *Proceedings of the 33rd Structures, Structural Dynamics, and Materials Conference*, AIAA, Washington, DC, 1535-1542.0.

21. Kim, H.B. and Park, Y.S. (1997) "Sensor placement guide for structural joint stiffness model improvement", *Mechanical System and Signal Processing*, vol. **11**, No.5, 651-672.

22. Law, S.S., Shi, Z.Y. and Zhang, L.M. (1998). "Structural damage detection from incomplete and noisy modal data." *Journal of Engineering Mechanics* vol. **124**, No. 11, 1280-1288.

23. Lim, T.W. (1992) "Actuator/sensor placement for modal parameter identification of flexible structures" *International modal analysis conference*, 1-13.

24. Lim, T.W., and Kashangaki, T.A. (1994). "Structural Damage Detection of Space Truss Structures using Best Achievable Eigenvectors", *AIAA Journal*, vol. **32**, No. 5, 1049-1057.

25. Messina, A., Williams, E.J. and Contursi, T. (1998). "Structural damage detection by a sensitivity and statistical-based method." *Journal of Sound and Vibration*, vol. **216**, No. 5, 791-808.

26. Messina, A., Contursi, T. and Williams, E.J. (1997) "Multi damage evaluation using natural frequency changes" *Proceedings of the 15th International Modal Analysis Conference*, Vol. **1**, 658-664.

27. Nelson, R.B. (1976) "Simplified calculation of eigenvector derivatives" *AIAA Journal*, vol. **14**, No. 9, 1201-1205.

28. Pandey, A.K., Biswas, M. and Samman, M.M. (1990) "Damage detection from changes in curvature mode shapes" *Journal of sound and vibration*, vol. **145**, No. 2, 321-332.

29. Penny, J.E.T., Friswell, M.I. and Garvey, S.D. (1994) "Automatic choice of measurement locations for dynamic testing" *AIAA Journal*, vol. **32**, No. 2, 407-414.

30. Rao, C.R. and Toutenburg, H. (1995). *Linear models: least squares and alternatives*, Springer.

31. Salama, M., Rose, T. and Garba, J. (1987). "Optimal Placement of Excitations and Sensors for Verification of Large Dynamic Systems", *Proceedings of the AIAA/ASME/ASCE/AHS 28th Structures, Structural Dynamics, and Materials Conference*, AIAA, Washington, DC, 1024-1031.

32. Shi, S.S., Law, S.S. and Zhang, L.M. "Damage localization by directly using incomplete mode shapes" submitted to *Journal of Engineering Mechanics*, ASCE (in press).

33. Shi, S.S., Law, S.S. and Zhang, L.M. (1998) "Structural damage detection from modal strain energy change" *Journal of Engineering Mechanics*.

34. Stabb, M. and Blelloch, P. "Application of flexibility shapes to sensor selection" 1255-1262.

35. Tasker, F.A. and Liu, C. (1995) "Variance-based sensor placement for modal identification of structures" *Journal of Guidance, Control and Dynamics*, vol. **18**, No. 3, 627-630.

36. Udwadia, F.E. and Garba, J.A. (1985) "Optimal sensor locations structural identification" JPL. *Proceedings of the Workshop on Identification and Control of Flexible Space Structures*, 247-261.

37. West, M.L, Milman, M. and Kissil, A (1996) "Mode shape expansion techniques for prediction: Experimental Evaluation" *AIAA Journal*, vol. **34**, No. 4, 821-829.

38. Xia, Y. and Hao, H. (2000) "Damage identification of structures with optimal measurement selection" *The Proceeding of Asia-Pacific Vibration Conference in Singapore 1999*, vol. **2**, 1100-1105.

39. Yap, K.C. and Zimmerman, D.C. (2000) "Optimal sensor placement for dynamic model correlation" *The Proceedings of 18th International modal analysis conference*, 607-612.

40. Zimmerman, D.C., Smith, S.W., Kim, H.M. and Bartkowicz, T.L. (1996) "An experimental study of structural health monitoring using incomplete measurement" *Journal of Vibration and Acoustics*, vol. **118**, 534-550.